Thesis for doctoral degree (Ph.D.)
2017

Molecular imaging of tau in the pathological cascade of Alzheimer's disease

Konstantinos Chiotis

Karolinska Institutet

From the Division of Translational Alzheimer Neurobiology
Department of Neurobiology, Care Sciences and Society
Karolinska Institutet, Stockholm, Sweden

MOLECULAR IMAGING OF TAU IN THE PATHOLOGICAL CASCADE OF ALZHEIMER'S DISEASE

Konstantinos Chiotis

Karolinska Institutet

Stockholm 2017

Cover illustration by Emelie Berg
All previously published papers were reproduced with permission from the publisher.
Published by Karolinska Institutet.
Printed by E-print AB 2017

ISBN 978-91-7676-855-6

Molecular imaging of tau in the pathological cascade of Alzheimer's disease

THESIS FOR DOCTORAL DEGREE (Ph.D.)

This thesis will be defended in Hörsalen, Novum, Floor 4, Huddinge
Tuesday, December 5th, 2017, at 10:00 a.m.

By

Konstantinos Chiotis

Principal Supervisor:
Professor Agneta Nordberg
Karolinska Institutet
Department of Neurobiology,
Care Sciences and Society
Division of Translational
Alzheimer Neurobiology

Co-supervisors:
Professor Ove Almkvist
Karolinska Institutet
Department of Neurobiology,
Care Sciences and Society
Division of Translational
Alzheimer Neurobiology

Dr. Stephen F. Carter
University of Manchester, UK
Institute of Brain, Behaviour
and Mental Health
Wolfson Molecular Imaging Centre

Dr. Laure Saint-Aubert
Toulouse University Hospital, Imaging Pole
ToNIC - Toulouse NeuroImaging Centre -
UMR1214 INSERM/University Toulouse 3
France

Opponent:
Professor Gil Rabinovici
University of California,
San Fransisco, USA
Department of Neurology
Memory and Aging Center

Examination Board:
Professor Per Svenningsson
Karolinska Institutet
Department of Clinical Neuroscience

Professor Irina Alafuzoff
Uppsala University
Department of Immunology,
Genetics and Pathology

Associate professor Sebastian Palmqvist
Lund University
Department of Clinical Sciences
Clinical Memory Research Unit

This thesis is dedicated to the patients and their relatives.

Οὐ γὰρ ὡς ἀγγεῖον ὁ νοῦς ἀποπληρώσεως ἀλλ΄
ὑπεκκαύματος μόνον ὥσπερ ὕλη δεῖται, ὁρμὴν
ἐμποιοῦντος εὑρετικὴν καὶ ὄρεξιν ἐπὶ τὴν ἀλήθειαν.

— Πλούταρχος, *Περί του ακούειν*

For the correct analogy for the mind is not a vessel
that needs filling, but wood that needs igniting –
no more – and then it motivates one towards
originality and instils the desire for truth.

— Plutarch, *On listening*

ABSTRACT

The pathology of Alzheimer's disease (AD) is characterised by the misfolding and aggregation of amyloid-β (Aβ) into extracellular plaques and aggregation of tau into intracellular neurofibrillary tangles. Recent advances in molecular imaging have allowed the development of positron emission tomography (PET) tracers for the *in vivo* detection of Aβ plaques while current efforts focus on the evaluation of recently proposed tracers targeting tau pathology. This thesis is composed of three main parts. Part one compares two Aβ PET tracers ([^{11}C]PIB and [^{18}F]florbetapir) when administered to different but matched patient cohorts, and explores the effect of age on the distribution of Aβ-positive PET scans. Part two focuses on the first *in vivo* evaluation of the tau-specific tracer [^{18}F]THK5317, using a longitudinal multi-modal design, in a sample of cognitively normal volunteers, patients at different clinical stages of AD and individual patients with atypical parkinsonism. The third part describes the direct *in vivo* comparison of the binding properties of two tau-specific tracers ([^{11}C]THK5351 and [^{11}C]PBB3) when injected into the same patients with AD on the same day. The results indicated that, firstly, the binding of the Aβ-specific PET tracers, [^{11}C]PIB and [^{18}F]florbetapir, was highly comparable in individuals from different cohorts. Furthermore, age plays an important role in the distribution of Aβ-positive PET scans, with the oldest old patients with cognitive complaints appearing to benefit substantially from clinical assessment with Aβ PET. Secondly, the tracer [^{18}F]THK5317 detected the expected load and regional distribution of tau pathology *in vivo* in a sample of patients with AD and patients with atypical parkinsonism. The distribution of [^{18}F]THK5317 binding differed from that of Aβ deposition in patients with AD, although regional correlations existed, indicating areas where Aβ and tau pathologies were co-located. The regional load of tau pathology ([^{18}F]THK5317) was associated with measures of global cognition and episodic memory, with local hypometabolism playing a mediating role in this relationship. Longitudinally, a heterogeneous pattern of changes was observed in the binding of the tau tracer [^{18}F]THK5317 in patients with AD, in contrast to the homogeneous changes in glucose metabolism that better tracked cognitive deterioration. The build-up of tau pathology ([^{18}F]THK5317) and the development of local hypometabolism appeared temporally dissociated, with a stronger relationship detected between the two when hypometabolism changes became more prevalent, in the later stages of the disease. Finally, different tau-specific tracers ([^{11}C]THK5351 and [^{11}C]PBB3) seemed to bind *in vivo* to different molecular targets; [^{11}C]PBB3 binding appeared to correlate closer to Aβ deposition, while [^{11}C]THK5351 binding followed the expected regional pattern of tau pathology in AD and related closer to downstream markers of the disease. Further investigation of the existing PET tracers and development of new tracers is required for shedding light on the pathological processes that contribute to neurodegeneration in AD and for developing clinical markers that allow early and highly accurate discrimination between different proteinopathies.

LIST OF PUBLICATIONS

The thesis is based on the following original articles.

I. **Chiotis K**, Carter SF, Farid K, Savitcheva I, Nordberg A; Diagnostic Molecular Imaging (DiMI) network and the Alzheimer's Disease Neuroimaging Initiative. Amyloid PET in European and North American cohorts; and exploring age as a limit to clinical use of amyloid imaging.
Eur J Nucl Med Mol Imaging. 2015 Sep;42(10):1492-506.

II. **Chiotis K**, Saint-Aubert L, Savitcheva I, Jelic V, Andersen P, Jonasson M, Eriksson J, Lubberink M, Almkvist O, Wall A, Antoni G, Nordberg A. Imaging *in vivo* tau pathology in Alzheimer's disease with THK5317 PET in a multimodal paradigm.
Eur J Nucl Med Mol Imaging. 2016 Aug;43(9):1686-99.

III. Saint-Aubert L, Almkvist O, **Chiotis K**, Almeida R, Wall A, Nordberg A. Regional tau deposition measured by [^{18}F]THK5317 positron emission tomography is associated to cognition via glucose metabolism in Alzheimer's disease.
Alzheimers Res Ther. 2016;8(1):38.

IV. **Chiotis K**, Saint-Aubert L, Rodriguez-Vieitez E, Leuzy A, Almkvist O, Savitcheva I, Jonasson M, Lubberink M, Wall A, Antoni G, Nordberg A. Longitudinal changes of tau PET imaging in relation to hypometabolism in prodromal and Alzheimer's disease dementia.
Mol Psychiatry. 2017; Epub 2017 May 16.

V. **Chiotis K**, Stenkrona P, Almkvist O, Stepanov V, Ferreira D, Arakawa R, Takano A, Westman E, Varrone A, Okamura N, Shimada H, Higuchi M, Halldin C, Nordberg A. Dual tracer tau PET imaging reveals different molecular targets for ^{11}C-THK5351 and ^{11}C-PBB3 in the Alzheimer brain.
Manuscript in preparation.

SELECTION OF RELATED PUBLICATIONS

This is an excerpt of related publications by the author, containing supporting evidence, or revising the existing literature.

Original articles

Rodriguez-Vieitez E, Leuzy A, **Chiotis K**, Saint-Aubert L, Wall A, Nordberg A. Comparability of [^{18}F]THK5317 and [^{11}C]PIB blood flow proxy images with [^{18}F]FDG positron emission tomography in Alzheimer's disease.
J Cereb Blood Flow Metab. 2017;37(2):740-749.

Jonasson M, Wall A, **Chiotis K**, Saint-Aubert L, Wilking H, Sprycha M, Borg B, Thibblin A, Eriksson J, Sörensen J, Antoni G, Nordberg A, Lubberink M. Tracer kinetic analysis of (S)-^{18}F-THK5117 as a PET tracer for assessing tau pathology.
J Nucl Med. 2016 Apr;57(4):574-81.

Review articles

Frisoni GB, Boccardi M, Barkhof F, Blennow K, Cappa S, **Chiotis K**, Démonet JF, Garibotto V, Giannakopoulos P, Gietl A, Hansson O, Herholz K, Jack CR Jr, Nobili F, Nordberg A, Snyder HM, Ten Kate M, Varrone A, Albanese E, Becker S, Bossuyt P, Carrillo MC, Cerami C, Dubois B, Gallo V, Giacobini E, Gold G, Hurst S, Lönneborg A, Lovblad KO, Mattsson N, Molinuevo JL, Monsch AU, Mosimann U, Padovani A, Picco A, Porteri C, Ratib O, Saint-Aubert L, Scerri C, Scheltens P, Schott JM, Sonni I, Teipel S, Vineis P, Visser PJ, Yasui Y, Winblad B. Strategic roadmap for an early diagnosis of Alzheimer's disease based on biomarkers.
Lancet Neurol. 2017 Aug;16(8):661-676.

Chiotis K, Saint-Aubert L, Boccardi M, Gietl A, Picco A, Varrone A, Garibotto V, Herholz K, Nobili F, Nordberg A; Geneva Task Force for the Roadmap of Alzheimer's Biomarkers. Clinical validity of increased cortical uptake of amyloid ligands on PET as a biomarker for Alzheimer's disease in the context of a structured 5-phase development framework.
Neurobiol Aging. 2017 Apr;52:214-227.

Saint-Aubert L, Lemoine L, **Chiotis K**, Leuzy A, Rodriguez-Vieitez E, Nordberg A. Tau PET imaging: present and future directions.
Mol Neurodegener. 2017;12(1):19.

TABLE OF CONTENTS

LIST OF ABBREVIATIONS

Aβ	Amyloid-β
AD	Alzheimer's disease
ADNI	Alzheimer's disease neuroimaging initiative
ApoE4	Apolipoprotein E ε4
APP	Amyloid precursor protein
BP_{ND}	Non-displaceable binding potential
CBD	Corticobasal degeneration
CSF	Cerebrospinal fluid
DiMI	Diagnostic molecular imaging
DVR	Distribution volume ratio
[^{18}F]FDG	2-[^{18}F]fluoro-2-deoxy-D-glucose
FSIQ	Full-scale intelligence quotient
MAPT	Microtubule-associated protein tau
MCI	Mild cognitive impairment
MMSE	Mini-mental state examination
MNI	Montreal Neurological Institute
MAO	Monoamine oxidase
MRI	Magnetic resonance imaging
NFT	Neurofibrillary tangle
PET	Positron emission tomography
PSP	Progressive supranuclear palsy
ROI	Region of interest
SCD	Subjective cognitive decline
SUVR	Standardised uptake value ratio
TDP-43	TAR DNA-binding protein 43

1 INTRODUCTION

1.1 FROM NORMAL AGEING TO DEMENTIA

1.1.1 Ageing

Age-related progressive decline in intrinsic physiological functioning, associated with increased morbidity and mortality, is a common definition of ageing. [1,2] In the brain, normal ageing is linked with various structural and functional changes that are associated with a gradual decline in specific cognitive functions (e.g. processing speed, memory, etc.), which do not interfere with the activities of daily living. [3] However, the links between normal cognitive ageing and the age-related neurodegenerative diseases that lead to substantial cognitive deficits and functional disability remain elusive.

1.1.2 Dementia

Dementia can be described as the acquired loss of cognitive function, severe enough to interfere with daily life, caused by brain disease or injury. [4] According to the Diagnostic and Statistical Manual of Mental Disorders, 5th edition, the diagnosis of major neurocognitive disorder (previously dementia) diagnosis is mainly based on evidence of significant cognitive decline from a previous level of performance in one or more cognitive domains (complex attention, executive function, learning and memory, language, perceptual-motor, or social cognition), with these cognitive deficits interfering with independence in everyday activities. The diagnosis is made after the exclusion of other mental disorders that could explain the cognitive deficits (e.g. major depressive disorder, schizophrenia). [5]

According to the Centers for Disease Control and Prevention USA, dementia is the sixth leading cause of death, behind heart disease, cancer, chronic lower respiratory diseases, accidents and stroke. More specifically, one in three seniors die with dementia, and 46 million people are estimated to live with dementia worldwide. [6] In Sweden it is estimated that more than 160,000 people suffer from dementia at the moment, [7] a prevalence comparable to that in other European countries. It is worth mentioning that, as age is the strongest known risk factor for dementia, the prevalence of dementia is expected to nearly double every 20 years, due to the global increase in population size and life expectancy, according to the World Alzheimer Report. [8] Dementia is not only associated with disability and mortality but also with dependence and societal costs, which place a great burden on families, communities and societies, especially since dementia is a terminal condition and the patients live for many years after the onset of symptoms. [9] It is noteworthy that the total worldwide cost of dementia in 2015 was US$ 818 billion and is set to reach US$ 2 trillion annually by 2030. [8] The annual cost of dementia in Sweden is calculated to exceed the SEK 60 billion in total, or SEK

398,000 per person with dementia per year. [10] A growing body of evidence illustrates the dramatic increase in global prevalence and societal costs of the 'dementia epidemic' [11] and highlights the need for prioritising dementia in the public health research agenda internationally.

1.1.2.1 The spectrum of dementia

The set of symptoms grouped under the general term dementia do not refer to a single clinico-pathological entity, but rather to several diseases with distinct characteristics, although a substantial clinical and pathological overlap between them has been observed. Alzheimer's disease (AD) is the most common neurodegenerative disorder and cause of dementia, accounting for 50-70% of all dementia cases. [12] Other causes of dementia include frontotemporal lobar degeneration, vascular dementia, Lewy body disease, etc. (Figure 1). It should be noted that dementias with mixed underlying pathologies are a common finding; these show increased prevalence with increasing age. [13] Finally, other diseases have been linked to dementia (e.g. Down's syndrome, traumatic brain injury, Parkinson's disease, Huntington's disease, Creutzfeldt-Jakob disease) or dementia-like syndromes that may be reversed with the appropriate treatment (e.g. delirium, pseudodementia, infections, etc.).

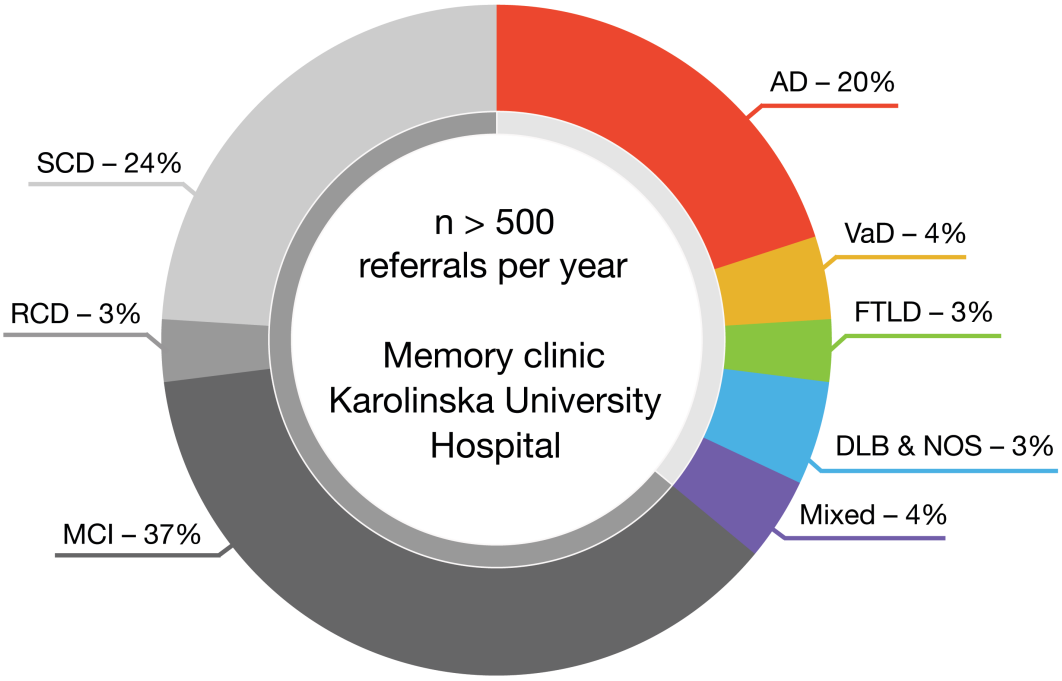

Figure 1. Pie chart illustrating the distribution (percentage, %) of diagnoses following memory assessment of more than 500 patients at the memory clinic, Karolinska University Hospital, Sweden, over one year (data from 2015). The coloured slices show the frequency of a diagnosis of dementia syndrome (34% in total). DLB = dementia with Lewy bodies; FTLD = frontotemporal lobar degeneration; Mixed = mixed dementia; NOS = dementia not otherwise specified; RCD = reversible cognitive disorder due to other medical conditions; VaD = vascular dementia.

1.1.3 Mild cognitive impairment

Mild cognitive impairment (MCI) is a clinical diagnosis with heterogeneous underlying causes that is thought to represent an intermediate stage between normal ageing and the diagnosis of dementia. [14] The diagnosis is assigned in the presence of objective cognitive decline in one or more cognitive domains that is not expected for the age and education of the patient, and normal activities of daily living in the absence of a dementia disorder. Subsequent revisions of the diagnostic criteria have classified patients with MCI into four categories based on the impairment of memory and/or other cognitive domains; [15] predominant impairment of memory has been more closely associated with later progression to AD. [16,17] The diagnosis of MCI represents a risk factor for a subsequent dementia diagnosis, [18] although not all patients will eventually develop dementia; a substantial number of patients will remain stable or even reverse to normal cognition over time. [19,20]

1.1.4 Subjective cognitive decline

A substantial percentage of patients presenting with cognitive complaints are discharged with a clinical diagnosis of subjective cognitive decline (SCD) (Figure 1). The diagnosis is made in the presence of a self-perceived decline in cognitive performance, not related to an acute event, and normal performance on standardised cognitive tests, adjusted for individual age and educational attainment. [21,22] Individuals with SCD represent an etiologically heterogeneous group with a subset of individuals developing objective cognitive deficits in the future. Although observations suggest that SCD is a risk factor for future development of MCI or dementia, [23-26] the relationship over time between subjective and objective cognitive decline remains unclear and has attracted great interest from the scientific community.

1.2 ALZHEIMER'S DISEASE

In 1984, McKhann, et al. [27] in a working group established by the National Institute of Neurological and Communicative Disorders and Stroke and the Alzheimer Disease and Related Disorders Association (now Alzheimer's Association), defined AD as 'a brain disorder characterised by progressive dementia that occurs in middle or late life'. The pathological characteristics of the disease include the presence of neurodegeneration, neuritic plaques and neurofibrillary tangles (NFTs), as discussed below. Clinically, the disease usually manifests after the sixth decade of life, typically starting with impairment of short-term memory early in the disease course, before the development of more extensive cognitive deficits. However, the clinical presentation of the disease can be heterogeneous, with different clinical phenotypes described, [28-30] and substantial overlap could exist in the clinical symptomatology of AD and other dementia syndromes. [31]

According to the most widely accepted diagnostic criteria, [16] a diagnosis of AD can be made clinically in the presence of a progressive dementia disorder with two confidence levels

(namely, possible and probable). A probable diagnosis is made in the presence of dementia with deficits in at least two cognitive domains, progressive cognitive decline, no disturbance of consciousness, and onset of the disease after 40 years of age and after the exclusion of other systemic or brain diseases; a possible diagnosis is made with an atypical clinical presentation or in the presence of other significant diseases. Finally, a definite diagnosis of AD can only be assigned in the presence of histopathological evidence of the disease in autopsy or biopsy specimens. [32] The level of uncertainty described in the clinical criteria for AD reflects the only moderate agreement between the clinical and neuropathological diagnoses, [33] as well as the absence, until very recently, of reliable laboratory or *in vivo* imaging markers of the underlying pathology.

While the cause of AD remains elusive, a number of risk factors have been identified. Specifically, increasing age, carriage of the apolipoprotein E ε4 (ApoE4) allele, family history and low educational attainment are associated with increased prevalence of sporadic AD. [34-36] A number of modifiable cardiovascular risk factors have been associated with increased risk of AD, including the presence of diabetes, obesity, smoking, hypertension, hypercholesterolaemia, and the lack of physical activity. [37]

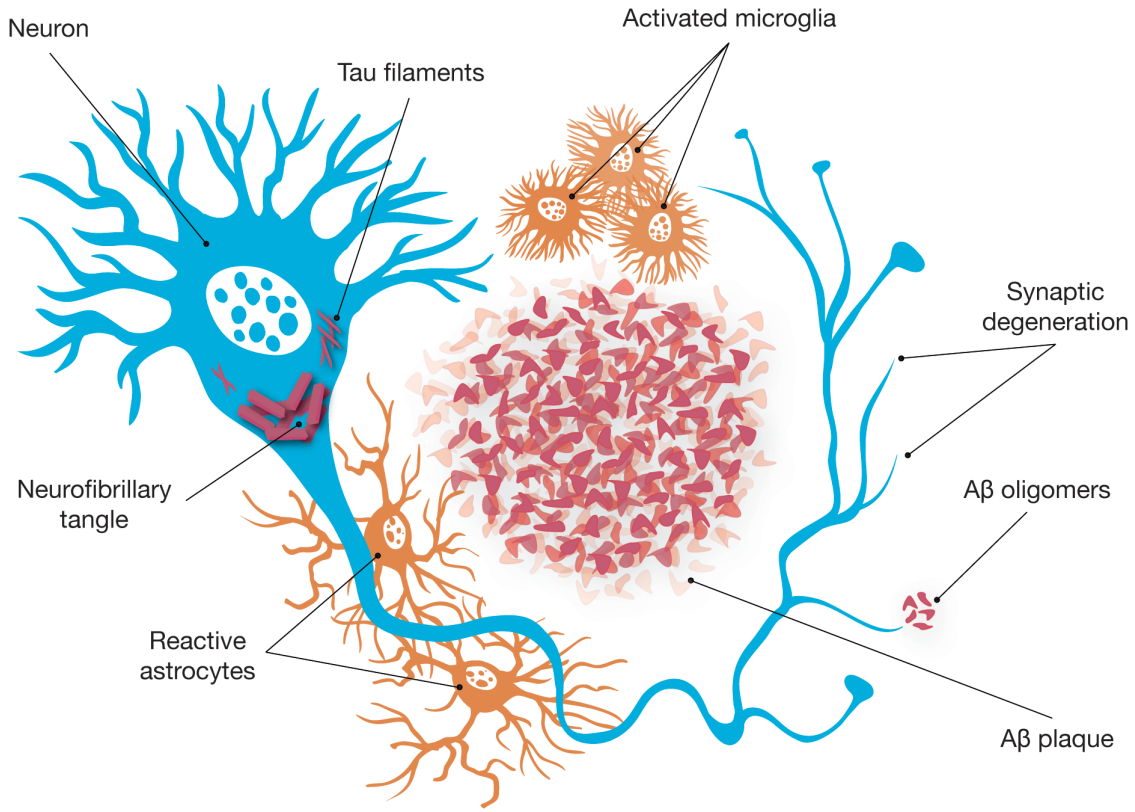

Figure 2. Illustration of the main pathological features of AD. Extracellular deposits of Aβ fibrils together with other proteins form the Aβ plaques, while intracellular deposits of tau filaments form the neurofibrillary tangles in AD. Inflammatory cells (i.e. reactive astrocytes and activated microglia) surround the Aβ plaques.

1.2.1 Neuropathology

Alois Alzheimer in 1906 was the first to identify and describe the neuropathological characteristics of a 'peculiar severe disease process of the cerebral cortex' later named after him, as Alzheimer's disease. The characteristics of AD in the first patient to be described consisted of the presence of miliary foci of silver-staining deposits (later known as neuritic plaques), and bundles of fibrils (later known as NFTs), along with atrophy in the brain. [38]

1.2.1.1 Amyloid-β plaques

Amyloid-β (Aβ) plaques are extracellular fibrillar deposits of insoluble Aβ protein (Figure 2). [39,40] Aβ protein is formed by the cleavage, by β- and γ-secretases, of the parent molecule, the amyloid precursor protein (APP; gene located on chromosome 21), an integral membrane protein. [41,42] Aβ is released extracellularly, and under normal conditions is mainly cleared into the cerebrospinal fluid (CSF) and later removed by the blood. [43] An imbalance between Aβ production and clearance in AD is thought to lead to the abnormal accumulation of the protein. [44] Aβ monomers aggregate into oligomers and these, based on the conformation they adopt, can be categorised into fibrillar-insoluble (β-sheet structure) or prefibrillar-soluble forms. [45] The insoluble forms are further aggregated into longer $A\beta_{40}$ or $A\beta_{42}$ β-sheet fibrils (Figure 3). Of note, $A\beta_{42}$ is considered the most toxic species of Aβ. The Aβ fibrils together with other deposited proteins (e.g. ApoE, interleukins, complement, etc.) form the extracellular Aβ plaques. [46] Two types of plaque have been described, based on their morphology; diffuse and dense-cored plaques. [47] Neuritic plaques are a specific subtype of dense-cored plaques that consist of Aβ deposits surrounded by dystrophic neurites rich in deposits of abnormally hyperphosphorylated tau protein. [48]

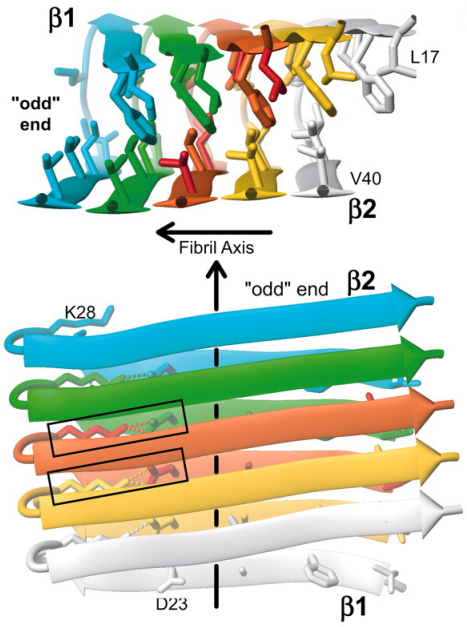

Figure 3. The 3D structure of an $A\beta_{42}$ fibril obtained by using hydrogen-bonding constraints in quenched hydrogen/deuterium-exchange nuclear magnetic resonance. The fibril consists of two stacked, parallel β-sheets. Adapted with permission from Luhrs, T. et al. 3D structure of Alzheimer's amyloid-beta(1-42) fibrils. Proceedings of the National Academy of Sciences of the United States of America **102**, 17342-17347, (2005). Copyright 2005 National Academy of Sciences.

The evolution of the regional distribution of Aβ plaques during the course of AD has been described in detail; the neocortex is the first to be involved (Phase 1), followed by the hippocampus and entorhinal cortex (Phase 2), the basal ganglia (Phase 3), the brainstem (Phase 4) and finally, the cerebellum (Phase 5). [49,50] The development of Aβ plaques is thought to start affecting the cortex in 4% of all neuropathology cases in the fourth decade, with Aβ pathology estimated to become prevalent in

more than 50% of all individuals in the eighth decade of life. [51] Given the fact that a diagnosis of AD is typically made after the sixth decade and that the incidence rate of clinical AD, even in the eighth decade, does not exceed the 5%, [52] it is apparent there is a long preclinical phase of Aβ accumulation and that a large number of individuals carry a substantial amount of Aβ pathology without ever developing the disease.

1.2.1.2 Tau pathology

The bundles of fibrils (NFT) that Alois Alzheimer described were in fact intraneuronal aggregates of the abnormally hyperphosphorylated microtubule-associated protein tau (MAPT) (Figure 2). [53] Tau protein, a cytoskeletal component that is abundant in the neuronal axons, plays an important role in regulating neuronal growth and axonal transport and stabilising the structure of the microtubules, a function that is regulated by the normal phosphorylation of tau. [54,55] More specifically, the dephosphorylated tau binds to the microtubules and promotes their polymerisation, while its phosphorylation causes tau to dissociate from the microtubules. Tau is encoded in the MAPT gene in chromosome 17, and alternative mRNA splicing of the gene leads to six possible tau isoforms, three with three and three with four microtubule-binding domain repeats (i.e. 3R and 4R, respectively). [56] While in the foetus the predominant form of tau is the 3R form, which binds less stably to microtubules, in the healthy adult brain the 3R and 4R isoforms are equally expressed. [57] Although tau is most abundant in neurons, astrocytes and oligodendroglia also contain tau, although this is essentially the 4R tau isoform. [58,59] Both 3R and 4R tau undergo pathological hyperphosphorylation in AD, in contrast to other less common neurodegenerative diseases involving accumulation of tau protein (aka tauopathies), where there is predominant involvement of either 3R or 4R tau. [60] The hyperphosphorylation is followed by the aggregation of tau into β-sheet paired helical filaments (Figure 4), which form the insoluble NFTs intracellularly. [53] Although, under normal conditions, tau is located mainly in the axons of the neurons, the aggregation of tau leads to its redistribution to the soma and dendrites of the affected neurites. [61] Three stages of aggregation of NFTs have been described, namely the pre-tangles (non-filamentous soluble aggregates), the intracellular mature tangles (condensed fibrillar deposits) and the extracellular ghost tangles (which arise after the death of the

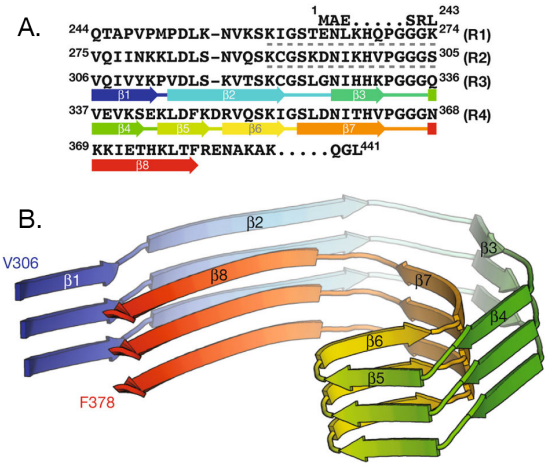

Figure 4. The 3D structure of the tau protofilament core obtained by cryo-electron microscopy. (A) Sequence alignment of the four microtubule-binding repeats (R1–R4) with the observed eight β-strand regions coloured from blue to red. (B) Rendered view of the secondary structure elements in three successive rungs. Adapted with permission from Macmillan Publishers Ltd: Nature, Fitzpatrick, A. W. P. *et al.* Cryo-EM structures of tau filaments from Alzheimer's disease. *Nature* **547**, 185-190, (2017). Copyright 2017.

neuron containing the mature tangles, named 'tombstone' lesions). [62,63] Recent evidence suggests that there are differences in the tau isoform profile in the different stages of NFT deposits. A profile shift is observed from the predominantly 4R tau deposits in the non-fibrillar pre-tangles to predominantly 3R tau in the ghost tangles, while equal expression of isoforms is reported in the mature NFT. [64] Based on autopsy studies tau pathology, but not Aβ accumulation, has been closely associated with both neuronal loss and cognitive impairment in patients with AD, and it is thought to be a marker of progression of AD. [65-68] However, although tau aggregation could lead, according to the current hypothesis, to cell death due to disruption of microtubule stability and axonal transport, the underlying mechanism is poorly understood. [55,69-71] To add to this uncertainty, there is experimental evidence suggesting that neurons can tolerate a substantial amount of tau pathology for longer intervals than expected, raising the possibility that NFT formation could even act protectively against neuronal loss. [72-74]

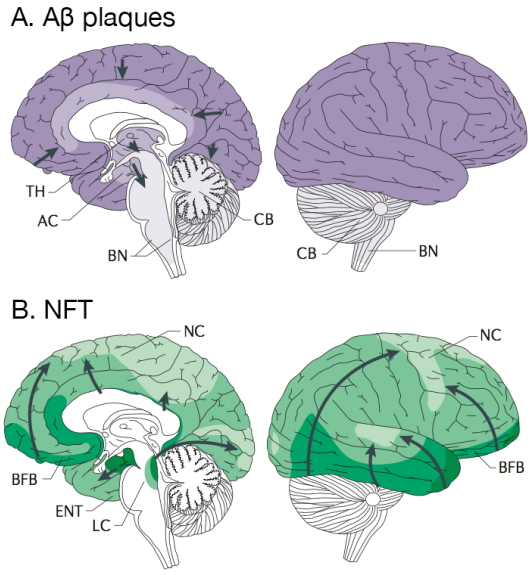

Figure 5. Illustration of the temporal spreading of (A) Aβ plaques and (B) NFTs in the AD brain. AC = allocortex; BFB = basal forebrain; BN = brainstem nuclei; CB = cerebellum; ENT = entorhinal cortex; LC = locus coeruleus; NC = neocortex; TH = thalamus. Adapted with permission from Macmillan Publishers Ltd: Nature reviews. Neuroscience, Brettschneider, J., Del Tredici, K., Lee, V. M. & Trojanowski, J. Q. Spreading of pathology in neurodegenerative diseases: a focus on human studies. *Nature reviews. Neuroscience* **16**, 109-120, (2015). Copyright 2015.

The regional distribution of NFTs in AD evolves in a predictable manner over time starting from the transentorhinal cortex and progressively affecting the hippocampus, the adjacent inferior temporal lobe, the cortical association areas and finally the primary cerebral cortices. [49,75] It should be noted that the exact area of initial NFT deposition remains controversial, since it is thought that the tau pathology could be detected in the brain stem, and more specifically in the locus coeruleus, before it affects the transentorhinal cortex. [76] Most autopsy studies published to date have highlighted the importance of the localisation of the NFT deposits, especially in relation to the cognitive performance of the individual affected. [77] While NFT pathology in the medial temporal lobe is considered to be asymptomatic, in other words to be an inevitable process of ageing, [51] spreading of the pathology to the adjacent neocortex has been associated with cognitive impairment, while severe dementia is thought to occur when the whole neocortex is affected. [78] The stereotypical propagation of tau pathology has led researchers to suggest that the pathology could spread in a prion-like manner. According to this hypothesis, the formation of misfolded tau aggregates in affected neurons could be transmitted to other neurons where the aggregates act as templates for the seeded aggregation of the native tau in the 'healthy' neuron. There is evidence of this from experimental studies in animal models and this represents a promising area for future research (for a detailed review, see [79-81]).

Although both Aβ plaques and NFTs follow stereotypical spatial spreading in the AD brain, the propagation profiles of the two pathologies are substantially different, as demonstrated in Figure 5. A long preclinical phase of NFT aggregation has been proposed, based on *post-mortem* studies; [82,83] data from these studies suggest that the formation of NFTs could even precede Aβ plaque deposition in the course of AD. [84-87]

1.2.1.3 Neurodegeneration

The AD brain is characterised by macroscopic atrophy with decreased brain weight and enlargement of the ventricles. [88] Microscopically, the neurodegeneration is expressed by neuronal loss and reduced synaptic density in both allo- and neo-cortical areas, which correlates closely with the cognitive function of the patient (Figure 2). [89-92] More specifically, changes in synaptic integrity are observed, with degeneration of the axons and subsequent neuronal death. [93,94]

1.2.1.4 Neuroinflammation

Neuroinflammation in AD is not limited to the presence of interleukins and component proteins in association with Aβ plaques. [95] Autopsy studies have revealed the existence of both activated microglia and reactive astrocytes proximal to Aβ plaques (Figure 2). [96-98] Microglial cells are inflammatory cells that can be primed (multiplied and activated) in response to their microenvironment. Activated microglia are characterised by pro-inflammatory and anti-inflammatory states, and are partly involved in the phagocytic clearance of Aβ. [99] Reactive astrocytes have diverse phenotypes, [100] and although they have been associated with the clearance of Aβ [101] their role seems more complex. Specifically, it has been suggested that reactive astrocytes could play an additional role in both Aβ accumulation and the induction of oxidative stress. [102-104]

1.2.1.5 Neuropathological criteria

Despite intense efforts to develop biomarkers that will detect *in vivo* changes in the AD brain, *post-mortem* neuropathological evaluation remains the gold standard in the diagnosis of AD. The recently described neuropathological criteria [32,105] for an AD diagnosis are based on a combination of the assessments of the phases of Aβ plaques development, [50] the stages of NFT spreading [49,106] and a semi-quantitative assessment of the neuritic plaque load. [107]

1.2.2 Amyloid cascade hypothesis

The amyloid cascade hypothesis, formulated in 1992 by Hardy and Higgins [108], is still the most widely accepted conceptualisation of the pathogenesis of AD. The factors that led to formulation of the hypothesis include the identification of mutations in the APP gene (chromosome 21) as deterministic for the development of autosomal dominant AD, [109,110] and the very high prevalence of the disease in patients with Down's syndrome (trisomy 21). [40,111,112] According to this hypothesis, Aβ plays a central role in the neuropathology of the disease, with its accumulation leading to the abnormal hyperphosphorylation of tau protein and neurodegeneration. However, through the years, a number of weaknesses have tested the validity of this hypothesis. [113] For example, Aβ deposition is common in cognitively normal elderly; [114] then the animal models with overexpression of the APP gene do not develop substantial neurodegeneration or the AD phenotype of cognitive impairment; [115,116] Aβ accumulation does not show a close relationship with cognitive impairment, especially at the symptomatic stages of the disease; [65] and anti-Aβ drugs have, so far, failed to change the course of the disease, at least in its later stages. [117-119]

Refinement of the amyloid hypothesis [120,121] and alternative models of AD pathogenesis has been proposed in order to account for the weaknesses of the hypothesis formulated by Hardy and Higgins [108]. Aβ-soluble oligomers are thought, now, as the most neurotoxic form of Aβ aggregates that could drive tau pathology, although our knowledge about their role remains fragmentary. [122-126] According to this hypothesis, the fibrillar Aβ plaques may not be harmful but will instead act as 'inert sinks' for the accumulation of Aβ oligomers.

Alternative models, where tau pathology or neuroinflammation are of central interest, have also been proposed, [84,121,127-129] although these have received less attention to date.

1.2.3 Cognitive performance

The term neuropsychological assessment is used to describe the administration of a number of tests for evaluation of the cognitive function and functional status of an individual. The assessment typically evaluates the performance in different cognitive domains (i.e. memory, perception, attention, language, visuospatial ability and executive function) and it is being used extensively in the clinical examination of patients with cognitive symptoms. On an individual level neuropsychological test results can be compared to age/education matched normative data (or z-scores from a population mean) and similarly results can be compared statistically on a group level e.g. age/education matched cognitively normal individuals compared to patient groups. Both individual and group level comparisons allow neuropsychologists to determine whether cognitive impairment is present in that person/group. The selective impairment of episodic memory is thought to be an early sign of AD, and has been associated with neurodegeneration in the medial temporal lobe, particularly the hippocampus. [130] Furthermore, the progression of the pathology in the neocortex is associated with additional impairment in other cognitive domains. [131] Overall, although

neuropsychological testing is very sensitive to the detection of cognitive deficits in relation to the cognitive background of the individual, [132] it is not highly accurate alone in the differential diagnosis of the underlying pathology. [133]

1.3 CORTICOBASAL DEGENERATION AND PROGRESSIVE SUPRANUCLEAR PALSY

Corticobasal degeneration (CBD) and progressive supranuclear palsy (PSP) are two neuropathological entities characterised by the aggregation of abnormally hyperphosphorylated tau protein; tau aggregates are localised in neurons (i.e. neurofibrillary tangles), astrocytes (i.e. tufted astrocytes for PSP and astrocytic plaques for CBD), as well as oligodendrocytes (i.e. coiled bodies). [134] In contrast to AD, in CBD and PSP 4R tau is predominantly involved, and straight tau filaments are formed. The involvement of basal ganglia is common to both PSP and CBD, while the involvement of other cortical and subcortical areas differs between the two; for example PSP commonly affects the brainstem and the dentate nucleus of the cerebellum while CBD affects several grey- and white-matter brain areas asymmetrically, with a greater load of pathology contralateral to the affected side. [60,135,136] Clinically both diseases are associated with the presence of atypical parkinsonism, executive cognitive deficits and other symptoms, including postural instability, ophthalmoparesis or progressive apraxia, depending on the regional distribution of the underlying pathology. [137-139] The clinical syndromes associated with PSP and CBD (PSP and corticobasal syndromes, respectively), however, could be difficult to distinguish, since the diseases show a substantial clinical and neuropathological overlap (Figure 6). [140-144] Moreover, these syndromes have also been associated with neuropathological evidence of AD or with the presence of tau-negative inclusions, which further complicates the reliable clinical diagnosis in those patients. [145,146]

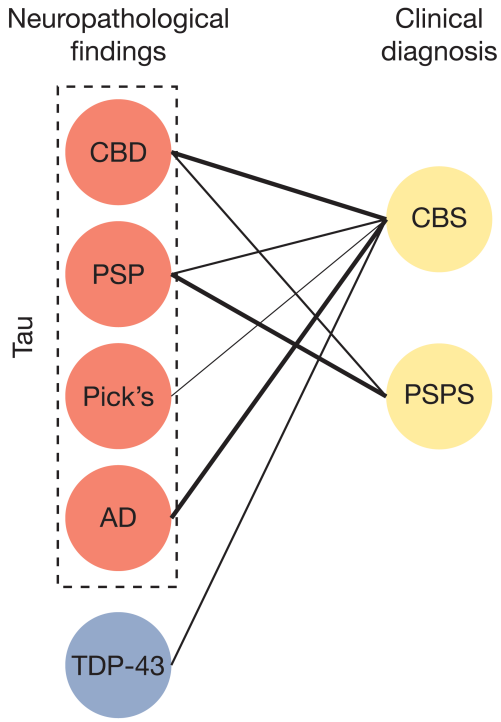

Figure 6. Atypical parkinsonian syndromes (right panel) and associated neuropathological findings (left panel). The weight of the strings in the diagram illustrates the approximate strength of the clinicopathological correlations. CBS = corticobasal syndrome; Pick's = Pick's disease; PSPS = progressive supranuclear palsy syndrome. Figure inspired by Miller, B. L. & Boeve, B. F. The behavioral neurology of dementia. 2nd edition, Cambridge University Press, (2016) and Rohrer, J. D. & Rosen, H. J. Neuroimaging in frontotemporal dementia. *International review of psychiatry* **25**, 221-229, (2013).

1.4 BIOMARKERS

> 'Biomarker: A characteristic that is objectively measured and evaluated as an indicator of normal biological processes, pathogenic processes, or pharmacologic responses to a therapeutic intervention' as defined by the Biomarkers Definitions Working Group. [147]

A number of biomarkers have recently been employed to help in the differentiation of neurodegenerative diseases and causes of dementia, aiming for early detection and staging of the pathology, and are also being used to monitor the therapeutic efficacy of disease-modifying drugs. [148] Investigation into the clinical validity of two of these, molecular imaging and CSF markers, has progressed furthest relative to other biomarkers.

1.5 MOLECULAR IMAGING

Advanced neuroimaging techniques have allowed imaging of structural and functional biological abnormalities *in vivo*. Computed tomography, magnetic resonance imaging (MRI) and positron emission tomography (PET) are only some of the developed imaging technologies; each modality presents with different advantages and limitations. While computed tomography and structural MRI were developed for imaging the structure of systems clinically, PET allows the imaging and quantification of biochemical processes *in vivo* by incorporating positron-emitting isotopes into molecular radiotracers. [149]

1.6 MAGNETIC RESONANCE IMAGING

Structural imaging of the brain with MRI offers highly sensitive detection *in vivo* of brain abnormalities such as atrophy, trauma, tumours, vascular changes (i.e. stroke, bleeding, etc.), mass lesions and other intracranial findings. MRI does not use ionising radiation but instead uses combination of magnetic fields, radio waves, and field gradients to image the anatomy of the brain with a wide range of contrasts. Several studies in the field of neurodegeneration have highlighted differences in terms of atrophy between cognitively normal individuals and patients with cognitive impairment, and have also shown that it is possible to discriminate between the different underlying causes of neurodegeneration and dementia, based on specific atrophy patterns. [150,151] More specifically, in AD atrophy changes have been typically observed in temporo-parietal areas, including the medial temporal lobe, [152] although atrophy variants have also been observed in patients with AD. [153] The extent of atrophy has been associated with *post-mortem* evidence of neuronal loss, with the underlying NFT pathology as well as with cognitive decline and is considered a very good marker of disease progression. [154-157] Visual scales of medial temporal atrophy [158] have been part of the diagnostic assessment in specialised memory units with good accuracy in discriminating between patients with dementia from cognitively normal volunteers, although it has proven less useful in differentiating between different causes of dementia. The use of automatic

procedures for measuring patterns of atrophy might lead to wider use of MRI imaging in the differential diagnosis of the different causes of cognitive impairment. [159]

Several MRI sequences have been developed in recent years to allow the imaging of different physiological processes, which widens the application of MRI in the field of neurodegeneration. These include imaging of cerebral blood flow with arterial spin labelling, imaging cerebral connectivity using diffusion weighted imaging sequences, measuring cerebral activation with functional MRI, and detecting levels of metabolites using spectroscopy sequences. [160-163] However, clinical validation of these techniques is still pending.

1.7 POSITRON EMISSION TOMOGRAPHY

The introduction of PET imaging allowed *in vivo* detection of the load and regional distribution of different molecular targets, based on the binding of specially designed tracers. The first human PET scanner was documented in 1976 at Washington University, St. Louis, USA, by Phelps, et al. [164] PET is based on the detection of a pair of 511 keV annihilation gamma-rays, which are produced after the β+ decay of a positron-emitting short-lived radioactive isotope. Radioactive isotopes are atoms with unstable nuclei that release energy when they undergo decay, in order to be transformed in a more stable state. For the purposes of PET, isotopes that will undergo positron-emitting decay shortly after production (i.e. that have a short half-life; e.g. ^{11}C, ^{18}F, ^{13}N and ^{15}O) are artificially produced in a particle accelerator called a cyclotron. These isotopes are incorporated into molecules (i.e. the molecules are labelled as tracers), which are known to target different biochemical processes, to form the radiotracer that will be injected into the patient. Following the injection, the radiotracer is distributed into specific areas in the body, based on its pharmacological characteristics, where it binds to its molecular target. When the isotope decays, the atom transforms one of its protons into a neutron and emits a positron. The positron travels a short distance before it 'meets' its anti-particle, the electron. The contact of the two will leads to their annihilation or, in other words, the transformation of their mass into energy, as detected by the production of an anti-

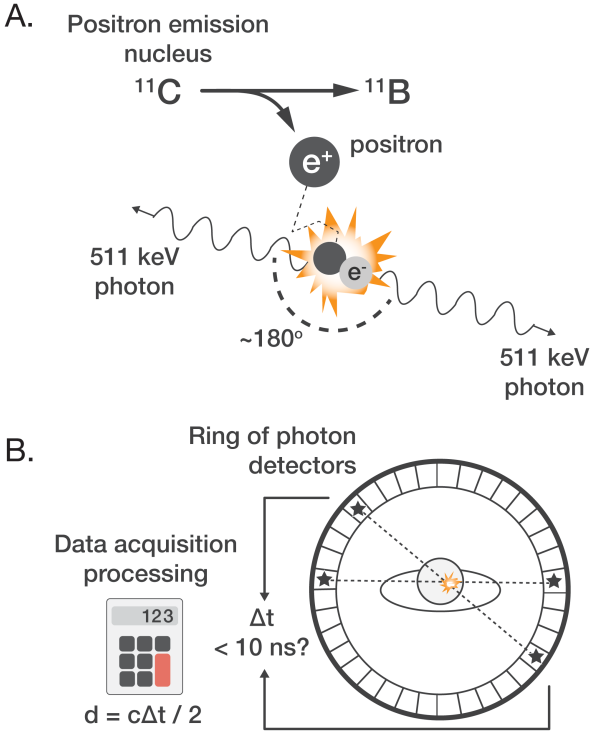

Figure 7. Illustration of the basic principles behind PET imaging. Δt = time between the arrival of each of the anti-parallel pair of photons; c = speed of light; d = distance from the detected annihilation to the midpoint of the scanner on the line connecting the coincidence events.

parallel (180°) pair of photons (gamma-rays; 511 keV each) (Figure 7A). The anti-parallel pair of photons is expected to reach detectors at each side of the ring of the PET scanner roughly at the same time ($\Delta t < 10$ ns). The scanner is able to record these coincidence events as deriving from the same annihilation. With the use of more advanced coincidence processing, the location of the annihilation can be determined on the line connecting the two activated photon detectors ($d = c\ \Delta t\ /\ 2$) (Figure 7B). The events recorded are later reconstructed as an image using computation algorithms. Detection of the pair of photons deriving from the same annihilation is the reason for the higher sensitivity of PET over other imaging modalities, even with the injection of very low concentrations of radiotracer. However, because of detector physics, PET is characterised by low resolution relatively to computed tomography or MRI, and therefore does not provide useful structural information. [165]

An ideal radiotracer should be able to penetrate the blood–brain barrier adequately without being a P-glycoprotein substrate, would have high affinity (binding affinity usually in nM range) and selectivity for the target with a low off-target signal, would have favourable pharmacokinetics for PET imaging (rapid brain uptake and wash-out), would lack radioactive metabolites able to cross the blood–brain barrier and, finally, would be safe for administration in low doses. [166] Different isotopes can be used for radiolabelling the tracers, each one with different advantages and disadvantages. Isotopes with a very short half-life (e.g. [^{11}C] with a 20 min half-life) have been very useful in the research setting, allowing multi-tracer PET imaging *in vivo* on the same day; they, however, require an on-site production. In contrast, isotopes with a longer half-life (e.g. [^{18}F] with a 109 min half-life) can be produced in a cyclotron centrally and the radiolabelled tracers can be delivered to geographically dispersed sites, thus allowing the clinical application of the radiotracer even in centres without access to highly-specialised facilities and personnel. More than 40 radiolabelled tracers targeting specific biological processes have been developed through the years for the study of brain diseases. [167]

1.7.1 Glucose consumption

2-[^{18}F]fluoro-2-deoxy-D-glucose ([^{18}F]FDG), a radiolabelled glucose analogue, is used as a PET tracer to measure metabolic glucose consumption within a targeted tissue. FDG is transported inside the cell, mediated by glucose transport proteins and is phosphorylated by hexokinase. However, unlike normal glucose, FDG cannot enter the glycolytic pathway and is trapped inside the cell, allowing the rate of trapping, and thus metabolic rates of glucose consumption to be approximated with dynamic PET imaging. Its use in neuroimaging, and dementia research, has been longstanding. A reduced [^{18}F]FDG signal is associated with neurodegenerative changes including neuronal dysfunction, changes in synaptic activity and neuronal death. [168-175] Recent evidence, however, is challenging the idea that the [^{18}F]FDG signal reflects neuronal activity exclusively, since activated astrocytes may also contribute to the observed signal. [176] However, the contribution of each cell type remains elusive.

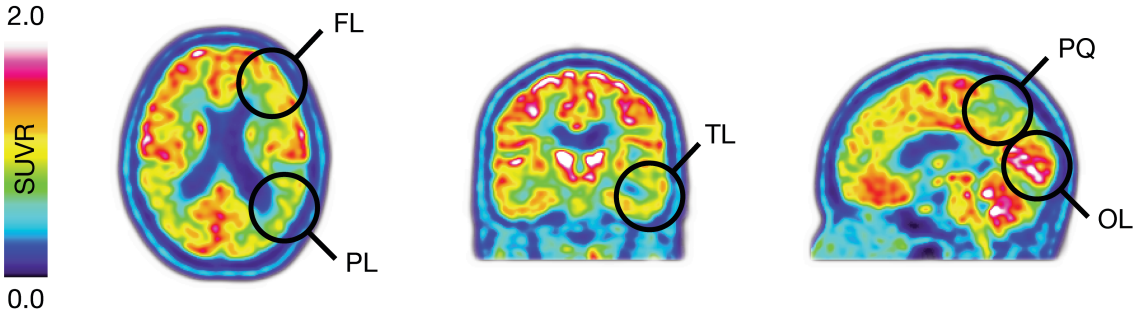

Figure 8. [^{18}F]FDG PET scan in a patient with a clinical diagnosis of probable AD, illustrating the areas typically affected in terms of glucose metabolism. The temporal (TL) and parietal (PL) lobes, including the precuneus (PQ), are primarily affected, and the frontal lobe (FL) is also (secondarily) affected. The metabolism of the occipital lobe (OL) remains relatively spared. The pons was used as the reference region for the quantification of [^{18}F]FDG uptake.

The uptake of [^{18}F]FDG is lower in patients with AD than in cognitively normal individuals, especially in the temporo-parietal association cortices, the precuneus and the posterior cingulate gyrus, also called the FDG signature regions for AD (Figure 8). [177,178] [^{18}F]FDG uptake declines over time in patients with AD, in these cortical regions; [179] the change in uptake is closely correlated to cognitive decline in the patients. [180] Moreover, the exact spatial patterns of low uptake of [^{18}F]FDG tend to reflect the different clinicopathological variants of AD, [181-183] as well as to differentiate with high specificity between AD and other causes of dementia, including the different types of frontotemporal lobar degeneration or Lewy body disease. [184] Changes in uptake of [^{18}F]FDG have been observed even earlier than the onset of dementia, in patients with MCI, [185] although the pattern of changes appears heterogeneous, probably because of the different causes of MCI. At the MCI stage, [^{18}F]FDG has moderate-to-high sensitivity and specificity for discriminating between patients who could later develop clinical AD and those who could develop other types of dementia. [150,186] The clinical validity of [^{18}F]FDG in the differential diagnosis of patients with cognitive complaints has been well established, [187] with [^{18}F]FDG PET currently being used in specialised memory units, typically as a second-line test where there is diagnostic uncertainty.

1.7.2 Fibrillar amyloid-β deposition

The identification of a fibrillar Aβ-specific tracer with favourable pharmacokinetics ([^{11}C]Pittsburgh compound B, [^{11}C]PIB) led to the first *in vivo* study in human published in 2004 (Figure 9A). [188] The PIB radiotracer was based on the structure of the fluorescent dye thioflavin T, which is widely used to detect beta-sheet structures, including Aβ fibrils and NFTs, in autopsied brain tissue or *in vitro* cultures. [^{11}C]PIB has high affinity for Aβ fibrils [189] and, injected *in vivo*, was adequately taken up and quickly washed out from the brains of the first study participants. [188] Patients with clinically probable AD have high binding of the tracer across the whole neocortex, with the medial temporal cortex relatively spared, in comparison with cognitively normal individuals (Figure 9B). Autopsy studies performed in patients who had undergone [^{11}C]PIB PET imaging *ante-mortem* have illustrated the selective

binding of [^{11}C]PIB in insoluble fibrillar Aβ deposits (predominantly dense-cored over diffuse plaques), including vascular Aβ pathology (i.e. cerebral amyloid angiopathy), and the strong correlation between *in vivo* [^{11}C]PIB binding and region-matched histopathological measures of Aβ pathology. Interestingly, in the cerebellum, a region commonly used as a reference for quantifying [^{11}C]PIB binding, diffuse Aβ plaques were not labelled with PIB. Moreover, PIB did not show evidence of binding to soluble forms of Aβ or to the NFTs. [179,190-192]

The short half-life of [^{11}C] (~20 min), however, precludes its use in centres without on-site radiochemistry facilities, as previously discussed. This led to the development of [^{18}F] Aβ PET tracers with longer half-lives (~110 min), which enabled them to be produced centrally and be transferred to geographically dispersed sites, thus enabling their widespread use for research and in the clinic. Derivatives of PIB were used for the [^{18}F] Aβ PET tracers as can be seen by their chemical structures (Figure 9A). All the [^{18}F] tracers were highly comparable

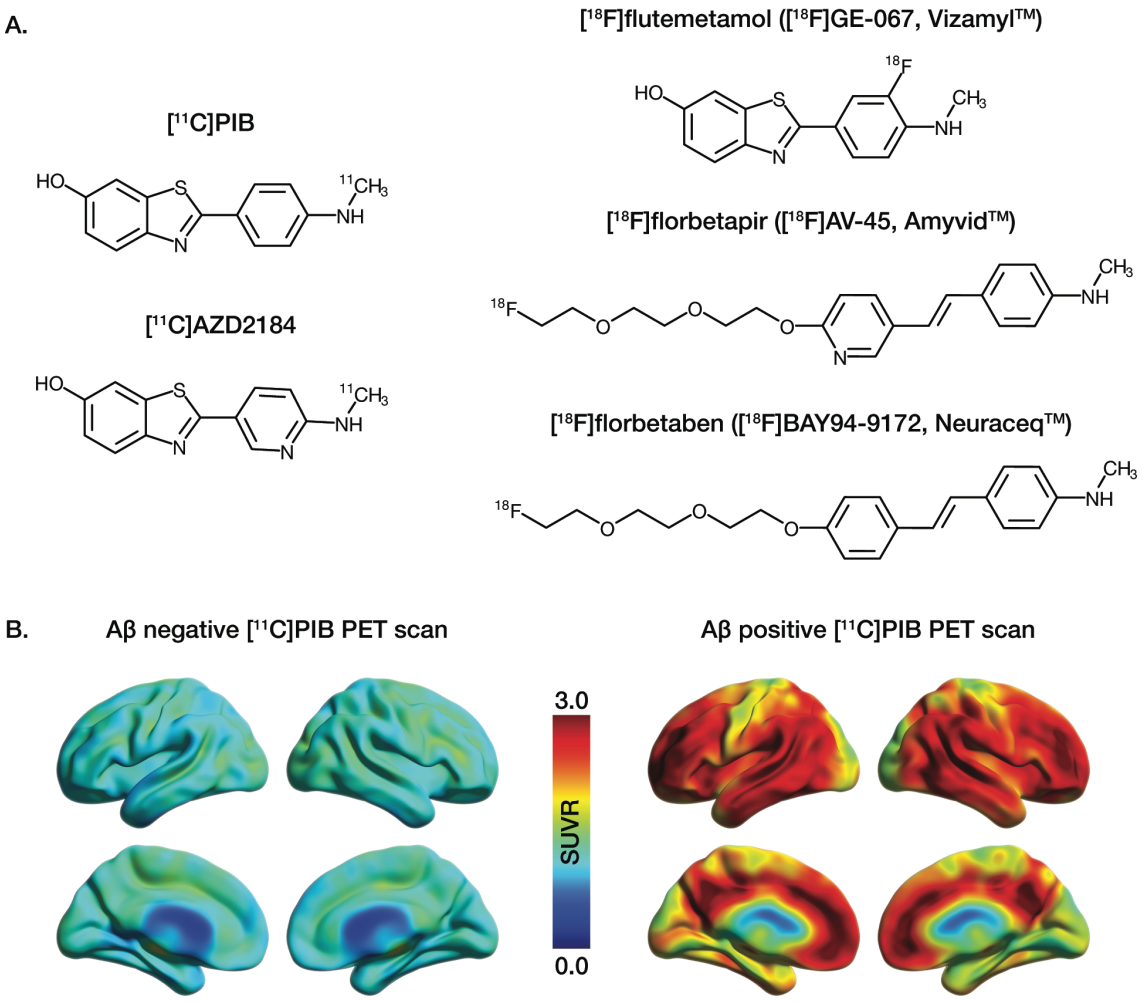

Figure 9. (A) Illustration of the chemical structures of Aβ-specific PET tracers. PIB and AZD2184 were labelled with [^{11}C] while flutemetamol, florbetapir and florbetaben were labelled with [^{18}F]. (B) Cortical projection of Aβ-positive and Aβ-negative PET scans. The scans were performed with [^{11}C]PIB in a cognitively normal individual (Aβ-negative; left panel) and a patient with a clinical diagnosis of probable AD (Aβ-positive; right panel). Cerebellar grey-matter was used as the reference region for quantifying [^{11}C]PIB binding.

with [^{11}C]PIB when examined in a head-to-head design, although they showed more extensive off-target binding. [193-195] However, the comparability of [^{11}C]PIB and the [^{18}F] Aβ tracers when investigated in separate patient cohorts remained largely unexplored.

Available *in vivo* evidence with the different tracers shows that in cognitively normal individuals the prevalence of Aβ-positivity (Aβ PET binding above the cut-off for positivity) increases in an age-related manner, [114] in agreement with previously published neuropathological studies, [51] with >30% of individuals over the age of 80 exhibiting pathological levels of fibrillar Aβ (measured by Aβ PET). [196] The presence of the ApoE4 allele is associated with up to three times higher prevalence of Aβ-positivity in cognitively normal individuals. [196] The build-up of Aβ deposition, as imaged with PET, is a slow process that is thought to start at the preclinical, presymptomatic stage of AD; it can take more than a decade before the tracer binding exceeds the threshold of Aβ pathology. The models based on longitudinal PET imaging also suggest that the pathology continues to build up for at least another decade before it reaches a plateau in patients with AD dementia. [179,197,198] Interestingly, patients with Aβ-negative MCI will not develop clinically probable AD – with a reported sensitivity of 96% – while patients with an Aβ-positive scan will be at high risk of the disease (specificity of 72%). [199-201] However, many patients with Aβ-positive MCI will not develop probable AD based on different longitudinal studies, which probably reflects the relatively short follow-up intervals as well as confirming the neuropathological evidence suggesting that a substantial number of elderly possess AD pathology but do not clinically manifest AD during their life span. [51]

The introduction of [^{18}F] Aβ PET tracers allowed the validity of Aβ PET to be evaluated easily before its clinical incorporation. Furthermore, large validation studies with the different tracers have indicated that *in vivo* Aβ PET imaging is able to accurately show Aβ pathology that was later confirmed *post-mortem* – with a sensitivity and specificity that reached or exceeded 90% – further supporting the utility of PET imaging as a biomarker of Aβ deposition in the differential diagnosis of syndromes associated with cognitive impairment. [202-206] Following the evidence from the validation studies, the US Food and Drug Agency and the European Medicines Agency recently approved three Aβ tracers ([^{18}F]florbetapir, [^{18}F]flutemetamol, [^{18}F]florbetaben) for excluding the presence of Aβ pathology in the clinical investigation of cognitive impairment. Since then, appropriate criteria for the clinical use of Aβ PET have been published, [207] although the impact of other patient characteristics (e.g. age or ApoE4 carrier status) on the utility of this biomarker remains unclear. On-going large multi-centre studies are investigating the clinical validity of Aβ PET imaging in greater detail in Europe (Amyloid imaging to prevent Alzheimer's disease; AMYPAD) and the USA (Imaging Dementia – Evidence for Amyloid Scanning; IDEAS). Both these studies, and others, aim to evaluate the performance of Aβ PET in the management of patients with cognitive impairment and the cost-effectiveness of this imaging modality in a clinical setting. [148]

1.7.3 Tau pathology

The wide spectrum of degenerative tauopathies [208] and the close relationship between tau pathology, neurodegeneration and cognitive measures in AD, as reported by autopsy studies, [65,66] raised interest in the development of PET radiotracers that would allow *in vivo* imaging of tau. The addition of tau PET to the imaging arsenal would allow more light to be shed on the pathological events that lead to neurodegeneration, the differentiation of tauopathies, and the development of new disease-modifying therapies. Everything started with the development of [^{18}F]FDDNP in 1999, a tracer that was originally designed to target Aβ pathology but that showed additional affinity for tau deposits. [209-211] However, the development of tau-specific PET tracers had been particularly challenging (Figure 10) [208,212] and it would take 10 more years before promising new tracers started to emerge. Tau is a very heterogeneous target since it exists in multiple isoforms, as discussed above, undergoes different post-translational modifications (i.e. phosphorylation, ubiquitination, truncation, etc.), [213] and forms different types of filaments and deposits depending on the underlying tauopathies (Table 1). [134,208,214,215] The localisation of tau deposits also varies, as deposits are found in neurons and glial cells, in grey and white-matter, and in areas commonly used as reference regions in PET (i.e. brainstem and cerebellum). Furthermore, tau deposits are characterised by complex dynamic changes over time with distinct maturation stages. To add to the complexity of imaging tau pathology, the deposits are predominantly intracellular, in contrast to Aβ pathology, and therefore the tracer will need to pass both the blood-brain barrier and the cell membrane to reach the target. Furthermore, the common co-localisation of tau and Aβ deposits (i.e. neuritic plaques), with relative abundance of Aβ deposits in AD, could further complicate evaluation of the specificity of a potential tau tracer. Finally, since 'normal' tau is practically invisible even with immuhistochemistry techniques, [216] the detection of 'abnormal' insoluble tau could be based on the adopted β-sheet conformations. However, caution is advised if this principle is applied to the design of a PET tracer, since the β-sheet formation is not specific to 'abnormal' tau but is the characteristic structure that is adopted by different misfolded proteins ('amyloids'), associated with neurodegeneration (e.g. TAR DNA-binding protein 43 (TDP-43), α-synuclein or Aβ), and this could limit the

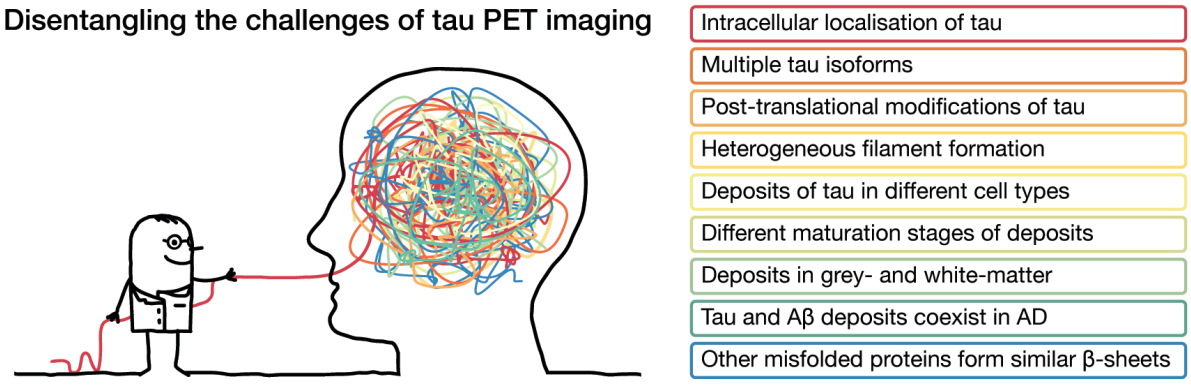

Figure 10. Illustration of the challenges related to the development of tau-specific PET tracers.

specificity of the tau tracer.

Table 1. Common tauopathies and related biochemical and neuropathological characteristics of the underlying tau pathology.

Tauopathy	Isoforms	Filaments	Histopathological findings		Location
			Neurons	Glial cells	
AD	3R ≈ 4R [a]	Paired helical >> Straight	NFTs Neuritic plaques Neuropil threads	–	Detailed staging by Braak and Braak [49], Delacourte, et al. [75]
CBD	4R > 3R	Straight >> Twisted	NFTs Neuropil threads Ballooned neurons	Astrocytic plaques Coiled bodies	Grey- and white-matter areas, striatum
PSP	4R > 3R	Straight	NFTs Neuropil threads	Tufted astrocytes Coiled bodies	Subthalamic nuclei, striatum, dentate nucleus, cortex [b]
Pick's disease	3R > 4R	Straight >> Twisted	Pick bodies Pick cells	–	Hippocampus, striatum, cortex

[a] shift to 3R predominance in the extracellular 'ghost' tangles; [b] variable involvement of the cortex

Several families of tracers have been developed during the past seven years. The most widely used tracers are [^{18}F]THK5317 and [^{18}F]THK5351, which were developed at Tohoku University, Japan, [^{18}F]AV-1451 (aka T807 or flortaucipir), which was developed by Siemens Medical Solution, USA, and sold to Avid Radiopharmaceuticals, USA (Eli Lilly & Co, USA), and [^{11}C]PBB3 which was developed by the National Institute of Radiological Sciences in Chiba, Japan (Figure 11A). The tracers showed *in vitro* high binding affinity to and specificity for tau deposits. Moreover, the binding patterns of the tracers in adjacent sections of AD brain tissue resembled the pattern of immunohistochemistry with tau-specific antibodies (e.g. AT8, PHF-1), further supporting the selectivity of the tracers for tau deposits. [217-222] There is so far scant evidence for specific targets of the different tracers on tau deposits, [223] and it would not come as a surprise if they bound to different molecular targets on tau pathology, given the heterogeneity of tau. Indeed, recent *in vitro* evidence has indicated that the different tracers may bind to different sites in the AD brain and are likely to image different aspects of 'abnormal' tau deposition in AD or other tauopathies. [224,225]

When the tracers were injected *in vivo,* they showed adequate brain uptake and rapid washout, although a radiolabelled metabolite of [^{11}C]PBB3 that was able to cross the blood-

brain barrier and complicate the quantification of tracer binding was reported. [226-228] Furthermore, the use of reference regions provided adequate accuracy in quantifying the tracer binding, although the use of short static acquisitions was reported not to be optimal since it could cause uncertainty in the binding measures. [229] The tracers are now starting to be used in continually growing groups of patients with AD and other tauopathies as well as in cohorts of cognitively normal elderly. The first studies showed preferential binding of the tracers in the temporal lobes of patients with AD with a clear discrimination between the patients and age-matched cognitively normal elderly (Figure 11B). [220,230-232] Early studies claimed that the binding of the tracers could even replicate the staging of the spreading tau pathology, [233-235] as defined by neuropathology studies, although only one case study in a patient with AD has been published to date, providing evidence of agreement between *in vivo* tracer ([^{18}F]THK5351) binding and *post-mortem* measures of tau pathology. [236] Evidence suggests a relationship between binding of the tau tracers and measures of Aβ load, neurodegeneration, and cognitive impairment, although the exact relationship between these markers remains largely unexplored (for a detailed review of the current literature please see Saint-Aubert, et al. [223]). [237-246] To date, there are no published studies investigating the longitudinal progression of tau pathology, as assessed by PET imaging, or the relationships

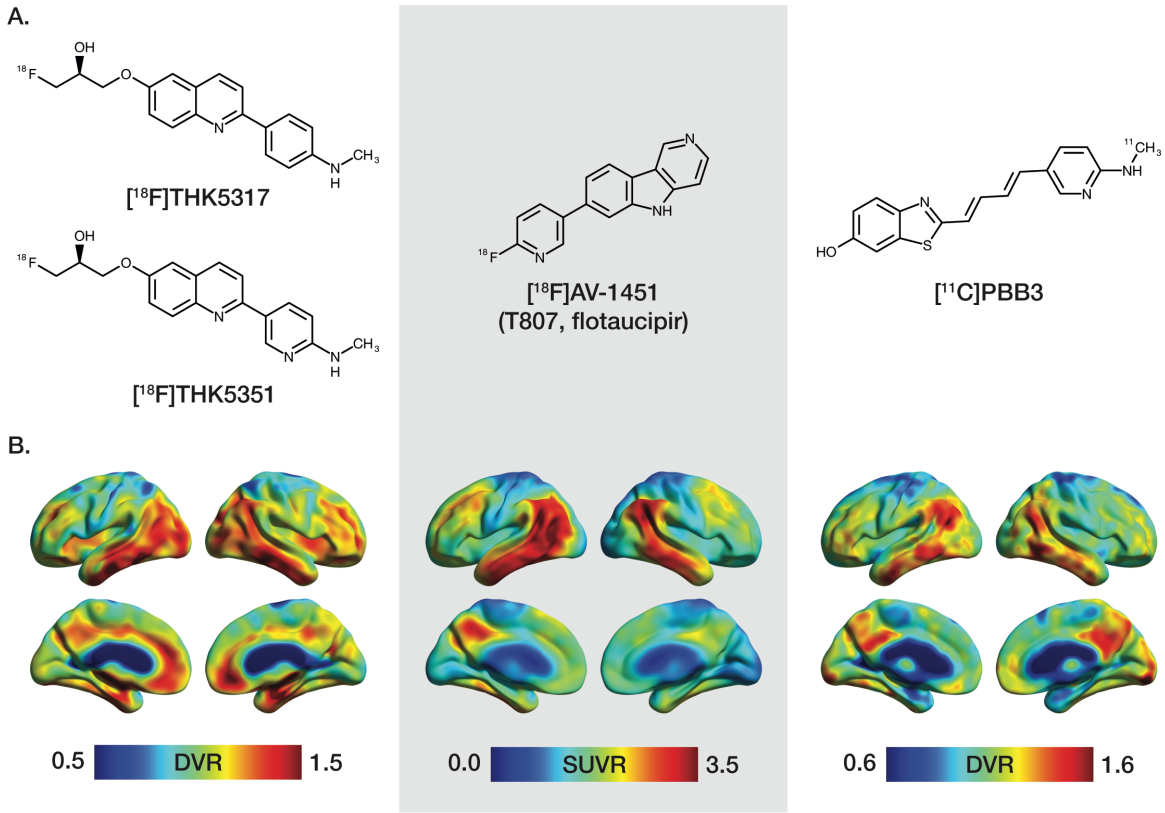

Figure 11. (A) Chemical structures of and (B) typical binding surface projections from Aβ-positive (based on their PET scans) patients with a clinical diagnosis of probable AD scanned with the most widely studied tau-specific PET tracers. Different patients were scanned with each tau PET tracer. The surface projection for the THK family of tracers was performed with [^{18}F]THK5317 PET data. The [^{18}F]AV1451 image derives from the ADNI database. Cerebellar grey-matter was used as the reference region for quantifying the binding of all tracers. The DVR was based on the Logan reference graphical and wavelet-aided parametric imaging methods for [^{18}F]THK5317 and [^{11}C]PBB3, respectively.

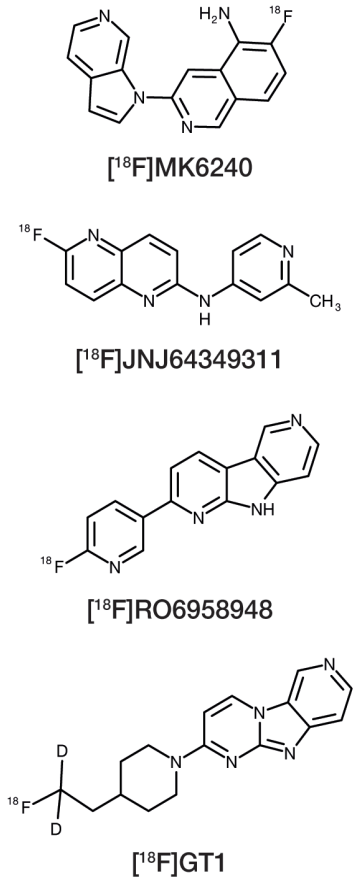

Figure 12. Chemical structures of newly developed tau-specific tracers that are considered to belong to the second generation of tracers with improved characteristics.

over time with other biomarkers of the disease, with the exception of the study included in this thesis (paper IV).

In patients with atypical parkinsonism and a clinical diagnosis associated with the presence of CBD or PSP pathologies, the tau tracers showed binding in brain areas expected from *post-mortem* studies. [220,247-252] Moreover, there was agreement between areas with high tracer binding and tau pathology in patients who underwent autopsy evaluation, further illustrating that these tracers could prove useful in non-AD tauopathies. [253-255] However, the fact that the tracers bind off-target to areas relevant for those tauopathies questions their usefulness in discrimination. Indeed, a recent study showed that there were no differences between patients with clinical PSP and cognitively normal participants. [256] Concerns about off-target binding of the tracers have been raised not only with regard to imaging non-AD tauopathies but also with regard to the general validity of the tracers. Several potential sources of off-target binding have been suggested, [236,257-261] although a thorough assessment, including direct comparisons between tracers, is pending. Newly developed tau-specific tracers are thought to have improved binding properties with lower off-target signal, although no *in vivo* data have been published so far (Figure 12).

1.8 CEREBROSPINAL FLUID MARKERS

The identification and quantification of Aβ in the CSF [262] led to the development of specific assays to measure the $A\beta_{42}$ isoform. The low levels of $A\beta_{42}$ in the CSF of AD patients are thought to reflect the deposition of $A\beta_{42}$ into plaques in the brains of these patients, and therefore its reduced clearance to the CSF. [263,264] Indeed, an inverse relationship between the neuropathological Aβ plaque load and CSF $A\beta_{42}$ measurements has been observed. [265,266] However, although part of the scientific community treats CSF $A\beta_{42}$ and Aβ PET as equivalent and interchangeable, a significant number of individuals have shown discordant profiles for the two markers of Aβ. [267-270] It cannot, therefore, be ruled out that the two biomarkers are capturing slightly different components of Aβ pathology. To add to this uncertainty, CSF $A\beta_{42}$ appears not to be a specific biomarker for AD pathology, since CSF $A\beta_{42}$ reductions have also been observed in other diseases (e.g. Creutzfeldt-Jakob disease, amyotrophic lateral sclerosis, multiple system atrophy). [271]

The development of CSF assays for measuring total and phosphorylated tau levels followed shortly after those for CSF $A\beta_{42}$. [272,273] Neuropathological studies, however, illustrated that the amount of NFTs detected *post-mortem* correlated only moderately with CSF total tau, [274] while the relationship with phosphorylated tau levels was more complex. More specifically, it appears that levels of NFTs correlate with measures of tau phosphorylated at threonine 231 [275] but not with tau phosphorylated at threonine 181, [276] the most common clinical measure of phosphorylated tau. Studies showing correlations of varying strengths between the binding of the newly developed tau-specific PET tracers and CSF tau measures have started to emerge, although doubts have been expressed that the two markers are reflecting the same component of tau pathology. [277-280]

1.9 DIAGNOSTIC ASSESSMENT OF COGNITIVE IMPAIRMENT

Most patients presenting with cognitive complaints will undergo clinical assessment at a primary care unit, according to national guidelines. [281] In Sweden, as part of the initial, routine assessment, a detailed history is taken from the patient and informant, followed by physical, including neurological, examination, evaluation of the patient's functional capacity to perform activities of daily living and evaluation of the patient's cognitive performance with brief tests (e.g. the MMSE and the clock-drawing tests, as measures of global cognitive and visuospatial, executive performance, respectively). Finally, the patient undergoes blood tests, and structural brain imaging (computed tomography or MRI), for exclusion of other causes of neurological symptoms. If there is uncertainty following the basic assessment or with cognitive complaints by relatively young patients (under the age of 65 yrs), it is advised that the patients are remitted to secondary specialised units for thorough investigation. This could include detailed cognitive assessment performed by a trained neuropsychologist, speech and language assessment by a qualified speech pathologist, electroencephalography, measurements of CSF markers or imaging with different PET tracers (i.e. [^{18}F]FDG PET or Aβ PET). The final diagnosis is often based on consensus from a committee composed of geriatricians, neurologists, clinical neuropsychologists, and specialist nurses.

1.10 REVISING THE CLASSICAL DIAGNOSTIC CRITERIA

The development of biomarkers has reconceptualised the diagnosis of AD. In recent years, two sets of different criteria for AD have been published that highlighted the use of biomarkers to identify AD accurately *in vivo*, [282-285] even before the onset of dementia, at the preclinical/presymptomatic and prodromal (i.e. MCI due to AD) stages of the disease, in contrast to the classical understanding that AD can only be diagnosed with certainty neuropathologically. Furthermore, these recent AD criteria have suggested that the available biomarkers can be categorised into two groups, based on whether they are specific to the underlying AD pathology (i.e. pathophysiological markers; Aβ PET and CSF measures for $A\beta_{42}$ and tau) or whether they can track downstream neurodegeneration indicative of the

regional spread of AD pathology (i.e. topographical markers; [^{18}F]FDG and atrophy in MRI). [282]

1.11 TIME COURSE OF THE ALZHEIMER'S DISEASE PATHOLOGY

In the past two decades, a number of researchers have sought to determine the hypothetical time courses of the underlying pathological changes in the brains of patients with AD. The first hypotheses were based on neuropathological studies and highlighted the presence of AD pathology in cognitively normal individuals, thus indicating the preclinical, silent stages of the disease. [82,83] The development of biomarkers has enabled the multi-modal and longitudinal evaluation *in vivo* of the different pathological processes in AD, and has subsequently led to revised models. These revised models incorporate measures of Aβ deposition, measures of cognitive impairment, and inflammatory and other markers of the disease. [286-288] (Figure 13) The incorporation of tau PET tracers in longitudinal, multi-modal cohorts of patients with AD may shed light on the temporal evolution of tau pathology.

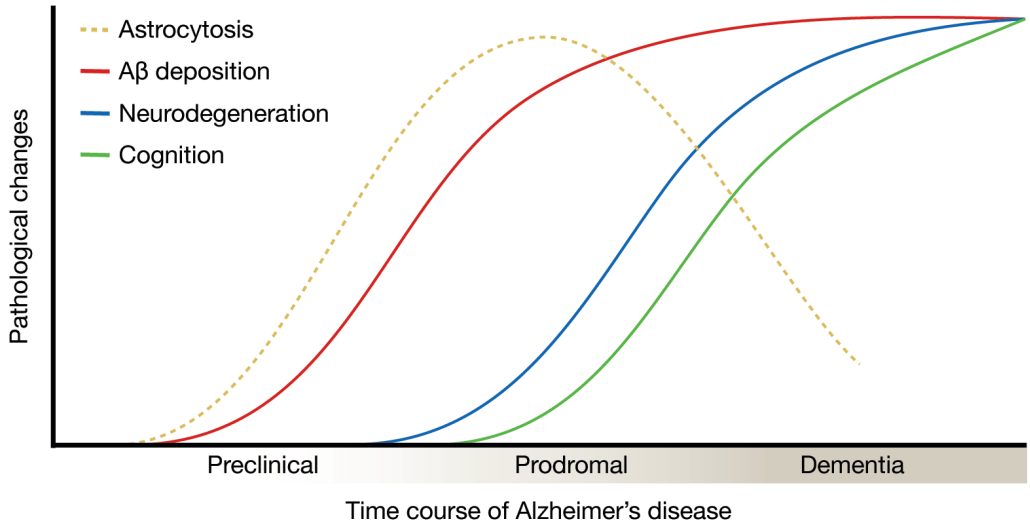

Figure 13. Tentative time course of the pathological changes during the development of AD based on Nordberg, A. Molecular imaging in Alzheimer's disease: new perspectives on biomarkers for early diagnosis and drug development. *Alzheimer's research & therapy* **3**, 34, (2011).

2 AIMS

This thesis aimed with the use of multi-modal PET imaging, to provide new insights on the pathological interplay between tau pathology, neurodegeneration and Aβ deposition, which underlie the cognitive impairment in AD. The specific aims for each paper were:

In **paper I**, to compare the binding properties of two Aβ PET tracers ([^{11}C]PIB and [^{18}F]florbetapir) in unrelated but matched patient cohorts, and to examine the effect of age on the distribution of Aβ-positive scans.

In **paper II**, to evaluate, *in vivo*, the tau-specific PET tracer [^{18}F]THK5317 and to explore the relationship between binding of this tracer and markers of Aβ deposition ([^{11}C]PIB) and glucose metabolism ([^{18}F]FDG), in a sample of cognitively normal volunteers, patients with clinical diagnosis of AD (prodromal or dementia), and individual patients with atypical parkinsonism.

In **paper III**, to investigate the regional relationship between *in vivo* tau pathology (using [^{18}F]THK5317 PET) and cognitive deficits in a cohort of patients with clinical diagnosis of AD (prodromal or dementia) and to examine the potential role of glucose metabolism ([^{18}F]FDG) as a mediator in this association.

In **paper IV**, to evaluate in a longitudinal multi-modal design the temporal spreading of tau pathology (using [^{18}F]THK5317 PET) in relation to changes in glucose metabolism ([^{18}F]FDG) and cognitive performance in patients with clinical diagnosis of AD (prodromal or dementia) and individual patients with atypical parkinsonism.

In **paper V**, to investigate *in vivo* the binding characteristics of two different tau-specific PET tracers (i.e. [^{11}C]THK5351 and [^{11}C]PBB3) when injected into the same patients with clinical diagnosis of AD (prodromal or dementia); and to explore the relationship between the tracer binding and other markers of the disease.

3 PARTICIPANTS AND METHODS

A thorough description of the participants and the methods applied in each study is presented in the respective articles/manuscripts. Specific methodological aspects are discussed in this section.

3.1 PARTICIPANTS

Different samples of patients and cognitively normal volunteers were included in the different papers. Below is a brief description of the participants in each study.

3.1.1 Paper I

The participants were derived from two multi-centre cohorts of healthy volunteers, patients with MCI and patients with probable AD. The Diagnostic Molecular Imaging (DiMI) consortium was a European-funded project that retrospectively collected, Aβ PET imaging data from five European centres; the data were analysed centrally with the aim of evaluating the utility of Aβ PET. The Alzheimer's Disease Neuroimaging Initiative (ADNI) is an on-going USA-based multi-centre study which aims to test whether serial MRI, PET (including Aβ PET), other biological markers, and clinical and neuropsychological assessment can be combined to measure the progression of MCI and early AD. The data obtained from the ADNI have been organised in an online, open-access database for the research community to use. The patients with MCI and probable AD in both cohorts fulfilled the classical diagnostic criteria. [14,27,289] We used data from 213 DiMI and 916 ADNI participants, which included a mixture of healthy volunteers, patients with MCI and patients with probable AD. For the comparison with the DiMI cohort, we used an age-, gender-, and MMSE-matched group of participants from the ADNI. For the comparison between age groups, we divided the ADNI sample into two gender- and MMSE-matched groups, based on an age threshold of 75 yrs (n = 363 in each age group).

3.1.2 Papers II-V

All patients included in papers II-V were recruited from the Memory Clinic at the Department of Geriatric Medicine, Karolinska University Hospital, Stockholm, Sweden, after thorough clinical investigation including medical history, physical examination, laboratory blood tests, ApoE genotyping, neuropsychological assessment, CSF sampling and structural imaging. For paper II, 13 patients with MCI, nine with probable AD and two with atypical parkinsonian syndromes (one with possible CBD [138] and one with probable PSP [137]) were recruited. A subgroup of the patients from paper II was included in the analyses for paper III,

with a smaller subset of the same sample completing a longitudinal follow-up for paper IV. For paper V, a new group of five patients with MCI and four with probable AD were recruited. The diagnosis was based on the consensus of a committee, which included geriatricians, neurologists, clinical neuropsychologists, and specialist nurses. Although all participants were clinically diagnosed according to the classical criteria for MCI and AD, [14,27] for the purpose of these projects the patients were reclassified based on the new research criteria for AD. [282] More specifically, patients with MCI or AD and Aβ PET or CSF ($A\beta_{42}$ and tau) evidence of AD brain pathology were classified to prodromal AD or AD dementia groups, respectively. According to this classification, for paper I, 11 patients fulfilled the criteria for prodromal AD and nine for AD dementia. For paper V, five participants were classified in the prodromal AD and four in the AD dementia groups.

Nine cognitively normal volunteers (five young and four elderly) were also recruited in paper II for validation purposes. The inclusion criteria for the cognitively normal volunteers included the absence of cognitive complaint, prior head injury, or known neurological/psychiatric disorder. They were all non-smokers and free from medication.

3.2 COMPLIANCE WITH ETHICAL AND REGULATORY STANDARDS

All participants and their caregivers provided written informed consent prior to all investigations and all procedures performed were in accordance with the ethical standards of the institutional and national research committee and with the 1964 Helsinki Declaration and its later amendments, or comparable ethical standards. All studies were approved by the Regional Ethical Review Board in Stockholm, Sweden, and the Radiation Safety committees at the Karolinska University Hospital in Stockholm and the Uppsala University Hospital in Uppsala, Sweden. The study reported in paper V was additionally approved by the Medical Products Agency in Sweden since the protocol included the intravenous injection in patients with a novel PET tracer ([^{11}C]THK5351).

3.3 NEUROPSYCHOLOGICAL ASSESSMENT

All the participants described above underwent extensive neuropsychological assessment, at their respective clinics for the multi-centre studies (DiMI and ADNI) (paper I) or at the Memory Clinic at the Department of Geriatric Medicine, Karolinska University Hospital, Stockholm, Sweden, for the studies included in papers II-V. For papers II-V, the participants underwent baseline assessment, with the participants of the only longitudinal study (paper IV) undergoing additional follow-up neuropsychological evaluation (median interval = 17 months; interquartile range = 15:18).

3.3.1 Paper I

MMSE was selected as a measure of global cognitive function over other more detailed neuropsychological tests because of the wide heterogeneity in the neuropsychological batteries used among the different centres (DiMI) or between the different cohorts (DiMI versus ADNI).

3.3.2 Paper II-V

Global cognition and episodic memory tests were selected to characterise the participants in papers II-V, and to perform regression analyses against PET imaging measures (papers III-V). For the regression analyses, the MMSE and the full-scale intelligence quotient (FSIQ), which is based on five subtests from the Wechsler adult intelligence scale (Similarities, Information, Block Design, Digit Span, and Digit Symbol), [290] were used as measures of global cognition. The FSIQ was presented either alone or in relation to the premorbid cognitive function of the individual, as assessed with the irregularly spelled words subtest from the Swedish National Adult Reading Test. [291] Encoding and delayed recall from the Rey auditory verbal learning test, and delayed recall from the Rey-Osterrieth complex figure test were used for regression analyses for episodic memory (Table 2). The results of all the neuropsychological tests were reported following a z-score transformation for comparison with a reference group of age-matched cognitively normal volunteers. [292]

Table 2. Neuropsychological tests used in this thesis for cognitively assessing the participants.

Global cognition	Episodic memory
MMSE	Rey auditory verbal learning; encoding
FSIQ	Rey auditory verbal learning; delayed recall
Decline in FSIQ from premorbid cognitive function	Rey-Osterrieth complex figure; delayed recall

3.4 MULTI-MODAL PET DESIGN

The multi-modal PET design used in all the papers described in this thesis was a powerful tool that enabled the detailed *in vivo* characterisation of different aspects of the AD pathophysiology at the same time point. This approach is based on the injection of different radiotracers on the same day or in close temporal proximity, to the same participant. Apart from the evaluation of different pathophysiological processes, this approach enables the unbiased, direct comparison of different radiotracers in the same individual on the same day, as described in paper V. Tracers with [^{11}C] labelling were preferred for 'multi-tracer' imaging

on the same day, because of the very short half-life of the isotope, which allows imaging with two, or even more radiotracers with an interval of just a few hours between injections.

3.4.1 Image acquisitions

3.4.1.1 Paper I

Aβ PET imaging data were available for all participants from the DiMI and ADNI cohorts, ([^{11}C]PIB and [^{18}F]florbetapir, respectively); [^{18}F]FDG imaging data were available only for the ADNI cohort. PET acquisitions were performed on different PET scanners with different protocols for every centre within the different cohorts. A 3D T1 MRI sequence was available for a subset of 151 participants from the DiMI cohort and all 916 ADNI participants.

3.4.1.2 Papers II-IV

All patients in papers II-IV underwent, in close temporal proximity, baseline tau, Aβ and glucose metabolism PET imaging using [^{18}F]THK5317, [^{11}C]PIB and [^{18}F]FDG, respectively. The healthy volunteers underwent only tau ([^{18}F]THK5317) PET imaging, with the exception of the elderly who underwent an additional Aβ ([^{11}C]PIB) PET scan to exclude the presence of underlying Aβ pathology. All participants underwent a 3D T1 MRI sequence at baseline. The patients involved in longitudinal investigations underwent follow-up [^{18}F]THK5317 and [^{18}F]FDG PET imaging scans after a median interval of 17 months (interquartile range = 15:18) (paper IV). All [^{18}F]THK5317 and [^{11}C]PIB PET acquisitions were dynamic (0-60 min) and performed on an ECAT EXACT HR+ scanner (Siemens/CTI) or a Discovery ST PET/CT scanner (GE) at the Uppsala PET centre, Uppsala, Sweden. The [^{18}F]FDG PET acquisitions were static (30-45 min) and were performed on a Biograph mCT PET/CT scanner (Siemens) at the Department of Nuclear Medicine, Karolinska University Hospital Huddinge, Stockholm, Sweden.

3.4.1.3 Paper V

All patients in paper V underwent imaging with the tau-specific PET tracers [^{11}C]THK5351 and [^{11}C]PBB3 on the same day, as well as with the Aβ PET tracer [^{11}C]AZD2184 within a week. All PET acquisitions were dynamic (0-90 min for [^{11}C]THK5351 and 0-60 min for [^{11}C]PBB3 and [^{11}C]AZD2184) and were performed on a high-resolution research tomograph (HRRT, Siemens/CTI) at the Centre for Psychiatry Research, Karolinska Institutet, Stockholm, Sweden. A 3D T1 MRI sequence was also acquired for all patients, within three months from the PET investigations.

3.4.2 Test-retest evaluation

As part of the investigations for paper II, five patients (four with prodromal AD and one with possible CBD) underwent a second PET scan with [^{18}F]THK5317 within one month of the first investigation. This aimed to evaluate, for the first time, the test-retest variability of the tracer.

3.4.3 Image pre-processing

3.4.3.1 Paper I

The [^{11}C]PIB and [^{18}F]florbetapir imaging data were non-linearly spatially normalised to population-specific PET templates in the Montreal Neurological Institute (MNI) space for both tracers (SPM5), where the tracer binding was quantified. The [^{18}F]florbetapir template was based on the procedure previously applied to the [^{11}C]PIB data. [201,293] Briefly, 207 [^{18}F]florbetapir images were co-registered to their respective T1 MRI sequences, and were later normalised to MNI space using the non-linear transformation matrix from the individual T1 MRI sequence segmentations. An average [^{18}F]florbetapir image was subsequently created and used as a template for the spatial normalisation of all [^{18}F]florbetapir imaging data to MNI space.

3.4.3.2 Papers II-IV

The individual [^{18}F]THK5317, [^{11}C]PIB and [^{18}F]FDG imaging data were co-registered to the individual native T1 MRI sequences (SPM8), where the binding/uptake of the tracers was quantified.

3.4.3.3 Paper V

A different approach was selected for preserving the high-resolution of the PET imaging data in paper V. The T1 MRI sequences of the individual patients were co-registered to the individual [^{11}C]THK5351, [^{11}C]PBB3 and [^{11}C]AZD2184 imaging space (SPM12). The tracer binding was quantified in the native PET space, which was different for each imaging modality.

3.4.4 Quantification of tracer binding

For the regional quantification of the tracer binding/uptake, we employed regions of interest (ROIs) from different brain atlases for each paper, based on the research question and hypothesis. [294-299] For all studies, in addition to the individual ROIs employed, a composite

isocortical ROI was created to quantify the Aβ PET data, calculate the cut-offs for Aβ positivity, and classify the participants in the 'Aβ-positive' and 'Aβ-negative' groups.

3.4.4.1 Paper I

A simplified atlas was used in paper I because of the widespread binding of the Aβ tracers in the whole isocortex. Grey-matter ROIs, based on the available MRIs from the DiMI cohort, [201] were created because of the lack of T1 MRI sequences for all of the DiMI cohort, and were later applied to the Aβ PET scans of all study participants (DiMI and ADNI).

For [^{11}C]PIB and [^{18}F]florbetapir, standardised uptake value ratio (SUVR) images were created (over the time intervals 40-60 min and 50-70 min, respectively), and used to quantify the tracer binding. A cerebellar grey-matter ROI was used as reference for the [^{11}C]PIB images and a whole cerebellar ROI was used for the [^{18}F]florbetapir images.

3.4.4.2 Papers II-V

Grey-matter was parcellated from T1 MRI sequences using SPM (SPM8, SPM12). Grey-matter binary masks were created from this parcellation, and these were later applied to anatomical atlases for the creation of individual grey-matter ROIs. In papers II-III, in which [^{18}F]THK5317 binding was evaluated for the first time *in vivo*, grey-matter ROIs covering the whole brain were applied to all PET tracers. In contrast, for papers IV-V, we selected grey-matter ROIs predominantly in the temporal cortex, in agreement with the findings of papers II-III and the known regional distribution of tau pathology, as described by autopsy studies. [49,75]

A voxel-wise, reference region-based approach was adopted for the kinetic modelling of the dynamic [^{18}F]THK5317 PET imaging data. The Logan graphical method, with reference to the cerebellar grey-matter ROI, was applied to the dynamic data over the time interval 30-60 min to create the distribution volume ratio (DVR) images, a method that has been validated against arterial sampling-based quantification of the tracer binding. [227,300] Summation images (40-60 min) were used for [^{11}C]PIB and static images (30-45 min) were used for [^{18}F]FDG to create SUVR images, with reference to the cerebellar grey-matter and pons, respectively. The resulting [^{18}F]THK5317 DVR and [^{11}C]PIB and [^{18}F]FDG SUVR images were sampled with the grey-matter ROIs.

The quantification of the [^{11}C]THK5351, [^{11}C]PBB3 and [^{11}C]AZD2184 dynamic PET imaging binding data was modelled using the wavelet-aided parametric imaging method, [301] which allows the creation of high-resolution, noise-robust, non-displaceable binding potential (BP_{ND}) images. The cerebellar grey-matter ROI was used as reference for the creation of the BP_{ND} images, which were subsequently sampled with the grey-matter ROIs. The wavelet-

aided parametric imaging method was first compared to other kinetic models for validation purposes. [226,227,300,302]

3.4.5 Partial volume effect correction

PET is characterised by low spatial resolution and the concentration of a radiotracer might therefore be over- or under-estimated in a given ROI due to potential 'spill-over' of the signal from neighbouring ROIs (aka partial volume effect). Different areas of the brain are differentially affected by the partial volume effect; ROIs neighbouring other ROIs that have a different target availability or ROIs with significant atrophy are liable to experience greater spill-over of the signal. Correction methods can be applied based on detailed structural information from the T1 MRI sequence. Specifically, these methods could theoretically compensate for the spill-over of the signal by assuming that different tissue classes in the brain (e.g. grey- and white-matter) [303] or even individual ROIs, [304] have a homogeneous signal. Two T1 MRI-based partial volume effect correction methods were applied to the PET data for the purposes of this thesis (papers II, III, V).

3.5 CORTICAL THICKNESS MEASURES

The thickness of the entorhinal cortex was measured for study V, in the T1 MRI sequence, with FreeSurfer image processing software (version 6.0, http://surfer.nmr.mgh.harvard.edu). The selection of the entorhinal cortex as a measure of medial temporal atrophy was based on previous evidence of a correlation between the binding of another tau-specific PET tracer ([^{18}F]AV-1451) with underlying atrophy in the same region. [305]

3.6 CEREBROSPINAL FLUID BIOMARKERS

As part of the routine clinical assessment, CSF samples from the patients were analysed at the Clinical Neurochemistry Laboratory, Gothenburg University, Mölndal, Sweden. The local reference values of <550 pg/mL for $A\beta_{42}$, >400 pg/mL for total tau, and >80 pg/mL for tau phosphorylated at threonine 181 were used to evaluate the presence of AD pathology in the patients.

3.7 STATISTICAL ANALYSES

Diverse statistical analyses (descriptive and inferential) were used in the respective papers based on the research question and hypothesis. Detailed descriptions of the different approaches used are reported in the respective papers. The approaches to correction for

multiple comparisons are also discussed in the individual papers. For the imaging data, analyses were performed in a ROI- and voxel-based manner, as discussed below.

3.7.1 Region of interest-based analyses

The selection of parametric or non-parametric approaches for group comparisons (analysis of variance or the non-parametric Kruskal-Wallis analogue for analysis of variance) and correlation analyses (Pearson or Spearman rank correlation coefficients) was based on the sample sizes and the probability distributions of the selected variables. To investigate the relationship between imaging modalities or between an imaging modality and other markers of the disease, linear models were constructed for cross-sectional and linear mixed effects models for longitudinal data. Mediation analyses were employed to explore the mediation effect of a variable in the relationship between a causal variable and an outcome variable. Individual annual rates of change in the tracer binding/uptake were calculated, based on the longitudinal data. The expectation-maximisation algorithm for Gaussian mixture models was employed for clustering groups of individuals based on the probability distribution of specific variables. The receiver operating characteristic analysis was used for defining the accuracy of Aβ and tau PET imaging in discriminating between cognitively normal volunteers and patients with AD, and for selecting optimal cut-off points. For each paper, the ROI-based analyses were performed using different versions of the SPSS (Armonk, New York, USA), XLSTAT (Addinsoft, New York, USA) or R software (R Foundation for Statistical Computing, Vienna, Austria, http://www.R-project.org/).

3.7.2 Voxel-based analyses

Group comparisons of the tracer binding were performed using standard non-parametric procedures based on permutation testing (SnPM13), because of the limited sizes of the individual groups. Paired t-tests were employed for investigating changes in the tracer binding/uptake over time (SPM8). Correlation analyses were carried out between the local binding/uptake results for the different tracers (BPM 3.1). Additional procedures included the creation of individual z-score maps for expressing the tracer binding/uptake for an individual in relation to a group of cognitively normal volunteers. The same maps were also assessed longitudinally for exploring the spread of the tracer binding/uptake in individual patients. Maps of the individual annual rates of change were made for the tracer binding/uptake based on the longitudinal data. All voxel-based analyses were performed in MATLAB 2012b (The MathWorks, Inc., Natick, Massachusetts, USA).

4 RESULTS AND REFLECTIONS

More detailed presentation and discussion of the results of each study is included in the respective articles/manuscripts. The main findings as well as some methodological considerations are described briefly below.

4.1 MAIN FINDINGS

4.1.1 Paper I – Amyloid-β PET imaging

4.1.1.1 Comparability of [^{11}C]PIB and [^{18}F]florbetapir PET imaging

The different Aβ PET tracers have shown similar binding properties when injected into the same participants, [193-195] although their comparability across different groups was uncertain. In our study, it was observed that the binding of [^{11}C]PIB and [^{18}F]florbetapir, when the tracers were injected into different individuals from different cohorts (DiMI and ADNI, respectively), showed high regional agreement as well as significant correlation across ROIs in the different diagnostic groups, which illustrates the similarities between the tracers (Figure 14). [^{11}C]PIB showed a higher discriminative ability between cognitively normal volunteers and patients with AD than [^{18}F]florbetapir (area under the curve = 0.931 vs 0.864,

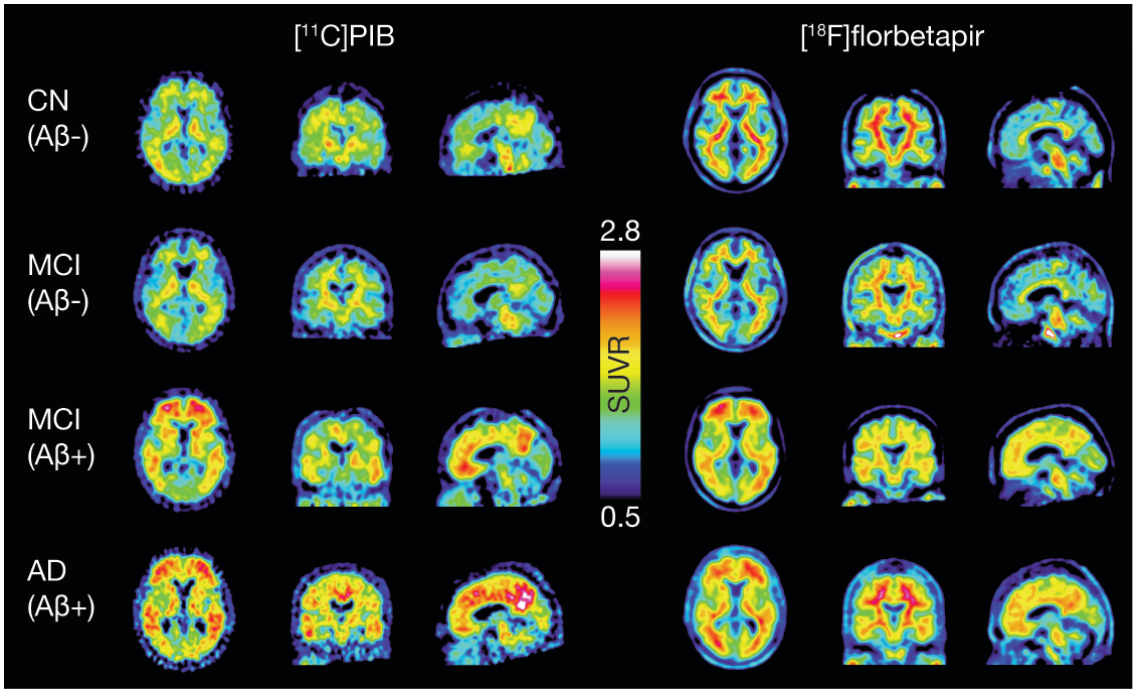

Figure 14. [^{11}C]PIB and [^{18}F]florbetapir SUVR images from age-, gender- and MMSE-matched cognitively normal volunteers (CN), patients with MCI (Aβ-negative and -positive) and patients with probable AD. The figure is adapted from Chiotis, K. *et al.* Amyloid PET in European and North American cohorts; and exploring age as a limit to clinical use of amyloid imaging. *European journal of nuclear medicine and molecular imaging* **42**, 1492-1506, (2015).

respectively), a finding that had previously been reported elsewhere, [195] although it was not investigated in detail. The wider dynamic range of SUVR values and lower off-target binding in white-matter that is observed for [^{11}C]PIB relatively to its [^{18}F] derivatives probably contributes to its higher discriminative ability, although it remains unclear if those differences could affect the clinical performance of the [^{18}F] Aβ tracers. The differences in discriminative ability between the tracers could alternatively be explained by other differences between the cohorts. Although we used matched groups of individuals, we cannot exclude that other covariates differed. For example, there was a difference in educational attainment between cohorts. The participants in the ADNI cohort were, on average, university graduates, whereas the average educational attainment of the participants in the DiMI cohort was equivalent to high-school graduates. The evidence from the literature suggests differences in the distribution of Aβ-positive PET scans depending on the educational attainment of the individuals, which could explain the differences in discriminative ability, although this phenomenon is not completely understood, especially among patients with AD. [196,306-311]

4.1.1.2 Effect of age on the distribution of amyloid-β-positive scans

The rapid development of Aβ PET imaging led to its approval by the regulatory agencies for clinical use in excluding AD pathology in individuals with cognitive impairment. However, several questions related to the clinical application of Aβ imaging remain unanswered, including the selection of patients (using demographic or clinical information) that would benefit the most by the incorporation of this expensive imaging technique in their clinical assessment. So far, appropriate use criteria based on the prevalence of different dementia syndromes have suggested that Aβ imaging should be used in patients younger than 65 years. [207] However, little is known on the potential effect of age on the clinical utility of Aβ imaging in patients with AD, especially across the wide range of ages affected by this disease. In the ADNI participants, we found that Aβ imaging performed better when discriminating between cognitively normal volunteers and patients with a clinical diagnosis of AD, who were younger (55-75yrs), rather than older (76-93 yrs) (sensitivity = 81 vs 72% and specificity = 70-80%, respectively). While we would expect a drop in specificity due to the age-related accumulation of Aβ in the population, [51] the drop in sensitivity probably reflected the substantial number of clinically diagnosed patients with AD in the older subgroup who actually did not carry Aβ pathology. A closer look at the distribution of Aβ PET measures sheds some light on the uncertain clinical diagnosis of the elderly patients. Specifically, the distribution was bimodal in the elderly patients, with a substantial number of individuals clearly Aβ-negative (n=15, 22%) (Figure 15). Furthermore, the same patients were less likely to be ApoE4 carriers (one out of 15) and, in general, had a pattern of [^{18}F]FDG uptake not suggestive of the presence of AD neurodegeneration. Neuropathology studies have pointed in the same direction, and our results were verified by a recent meta-analysis of Aβ PET imaging data; the prevalence of Aβ positivity decreases with increasing age in patients with a clinical diagnosis of AD, which indicates an increased clinical misdiagnosis of AD in the

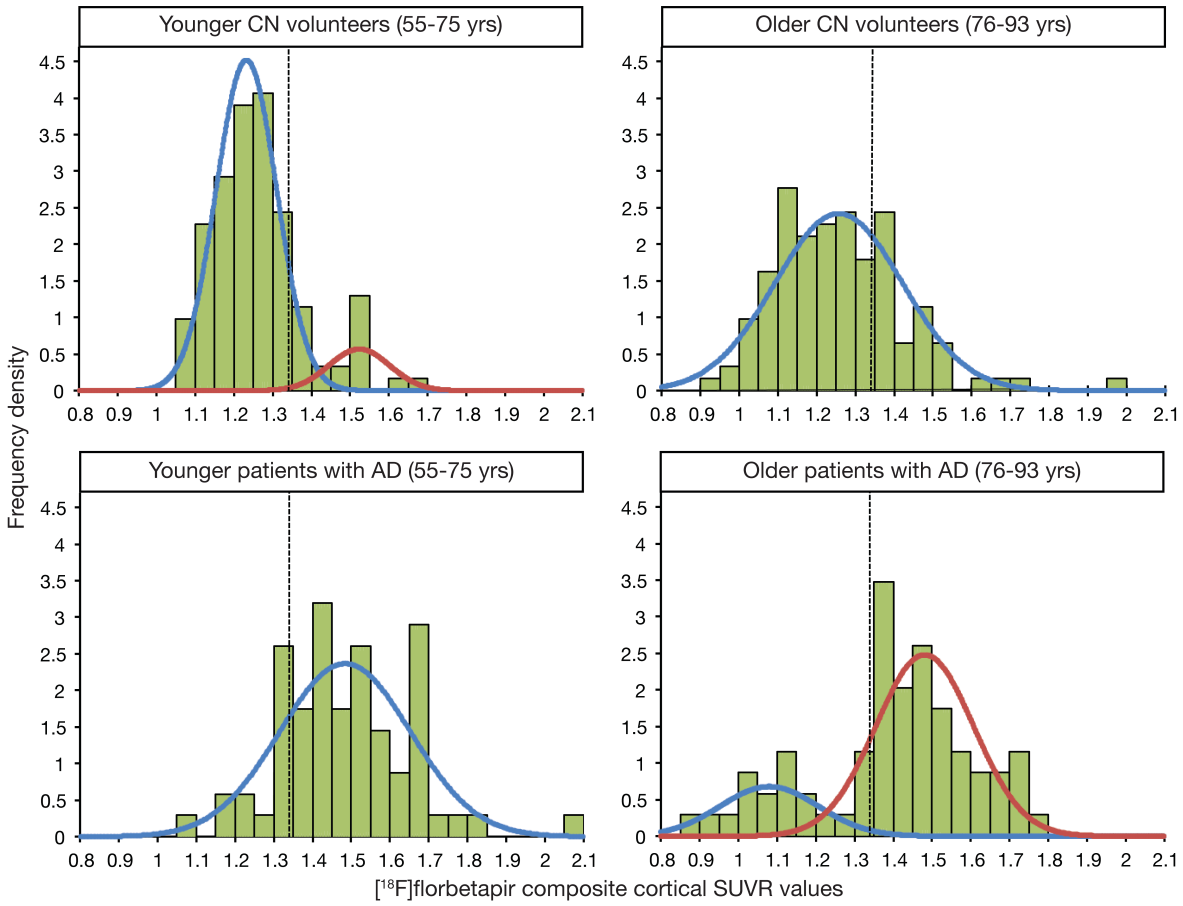

Figure 15. Frequency density plots of the [^{18}F]florbetapir composite cortical SUVR values in the two age groups of cognitively normal volunteers (CN) and patients with probable AD. The dashed line represents the cut-off for Aβ positivity with [^{18}F]florbetapir. The figure is adapted from Chiotis, K. *et al.* Amyloid PET in European and North American cohorts; and exploring age as a limit to clinical use of amyloid imaging. *European journal of nuclear medicine and molecular imaging* **42**, 1492-1506, (2015).

oldest-old in the absence of a reliable pathology marker. [311] Despite its exploratory nature, this study offers some insight into the increasing importance of Aβ PET imaging with increasing age in the diagnostic assessment of individuals with cognitive impairment. The on-going large, multi-centre studies (AMYPAD, IDEAS) that intend to evaluate the clinical performance of Aβ PET imaging offer a unique opportunity for enhancing our understanding of different clinical measures that could define subgroups of patients, where the use of such a biomarker would be more advantageous.

4.1.2 Papers II-V – Tau PET imaging in a multi-modal design

4.1.2.1 Binding of the tau tracer [^{18}F]THK5317 in patients with AD

The first *in vivo* evaluation of the tau-specific PET tracer [^{18}F]THK5317 in patients with AD (prodromal or dementia) detected high binding of the tracer predominantly in inferior and lateral temporal ROIs, regions that have been consistently associated with the presence of tau pathology in neuropathological studies of AD (Figure 16). [49,75] In contrast, the cognitively

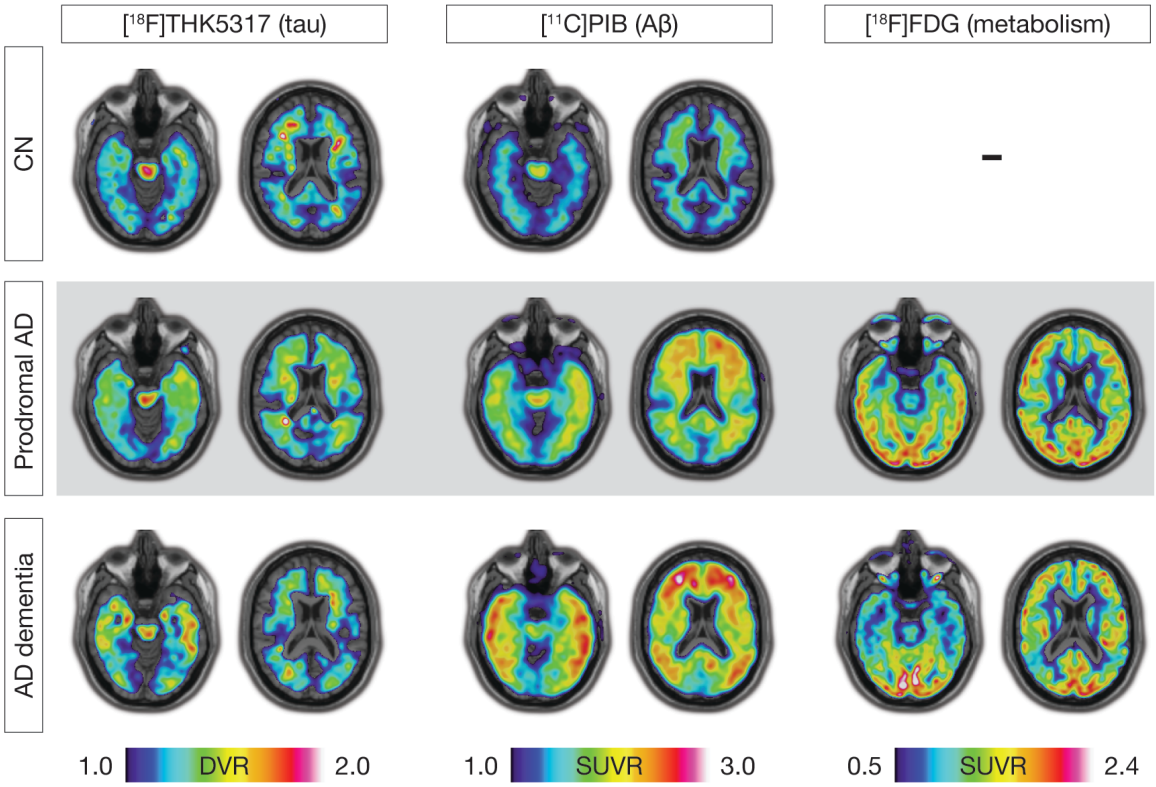

Figure 16. Sample [^{18}F]THK5317 DVR, [^{11}C]PIB SUVR and [^{18}F]FDG SUVR images from an elderly cognitively normal (CN) volunteer, a patient with prodromal AD and a patient with AD dementia. Cerebellar grey-matter was used as a reference region for [^{18}F]THK5317 and [^{11}C]PIB, and the pons was used for [^{18}F]FDG.

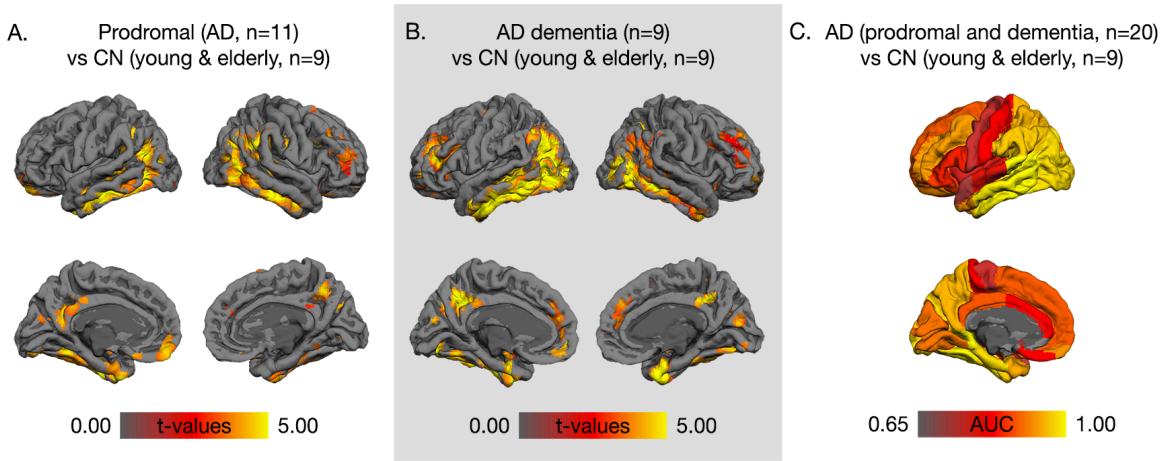

Figure 17. (A, B) Voxel-based group comparisons of [^{18}F]THK5317 binding between cognitively normal volunteers and patients with prodromal AD or AD dementia; the voxel-based comparisons were performed in SnPM13 and the results are presented after correction for multiple comparisons with the false discovery rate method ($p<0.05$). (C) ROI-based receiver operating characteristic analysis between all cognitively normal volunteers and all patients with AD (prodromal and dementia). The area under the curve (AUC) for every cortical ROI was reported. The figure is adapted from Chiotis, K. *et al.* Imaging in-vivo tau pathology in Alzheimer's disease with THK5317 PET in a multimodal paradigm. *European journal of nuclear medicine and molecular imaging* **43**, 1686-1699, (2016).

normal volunteers showed overall low binding of the tracer, with areas of high binding limited to the basal ganglia. Statistically significant differences were observed between patients with AD and cognitively normal volunteers predominantly in the temporal lobe as well as in other isocortical ROIs (Figure 17A, B). Furthermore, the ordering of ROIs with regard to discrimination between groups strongly resembled the suggested temporal evolution of tau pathology across the AD brain (Figure 17C), [75] in agreement with another study that used the same methodology but a different tau tracer (i.e. [^{18}F]AV-1451). [233] The findings of this study, together with *in vitro* evidence highlighting the specificity of this tracer for tau deposits, [218] suggest that [^{18}F]THK5317 could image the expected load and regional pattern of tau pathology *in vivo* in a cohort of cognitively normal volunteers and patients with AD. Similar findings have been reported in different cohorts, where different tau-specific PET tracers were used. [220,312]

The binding pattern of [^{18}F]THK5317 in patients with AD differed from that of the Aβ PET tracer [^{11}C]PIB (Figure 16), which further illustrates the differences between the targets of the two tracers. However, there were regional correlations between the two markers (Figure 18A), which may reflect the co-localisation of Aβ and tau deposits during the time course of AD, probably in the neuritic plaques. Similar findings have been reported for the tau PET tracer [^{18}F]AV1451. [243] Significant correlations between [^{18}F]THK5317 and neurodegeneration, as measured by glucose hypometabolism ([^{18}F]FDG), were regionally localised in areas vulnerable to neurodegeneration in the fronto-parieto-temporal lobes, including the precuneus, highlighting the close link between tau pathology and neurodegenerative changes (Figure 18B). [65-68] However, in contrast to other studies published with another tracer, the relationship between the tracer binding and the neurodegenerative changes was rather focal and did not occur across large cortical areas, [237,240,242] which could

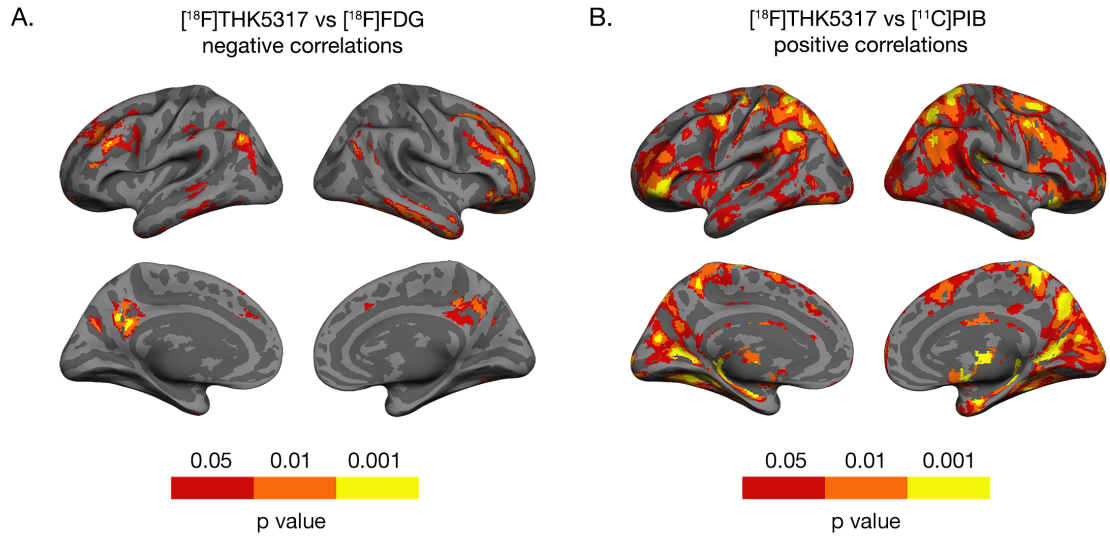

Figure 18. Voxel-based correlations between (A) [^{18}F]THK5317 (tau) and [^{11}C]PIB (Aβ) binding and (B) [^{18}F]THK5317 (tau) binding and [^{18}F]FDG (glucose metabolism) uptake. The correlation analyses were performed in BPM 3.1. No correction for multiple comparisons was applied. The figure is adapted from Chiotis, K. *et al.* Imaging in-vivo tau pathology in Alzheimer's disease with THK5317 PET in a multimodal paradigm. *European journal of nuclear medicine and molecular imaging* **43**, 1686-1699, (2016).

be attributed to our mildly impaired sample, where only a subset of patients had severe hypometabolic changes.

4.1.2.2 Relationship of tau pathology ([^{18}F]THK5317) with cognitive deficits

Binding of [^{18}F]THK5317 in patients with AD related negatively to measures of global cognition (MMSE, FSIQ) and episodic memory (encoding from the Rey auditory verbal learning and delayed recall from the Rey-Osterrieth complex figure tests) (Figure 19). The correlations, especially that with episodic memory, were predominantly observed in the temporal lobe, where the patients showed increased binding in comparison to a group of cognitively normal volunteers. Widespread hypometabolism ([^{18}F]FDG) in fronto-parieto-temporal areas related positively with measures of global cognition, while the relationship with episodic memory was somewhat more restricted spatially in comparison to

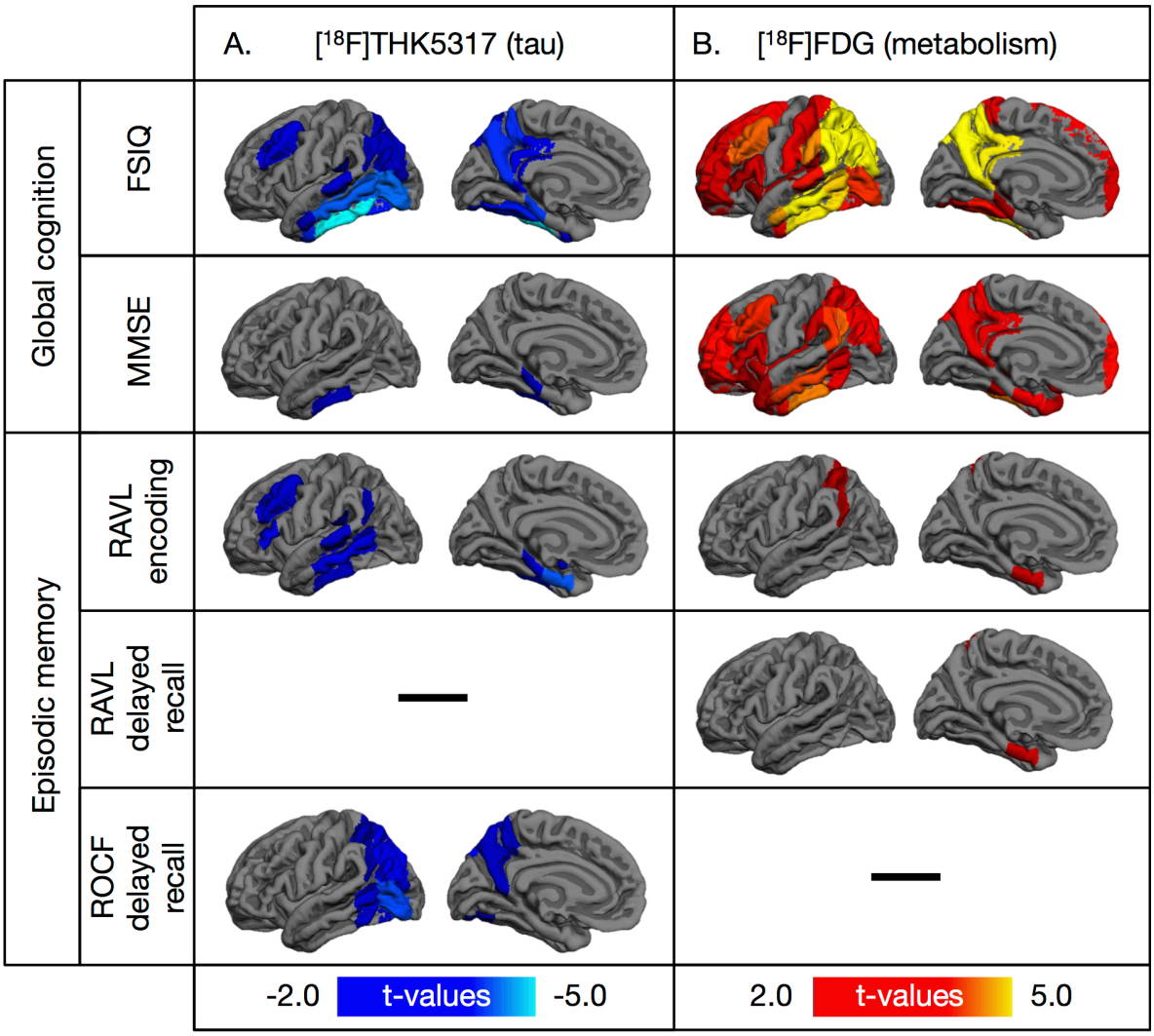

Figure 19. Surface projections describing the relationship of ROI-based tracer binding/uptake ([^{18}F]THK5317 and [^{18}F]FDG) with global cognitive and episodic memory performance in patients with AD. Linear models were employed for investigating relationships with t-values reported for significant associations ($p<0.05$). No correction for multiple comparisons was made. RAVL = Rey auditory verbal learning; ROCF = Rey-Osterrieth complex figure. The figure is adapted from Saint-Aubert, L. *et al.* Regional tau deposition measured by [^{18}F]THK5317 positron emission tomography is associated to cognition via glucose metabolism in Alzheimer's disease. *Alzheimer's research & therapy* **8**, 38, (2016)

[^{18}F]THK5317. From our evidence, tau pathology, relatively to glucose metabolism, seems to be more selective for episodic memory changes, while the opposite pattern was observed for global cognition. Similar correlations have been observed between the binding of other tau tracers and cognition in different patient samples. [231,234,237,313]

Based on current understanding, tau deposition could lead to neuronal dysfunction, neuronal death and finally cognitive deficits. [55,69-71] In order to test this hypothesis *in vivo*, we used mediation analyses to investigate possible causal relationships between tau deposition ([^{18}F]THK5317), glucose metabolism ([^{18}F]FDG) and cognition. Briefly, the prerequisite for those analyses was the presence of a statistically significant relationship of the mediator variable (glucose metabolism) with the other two variables (tau deposition and cognition). This condition was met for [^{18}F]THK5317 and [^{18}F]FDG binding/uptake in the ROIs of the temporal lobe and measures of global cognition. A mediating role of [^{18}F]FDG uptake was detected in the association of local [^{18}F]THK5317 binding with global cognitive measures. Thus, our cross-sectional data support the current hypothesis, according to which increased tau deposition leads to cognitive decline by causing local neuronal dysfunction (hypometabolism). Our findings are in line with those from another study, which incorporated CSF measures instead of PET imaging to trace tau pathology, [314] although the strength of our current work is the regional mapping of the pathological changes in the AD brain. A study published recently by Bejanin, et al. [315] further validates our observations by applying similar models with another tau tracer ([^{18}F]AV-1451).

4.1.2.3 Propagation of tau pathology ([^{18}F]THK5317) in a longitudinal design

Based on neuropathological evidence, it has been suggested that the regional spreading of tau pathology follows the clinical progression of AD in patients; [51,77,78] however, no longitudinal tau PET imaging study had been published, which validated these cross-sectional, *post-mortem* observations. In our study, we used a longitudinal design to investigate the temporal evolution (interval = 17 months) of tau pathology *in vivo* using PET ([^{18}F]THK5317) in relation to changes in glucose metabolism ([^{18}F]FDG) and cognitive performance in a group of patients with AD (prodromal or dementia). At a group level, no statistically significant increases in [^{18}F]THK5317 binding were observed over time (except for a restricted unilateral area in the left inferior temporal gyrus), while [^{18}F]FDG uptake declined significantly in widespread temporo-parietal areas (Figures 20, 21). In temporal ROIs, a statistically significant negative correlation was observed between baseline [^{18}F]THK5317 binding and annual rates of change of [^{18}F]THK5317 binding, which illustrates that the rate of tau deposition could even decelerate over time in ROIs with high tau burden at baseline. At an individual level, a heterogeneous pattern of increases in [^{18}F]THK5317 binding was observed, with differences observed between patients at different clinical stages of AD (prodromal or dementia). Binding was increased in more restricted isocortical areas in patients with prodromal AD in comparison to patients with AD dementia. This illustrates that, although no statistically significant differences were detected at a group level, there were

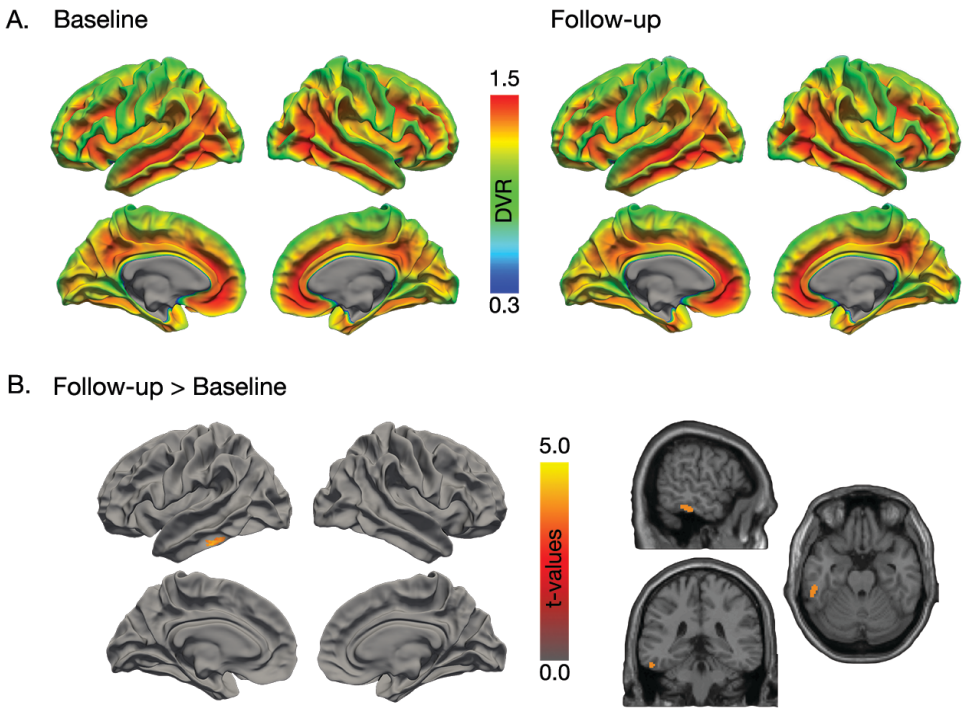

Figure 20. (A) Average baseline and follow-up DVR images from patients with AD (prodromal or dementia; n=16) with [^{18}F]THK5317, and (B) voxel-based paired t-tests (SPM8) evaluating the changes in binding over time (interval = 17 months). No correction for multiple comparisons was made (uncorrected p<0.001). The figure is adapted from Chiotis, K. *et al.* Longitudinal changes of tau PET imaging in relation to hypometabolism in prodromal and Alzheimer's disease dementia. *Molecular psychiatry*, (2017).

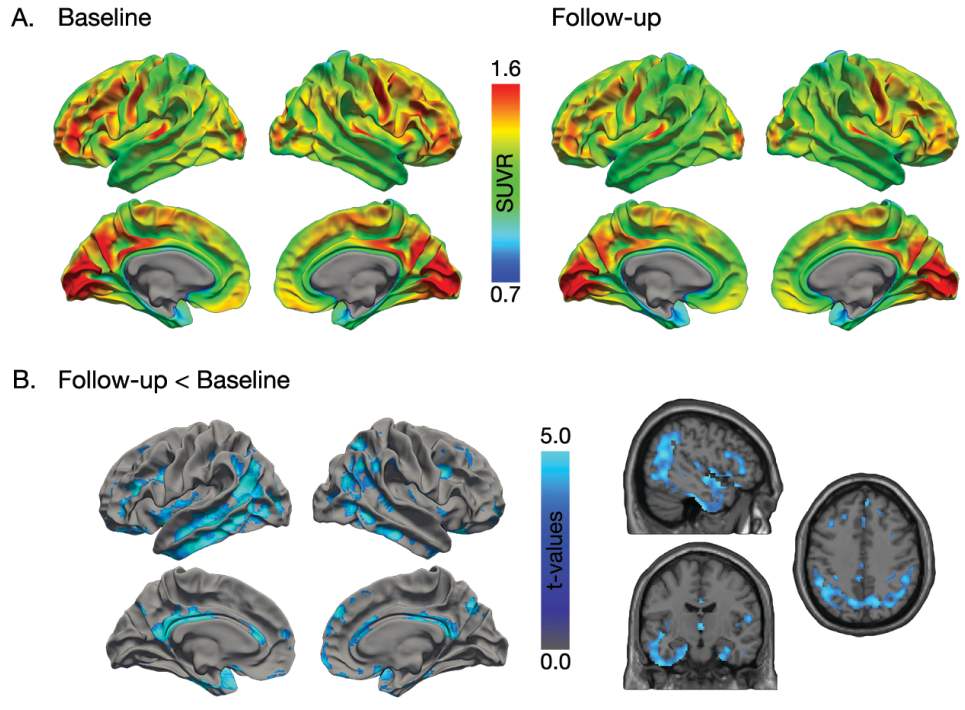

Figure 21. (A) Average baseline and follow-up SUVR images from patients with AD (prodromal or dementia; n=16) with [^{18}F]FDG, and (B) voxel-based paired t-tests (SPM8) evaluating the changes in uptake over time (interval = 17 months). No correction for multiple comparisons was made (uncorrected p<0.001). The figure is adapted from Chiotis, K. *et al.* Longitudinal changes of tau PET imaging in relation to hypometabolism in prodromal and Alzheimer's disease dementia. *Molecular psychiatry*, (2017).

substantial albeit heterogeneous differences at an individual level. Similar heterogeneity was also observed, in terms of [^{18}F]THK5317 binding, at baseline in our patient sample.

Longitudinally, no relationship was observed between [^{18}F]THK5317 binding and [^{18}F]FDG uptake in the patients with AD, as assessed by linear mixed-effects models. However, a significant interaction was detected between [^{18}F]THK5317 binding and the time points of investigations (baseline and follow-up) with regard to the [^{18}F]FDG uptake. Specifically, at follow-up the relationship between [^{18}F]THK5317 binding and [^{18}F]FDG uptake was closer than at baseline. In other words, although tau pathology and hypometabolism do not seem to go hand-in-hand over time, the relationship becomes closer as the disease progresses, i.e. as hypometabolism becomes more severe. Cross-sectional *in vivo* observations with another tau tracer ([^{18}F]AV-1451) in samples of patients at different stages of the disease, further supported the idea of a closer relationship between tau pathology and neurodegeneration at late symptomatic stages of AD (dementia). [240,242,246,316] Altogether, our findings indicate the existence of a lag phase between the build-up of tau pathology and the development of hypometabolic, neurodegenerative changes. This is in line with some experimental data showing that neurons can tolerate a substantial amount of tau pathology, through compensatory mechanisms, before exhibiting major degenerative changes. [72-74]

4.1.2.4 Binding of the tau tracer [^{18}F]THK5317 in patients with atypical parkinsonism

A neuropathological diagnosis of CBD and PSP is made in the presence of tau-positive deposits, although distinct types and regional distributions of the deposits characterise the two diseases (Table 2). [317,318] Both diseases have been associated with clinical symptomatology in the spectrum of atypical parkinsonism with broad overlap between their clinical presentations. Two patients clinically diagnosed with possible CBD and one with probable PSP underwent multi-modal PET imaging as part of our studies (paper II, IV). All three patients were negative for Aβ deposition ([^{11}C]PIB PET), they exhibited hypometabolic changes ([^{18}F]FDG PET) consistent with the presence of CBD and PSP pathology, respectively, and the regional distribution of their [^{18}F]THK5317 binding differed substantially from that in patients with AD. [^{18}F]THK5317 binding was higher in the two patients with possible CBD than in the cognitively normal volunteers, in areas consistent with the expected distribution of tau pathology in this disease; [135] both patients showed increased binding in the basal ganglia and cortical areas, while one of the them also showed extensive binding in the white-matter (Figure 22). The patient with probable PSP showed high [^{18}F]THK5317 binding, predominantly in the basal ganglia and midbrain, in agreement with previously published neuropathological studies. [136] Our findings are in line with evidence presented using different tau PET tracers, [220,247-252] and illustrate the promise held by the existing tracers for differentiating between syndromes associated with different tauopathies.

The two patients with possible CBD underwent follow-up [^{18}F]THK5317 and [^{18}F]FDG PET imaging after intervals of 17 and 24 months. At follow-up, [^{18}F]THK5317 binding in both

patients had increased in the basal ganglia as well as other cortical areas, including the frontal lobe (Figure 22). Decreases were observed in [^{18}F]FDG uptake over this time. Tau imaging with [^{18}F]THK5317 could thus prove more useful in tracking neurodegeneration longitudinally in non-AD rather than AD tauopathies, at least in the symptomatic stages of these diseases. However, because only two cases of possible CBD were investigated, without autopsy validation, we advise caution in the interpretation of our findings.

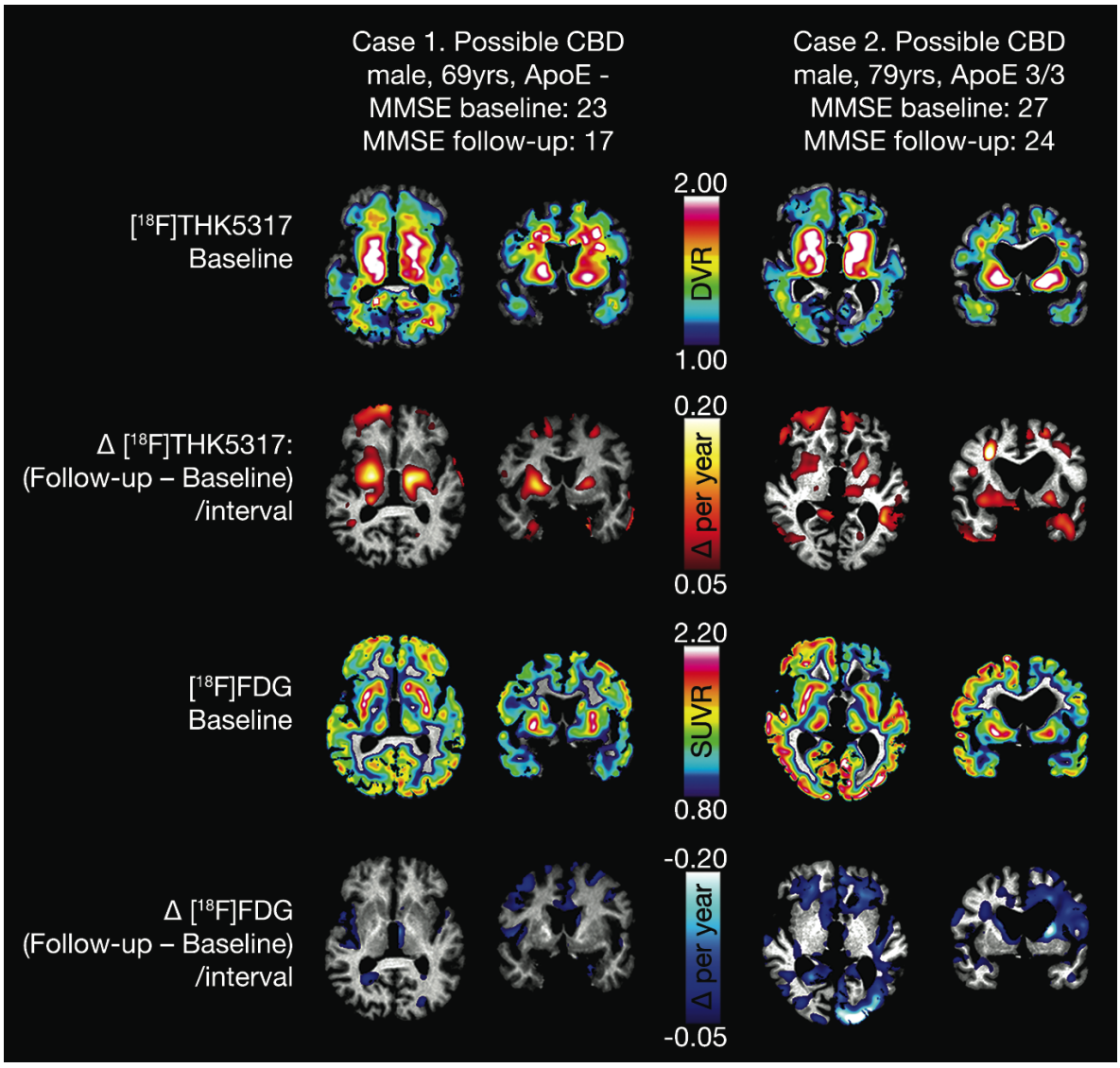

Figure 22. [^{18}F]THK5317 DVR and [^{18}F]FDG SUVR baseline images as well as annual rate of change maps (Δ DVR/SUVR per year) for the binding/uptake of the two tracers in the two patients with clinical diagnosis of possible CBD. The figure is adapted from Chiotis, K. *et al.* Longitudinal changes of tau PET imaging in relation to hypometabolism in prodromal and Alzheimer's disease dementia. *Molecular psychiatry*, (2017).

4.1.2.5 Differences between tau-specific tracers; relationship to other markers of AD

Similar findings have been presented *in vivo* when chemically different tau PET tracers were administered to different patients with AD or non-AD tauopathies, as discussed above. [223] However, head-to-head comparisons of those tracers in the same individuals were lacking. In our study, the tau tracers [^{11}C]THK5351 (successor of THK5317) and [^{11}C]PBB3 were injected on the same day into the same patients, who were diagnosed with clinical AD (prodromal or dementia), to compare their binding properties. [^{11}C]THK5351 bound with a higher load in the brains of the patients, than [^{11}C]PBB3, with both tracers exhibiting high binding in the temporal lobe, as well as other isocortical ROIs (Figure 23). However, the regional distribution of [^{11}C]THK5351 and [^{11}C]PBB3 binding differed substantially, especially within the temporal lobe. More specifically, while [^{11}C]THK5351 showed the highest binding in the medial relative to the lateral temporal lobe, the opposite pattern was detected for [^{11}C]PBB3. The binding of [^{11}C]PBB3, but not of [^{11}C]THK5351, resembled that of the Aβ tracer [^{11}C]AZD2184 in the temporal lobe and strong positive correlations were observed between the binding of [^{11}C]PBB3 and [^{11}C]AZD2184. Measures of tau in the CSF, and downstream markers of AD such as entorhinal cortex atrophy and global cognitive performance were more closely related to the binding of [^{11}C]THK5351, than to that of [^{11}C]PBB3. The differences in the load and regional distribution of the binding suggest different molecular targets for the two tau PET tracers. The correlations of the [^{11}C]PBB3 binding with the binding of the Aβ tracer, suggest that [^{11}C]PBB3 could bind preferentially to tau deposits co-localised with Aβ pathology (i.e. neuritic plaques). [319,320] In contrast, the

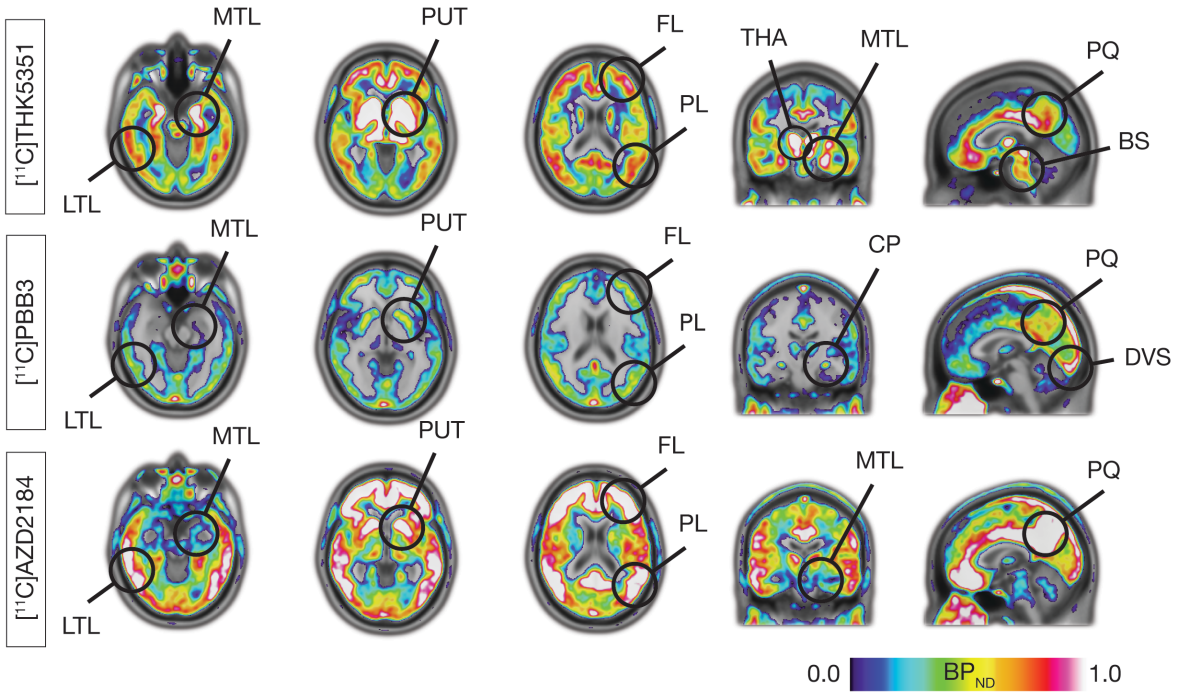

Figure 23. Average [^{11}C]THK5351 (tau), [^{11}C]PBB3 (tau) and [^{11}C]AZD2184 (Aβ) BP_{ND} images for the patients with AD (prodromal or dementia; n = 9). BS = brainstem; CP = choroid plexus; DVS = dural venous sinus; FL = frontal lobe; LTL = lateral temporal lobe; MTL = medial temporal lobe; PQ = precuneus; PL = parietal lobe; PUT = putamen; THA = thalamus.

pattern of [^{11}C]THK5351 binding matched the expected spatial distribution of tau pathology in AD better, suggesting binding of the tracer to a wider range of tau deposits. [75,321]

4.2 METHODOLOGICAL CONSIDERATIONS

4.2.1 Tau PET imaging

4.2.1.1 Test-retest evaluation

Test-retest studies are crucial in the *in vivo* evaluation of the utility of novel tracers. [^{18}F]THK5317, when injected into the same patients within an interval of 37 days, showed excellent reproducibility, especially in regions of particular interest for tau pathology. In the temporal cortex, the average absolute difference in [^{18}F]THK5317 binding between test and retest was 1.83% (standard deviation = 1.00%). Low variability was also observed in ROIs considered affected by 'off-target' binding of the tracer, as discussed below. As an example, the average absolute difference in [^{18}F]THK5317 binding in the putamen between test and retest was 1.51% (standard deviation = 1.07%).

4.2.1.2 Off-target binding

The binding of [^{18}F]THK5317 and its successor [^{11}C]THK5351 was extensive in areas that are not expected to be affected significantly by tau pathology (likely, off-target binding) in cognitively normal volunteers or patients with early AD, [49] such as the basal ganglia, thalami and brainstem (Figures 23, 24). Binding in the basal ganglia appeared to be of higher intensity in the elderly compared with younger, cognitively normal volunteers, although there was very good discrimination in the same area between groups of cognitively normal volunteers and patients with AD (prodromal or dementia) or atypical parkinsonism. Off-target binding in the basal ganglia and thalami has been associated with binding of the tracer to monoamine oxidase B (MAO-B). [236] Although, the discrimination between patients with atypical parkinsonism and cognitively normal volunteers could indicate a tau component in the binding in those areas, the source of increased binding in patients with AD remains unexplored. Interestingly, the structurally different tau tracer [^{11}C]PBB3 was also

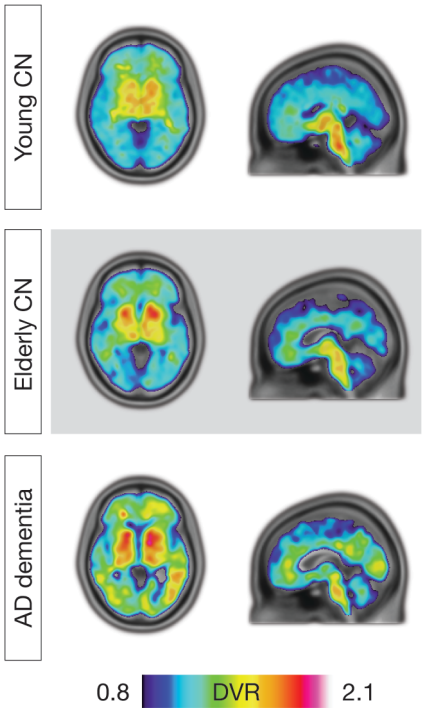

Figure 24. Sample [^{18}F]THK5317 DVR images illustrating the off-target binding of the tracer in areas such as the basal ganglia, thalamus and brainstem from a young cognitively normal (CN) volunteer (22 yrs), an elderly CN (58 yrs) and a patient with AD of the same age (58 yrs).

bound extensively to the MAO-B-rich basal ganglia in patients with AD, although the comparability of off-target binding sources between tracers remains elusive. Additional areas of off-target binding for [^{11}C]PBB3 were detected in vascular structures, including the choroid plexus and the dural venous sinuses (Figure 23).

4.2.1.3 Partial volume effect correction

The extensive off-target binding of the investigated tau tracers could potentially lead to spill-over of the signal to the adjacent ROIs, especially when conventional PET scanners with low spatial resolution (e.g. ECAT EXACT HR+ scanner and Discovery ST PET/CT) are used. We used different methods to correct for this partial volume effect. In the uncorrected [^{18}F]THK5317 DVR images no differences were observed in the hippocampus between the cognitively normal volunteers and patients with AD, possibly because of off-target tracer binding in the basal ganglia, which led to spill-over of signal. Application of partial volume effect correction accounted for the spill-over and revealed that the groups could be differentiated moderately well based on the load of tracer binding (Figure 25). A similar effect was observed in the anterior cingulate. For [^{11}C]THK5351 and [^{11}C]PBB3, the partial volume effect correction did not substantially affect the quantification of the tracer binding, probably because of the high-resolution of the PET system (HHRT), which minimised the spill-over between ROIs. However, it is appears that the use of these tracers in conventional scanners would result in substantial spill-over of the signal and therefore bias in the regional quantification of the tracer binding.

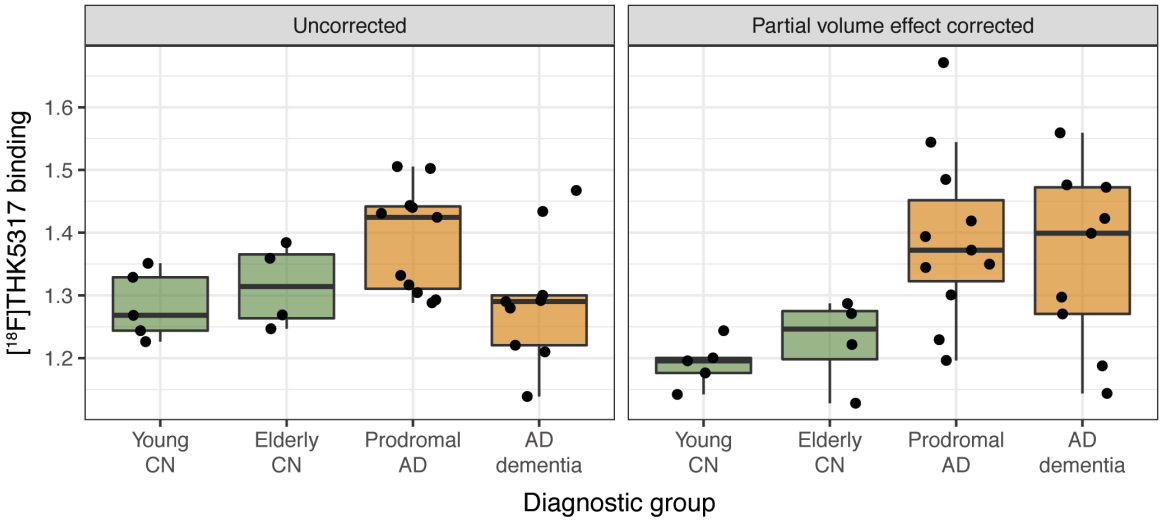

Figure 25. Boxplots of [^{18}F]THK5317 binding in the hippocampus before and after the application of partial volume effect correction across diagnostic groups. CN = cognitively normal volunteers. The figure is adapted from Chiotis, K. *et al.* Imaging in-vivo tau pathology in Alzheimer's disease with THK5317 PET in a multimodal paradigm. *European journal of nuclear medicine and molecular imaging* **43**, 1686-1699, (2016).

5 CONCLUDING REMARKS

- The developed Aβ-specific PET tracers, [^{11}C]PIB and [^{18}F]florbetapir, were highly comparable even when applied to different cohorts. The oldest old patients with cognitive complaints might benefit substantially from the use of Aβ PET as part of their clinical assessment.

- The tracer [^{18}F]THK5317 detected the expected load and regional distribution of tau pathology *in vivo* in a sample of patients with clinical AD (prodromal or dementia) and patients with atypical parkinsonism. The distribution of [^{18}F]THK5317 binding differed from that of Aβ deposition ([^{11}C]PIB) in AD, although there were regional correlations.

- The regional load of tau pathology ([^{18}F]THK5317) is associated with measures of global cognition and episodic memory. Local hypometabolism ([^{18}F]FDG) appeared to play a mediating role in this relationship.

- Heterogeneous patterns of change over time were observed in the binding of the tau tracer [^{18}F]THK5317 in patients with AD, in contrast to homogeneous changes in glucose metabolism ([^{18}F]FDG), which tracked cognitive deterioration better. The build-up of tau pathology and the development of local hypometabolism appeared temporally dissociated, at early symptomatic stages of AD, with a stronger relationship detected when hypometabolism changes become more prevalent in the later stages.

- The tau tracers [^{11}C]THK5351 and [^{11}C]PBB3 seem to bind to different molecular targets *in vivo*. Binding of [^{11}C]PBB3 appeared to be more closely related to Aβ deposition ([^{11}C]AZD2184), while [^{11}C]THK5351 binding followed the expected regional pattern of tau pathology in AD more closely and was more closely related to downstream markers of the disease.

6 FURTHER CONSIDERATIONS

Although the results of tau PET imaging are promising, a number of concerns have also been raised, predominantly related to the lack of thorough characterisation of the binding targets for each tracer, as discussed below. Therefore, caution is advised in interpreting the *in vivo* findings published to date. Future research should focus on validating the binding of the existing PET tracers as well as on developing new tracers with improved pharmacological properties, based on the lessons learned from the evaluation of the first generation of tracers.

6.1 SPECIFIC TARGETS OF TAU PET TRACERS

The specific targets of the developed tau PET tracers remain uncertain. Although all tracers have shown high specificity to tau pathology in *in vitro* studies, [223] the heterogeneity of tau deposits complicates the identification of their specific targets, in the absence of detailed validation studies. Furthermore, the differences in chemical structure of the existing tracers raise doubts about the comparability of their binding properties on the tau deposits. To date, studies directly comparing the *in vitro* binding of the tracers have highlighted differences in their binding characteristics. The tracers in the THK family (THK5317, THK5351) and AV-1451 appear to have similar binding properties in the AD brain while PBB3 has different properties, as illustrated by competition studies. [224,225] These observations have been reinforced by *in vivo* comparisons in the same patients with different tracers, both in paper V and the work of Jang, et al. [322]. Therefore, although we know very little about the specific targets of these tracers, we now understand that at least one of them (PBB3) binds to different molecular sites from the rather similar targets that THK5317, THK5351 and AV-1451 bind to. The identification of tracers binding to different aspects of tau pathology may have important implications for the differentiation of tauopathies, as well as for exploration of the temporal evolution of tau pathology in the diseased brain.

The determination of the 3D molecular structure of paired helical and straight tau filaments [323] could offer new insight into the development of future tau PET tracers. The use of computational simulation studies (*in silico* modelling) will allow detailed investigation of the tracer binding sites on the tau fibril in greater detail, as well as allow determination of whether the tracers preferentially bind to different types of tau filaments. In addition, more detailed characterisation of the tracer binding is expected with the *post-mortem* validation of tracer binding in end-of-life patients. These studies will reveal whether the tracers bind to different types of tau deposits or even to different maturation stages of these deposits. The elucidation of the binding characteristics is crucial for interpreting *in vivo* PET observations in both AD and non-AD tauopathies.

6.2 OFF-TARGET BINDING OF TAU PET TRACERS

The *in vivo* binding of the developed tracers to areas not expected to be affected by tau pathology, both in cognitively normal volunteers and patient groups was somehow largely neglected in the first *in vivo* studies, [219,220,231,324] probably as a result of the commercial interests surrounding the development of many of the tau-specific tracers. Briefly, recent studies have suggested off-target binding for the tracers to misfolded proteins other than tau (e.g. TDP-43, α-synuclein, Aβ), enzymes (e.g. MAO-A, MAO-B), and vascular structures.

6.2.1.1 Misfolded proteins

The preliminary evidence pointing to binding of tau tracers to misfolded proteins other than tau [257,258,325-328] has led to the 'tau-specificity' of these tracers being questioned. So far, PBB3 appears to have affinity for α-synuclein, the tracers of the THK family and AV-1451 show high binding *in vivo* in syndromes associated with TDP-43 pathology, and the THK tracer family could have some affinity for Aβ deposits, according to *in vitro* work. While the latter observations remain to be validated in *ante-/post-mortem* studies, concerns have been raised that these tracers might bind *in vivo* to multiple β-sheet structures ('amyloids'), although with a different affinity from that to tau pathology. If this proves to be the case, the clinical utility of the developed tracers would be undermined, since the discrimination between different neurodegenerative diseases characterised by the accumulation of misfolded proteins (aka proteinopathies) would be at least questionable.

6.2.1.2 Monoamine oxidase B

Extensive binding in the basal ganglia has been reported *in vivo* for AV-1451 and tracers of the THK family, in both cognitively normal volunteers and patients with AD. [250,329] However, the basal ganglia are minimally affected by tau pathology in both normal ageing and the early stages of AD. [49] The binding of the THK tracers to the basal ganglia has been attributed to off-target binding to MAO-B, [236] a finding that is consistent with the regional distribution of MAO-B in the brain. [330] However, a study that attempted to block the MAO-B signal *in vivo* by administering a MAO-B inhibitor prior to the THK5351 PET scan detected decreases in the signal compared to a baseline THK5351 investigation, irrespective of the cerebral distribution of MAO-B. Surprisingly, when the binding was quantified using a conventional reference region-based approach, no differences were noted in terms of binding before and after the administration of the inhibitor. This apparent discrepancy could derive from changes in the perfusion of the tracer following administration of a MAO-B inhibitor. In other words, the MAO-B inhibitor could lead to decreased delivery of the tracer across the whole brain, possibly through nitric oxide-mediated vasodilation, [331] which could mask small differences in the binding of THK5351 before and after administration of the inhibitor. Given the very strong correlation between AV-1451 and tracers of the THK family in the basal ganglia when

injected in the same patients, [322] it is conceivable that the source of off-target binding is – at least partly – similar for these tracers. Interestingly, as illustrated in paper V, PBB3 also binds *in vivo* to the MAO-B-rich basal ganglia. Altogether, the potential binding of chemically different tau tracers to the same off-target site might indicate the existence of similarities between binding sites on tau pathology and MAO-B. Detailed validation studies are required to determine the contribution of MAO-B in the *in vivo* signal of the developed tau tracers and to define the brain areas that are affected the most. Potential binding of the tracers to MAO-B has increased relevance in non-AD tauopathies, such as CBD and PSP, where ROIs with high MAO-B availability and tau pathology overlap (e.g. basal ganglia).

6.2.1.3 Vascular structures

AV-1451 and PBB3 both bind to vascular structures, which could complicate the quantification of the tracer binding in multiple ROIs. The source of this binding for AV-1451 has so far been attributed to multiple causes, [217,259,332] with no studies investigating further this issue for PBB3.

7 FUTURE OUTLOOK

The use of tau PET imaging for ever larger cohorts of patients with AD and non-AD tauopathies, and for cognitively normal elderly, could offer valuable insight on the temporal evolution of tau pathology in the diseased brain, as well as offering a useful tool for the differential diagnosis of different proteinopathies.

7.1 TEMPORAL EVOLUTION OF TAU PATHOLOGY

Tau PET *in vivo* studies with [^{18}F]THK5317, [^{18}F]THK5351 and [^{18}F]AV-1451 have indicated that lateral temporal cortical areas are already affected by tau deposition in the earliest symptomatic stages of AD (prodromal AD). [237,312,329] This suggests that tau propagates outside the medial temporal lobe already in the preclinical, presymptomatic phases of the disease, in agreement with previous models based on neuropathological data. [51,83] Data from several studies have suggested that tau deposition in the temporal lobe is related to markers of neurodegeneration and early cognitive deficit (i.e. episodic memory impairment), [237,246,315,329,333] with this relationships becoming stronger when neurodegenerative changes become more prevalent. [334] Based on these observations, it is conceivable that there is a lag phase between the build-up of tau pathology and the development of neurodegeneration, where the deposition of tau precedes the changes in markers of neurodegeneration and cognitive impairment. Although it is difficult to infer the temporal relationship between Aβ and tau depositions based on the current observations, the existence of Aβ-positive, cognitively normal volunteers with relatively low levels of tau in the lateral temporal lobe indicates that the spreading of tau pathology outside the medial temporal areas follows in time the cortical accumulation of fibrillar Aβ. [231] Overall, we suggest that tau pathology spreads early in the lateral areas of the temporal cortex before the onset of neurodegenerative changes and cognitive deficits, but after the cortical accumulation of Aβ plaques (Figure 26). Based on earlier evidence for other biomarkers, [286] we hypothesised a sigmoid-shaped curve for depicting the temporal course of tau pathology. Furthermore, it is likely, based on neuropathology data and early *in vivo* evidence, [49,233,234] that the proposed time course could be shift leftward or rightward on the time axis to better depict the earlier deposition of tau in the medial temporal lobe or the later spread in isocortical areas outside the temporal lobe, respectively. Future studies adopting a multi-modal design across the whole spectrum of the disease will improve our understanding of the temporal evolution of tau in the AD brain and offer a chance to validate the proposed model.

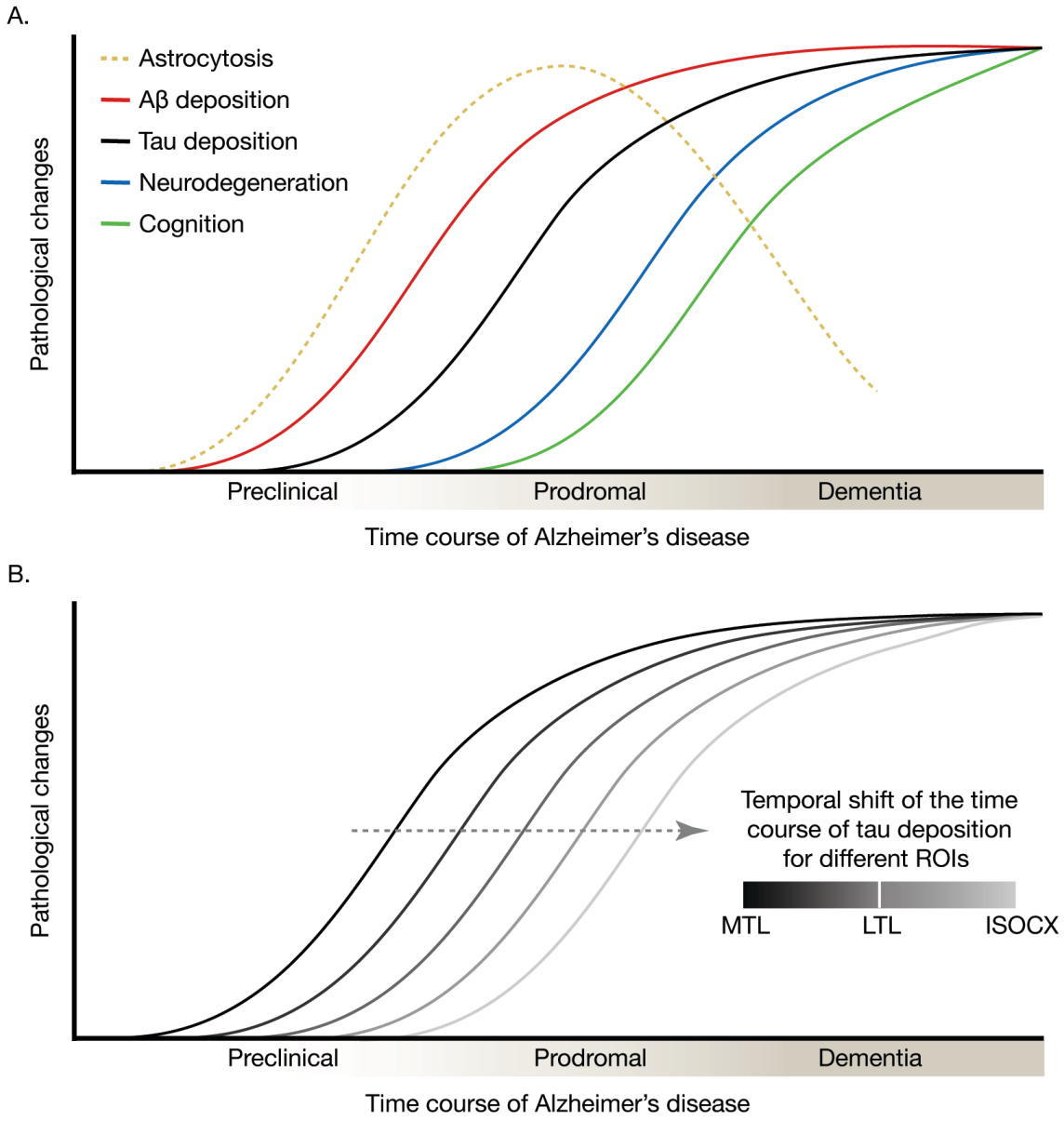

Figure 26. (A) Proposed model of the temporal ordering of the different pathological changes during the development of AD based on biomarker findings for astrocytosis, Aβ and tau deposition, neurodegeneration and cognitive impairment. (B) Temporal shift of the time course of the build-up of tau deposition for different brain ROIs. ISOCX = isocortex; MTL = medial temporal lobe; LTL = lateral temporal lobe.

7.2 CLINICAL UTILITY OF TAU PET IMAGING

The tau PET tracers have shown promising results at detecting the underlying load of tau pathology in clinically diagnosed AD and non-AD tauopathies that could lead to future breakthrough in the field of tauopathies. [220,230-232,246-252,329,334] Further research should concentrate on determining whether the different tau PET tracers can discriminate between patients diagnosed with AD or non-AD tauopathies as well as other non-tau-related proteinopathies, based on the load and regional distribution of the tracer binding. This differentiation could lead to great advances in the early, accurate clinical diagnosis, especially in the field of non-AD tauopathies, such as CBD and PSP, where there is, to date, a lack of reliable pathology markers able to be used in the clinic.

8 ACKNOWLEDGEMENTS

This thesis is the result of work by many hands. I am grateful to have had the opportunity to work together with so many wonderful people who have contributed to this work. I particularly wish to thank:

Primarily, **Agneta Nordberg**, my main supervisor, for your extraordinary passion and dedication in research, which has been deeply inspiring; for giving me freedom in my work but challenging my way of working and thinking; and for keeping the spirit of clinical work alive in me. It has been a privilege working with and learning from you as a PhD student.

Stephen Carter, for being my co-supervisor and friend over all these years; for teaching me the basics of neuroimaging, presentation and writing techniques; for being patient with me; for being there when I needed you through the open supervisor's hotline; and for the great time that we have every time we meet.

Laure Saint-Aubert, for being my hands-on supervisor and friend; for challenging me to develop technically and theoretically; for always taking the time to evaluate my work and always providing out-of-the-box suggestions. But mostly for introducing me to climbing; best PhD stress reliever ever.

Ove Almkvist, my co-supervisor, for your unique expertise in the group; for taking the time to thoroughly neuropsychologically investigate the patients included in this thesis; and for the useful feedback on the analyses performed.

Elena Rodriguez-Vieitez for being always curious, willing to help even at the busiest moments and for telling me not to stress and boosting my confidence; **Laetitia Lemoine** for answering all my unorthodox questions about *in vitro* studies and for funny moments at the office, at parties and at conferences; **Antoine Leuzy** for your admirable dedication determination, and for our fun chats at the office and over beers; and **Karim Farid** for bringing a more positive vibe to the office.

All collaborators from the Uppsala University Hospital PET centre, the Karolinska University Hospital Huddinge, the Department of Clinical Neuroscience and the Division of Clinical Geriatrics at Karolinska Institutet. Special thanks to **Anders Wall** for ensuring the problem-free investigation of all patients, **Irina Savitcheva** for taking care of the clinical PET scans, **Mark Lubberink** for expert advice on pharmacokinetic modelling of the PET imaging data, **Vesna Jelic** for insight into non-AD dementia, **Per Stenkrona** and **Zsolt Cselényi** for support during my work at the PET centrum in Solna, **Daniel Ferreira** and **Eric Westman** for your excellent work with the MRI data, **Rita Almeida** for the statistical input into my first project which really inspired me to continue developing my knowledge of statistics, and **Antona Wagstaff** for language editing all of my manuscripts.

Agneta Lindahl for taking care of each and every little or big administrative hurdle in the group. All present and past members of the division of **Translational Alzheimer Neurobiology** and the whole **Center for Alzheimer Research at Karolinska Institutet** for creating a stimulating atmosphere for research and a great place to work.

Elisabeth Chroni, my mentor, for your kindness and for introducing me to research; you are a role model and a continuous source of inspiration.

My family for, among other things, believing in me more than I do in myself, and for supporting my decision to move abroad and start a PhD. **My close friends**, for always showing how much you care; it is very inspiring to see you all chasing after your dreams. **Emelie** for standing by my side at every moment during this long PhD process, for being patient, supportive and affectionate, and for giving me a hug every time I felt discouraged.

Funding sources for all of the studies: Swedish Research Council (project 05817), the Swedish Foundation for Strategic Research (SSF), the Regional Agreement on Medical Training and Clinical Research (ALF) for Stockholm County Council, the Strategic Research Programme in Neuroscience at Karolinska Institutet, the Old Servants Foundation, the Sigurd and Elsa Goljes Memorial, the Axel Linder Foundation, the Gun and Bertil Stohne Foundation, the KI Funds, the Swedish Brain Fund, the Swedish Alzheimer's Foundation (Alzheimerfonden), the Dementia Foundation (demensfonden), the Wenner-Gren Foundation, the KTH-SLL grants and the EU FW7 large-scale integrating project INMiND (http://www.uni-muenster.de/INMiND). **Travel grants** attained for presenting these results at international conferences (AD/PD 2015, AAIC 2013 and 2016, HAI 2014). The **Diagnostic molecular imaging** initiative and the **Alzheimer's disease neuroimaging initiative** for the data used in the first study.

9 REFERENCES

1 Flatt, T. A new definition of aging? *Frontiers in genetics* **3**, 148, doi:10.3389/fgene.2012.00148 (2012).

2 Kasper, D. L. *et al.* Harrison's principles of internal medicine. (2015).

3 Harada, C. N., Natelson Love, M. C. & Triebel, K. L. Normal cognitive aging. *Clinics in geriatric medicine* **29**, 737-752, doi:10.1016/j.cger.2013.07.002 (2013).

4 Diagnostic and statistical manual of mental disorders: DSM-IV. *American Psychiatric Association* (1995).

5 Diagnostic and statistical manual of mental disorders: DSM-5. *American Psychiatric Association* (2013).

6 Wimo, A. *et al.* The worldwide costs of dementia 2015 and comparisons with 2010. *Alzheimer's & dementia : the journal of the Alzheimer's Association* **13**, 1-7, doi:10.1016/j.jalz.2016.07.150 (2017).

7 Nationell utvärdering – Vård och omsorg vid demenssjukdom – Rekommendationer, bedömningar och sammanfattning. *Swedish National Board of Health and Welfare - Socialstyrelsen* (2015).

8 Prince, M. *et al.* World Alzheimer Report 2015. *Alzheimer's Disease International* (2015).

9 Livingston, G. *et al.* Dementia prevention, intervention, and care. *Lancet*, doi:10.1016/S0140-6736(17)31363-6 (2017).

10 Wimo, A. *et al.* The societal costs of dementia in Sweden 2012 - relevance and methodological challenges in valuing informal care. *Alzheimer's research & therapy* **8**, 59, doi:10.1186/s13195-016-0215-9 (2016).

11 Larson, E. B., Yaffe, K. & Langa, K. M. New insights into the dementia epidemic. *The New England journal of medicine* **369**, 2275-2277, doi:10.1056/NEJMp1311405 (2013).

12 Winblad, B. *et al.* Defeating Alzheimer's disease and other dementias: a priority for European science and society. *The Lancet. Neurology* **15**, 455-532, doi:10.1016/S1474-4422(16)00062-4 (2016).

13 Schneider, J. A., Arvanitakis, Z., Bang, W. & Bennett, D. A. Mixed brain pathologies account for most dementia cases in community-dwelling older persons. *Neurology* **69**, 2197-2204, doi:10.1212/01.wnl.0000271090.28148.24 (2007).

14 Petersen, R. C. *et al.* Mild cognitive impairment: clinical characterization and outcome. *Archives of neurology* **56**, 303-308 (1999).

15 Winblad, B. *et al.* Mild cognitive impairment--beyond controversies, towards a consensus: report of the International Working Group on Mild Cognitive Impairment. *Journal of internal medicine* **256**, 240-246, doi:10.1111/j.1365-2796.2004.01380.x (2004).

16 Sarazin, M. *et al.* Amnestic syndrome of the medial temporal type identifies prodromal AD: a longitudinal study. *Neurology* **69**, 1859-1867, doi:10.1212/01.wnl.0000279336.36610.f7 (2007).

17 Ferman, T. J. *et al.* Nonamnestic mild cognitive impairment progresses to dementia with Lewy bodies. *Neurology* **81**, 2032-2038, doi:10.1212/01.wnl.0000436942.55281.47 (2013).

18 Petersen, R. C. *et al.* Practice parameter: early detection of dementia: mild cognitive impairment (an evidence-based review). Report of the Quality Standards Subcommittee of the American Academy of Neurology. *Neurology* **56**, 1133-1142 (2001).

19 Han, J. W. *et al.* Predictive validity and diagnostic stability of mild cognitive impairment subtypes. *Alzheimer's & dementia : the journal of the Alzheimer's Association* **8**, 553-559, doi:10.1016/j.jalz.2011.08.007 (2012).

20 Koepsell, T. D. & Monsell, S. E. Reversion from mild cognitive impairment to normal or near-normal cognition: risk factors and prognosis. *Neurology* **79**, 1591-1598, doi:10.1212/WNL.0b013e31826e26b7 (2012).

21 Jessen, F. *et al.* A conceptual framework for research on subjective cognitive decline in preclinical Alzheimer's disease. *Alzheimer's & dementia : the journal of the Alzheimer's Association* **10**, 844-852, doi:10.1016/j.jalz.2014.01.001 (2014).

22 Molinuevo, J. L. *et al.* Implementation of subjective cognitive decline criteria in research studies. *Alzheimer's & dementia : the journal of the Alzheimer's Association* **13**, 296-311, doi:10.1016/j.jalz.2016.09.012 (2017).

23 van Oijen, M., de Jong, F. J., Hofman, A., Koudstaal, P. J. & Breteler, M. M. Subjective memory complaints, education, and risk of Alzheimer's disease. *Alzheimer's & dementia : the journal of the Alzheimer's Association* **3**, 92-97, doi:10.1016/j.jalz.2007.01.011 (2007).

24 Jessen, F. *et al.* Prediction of dementia by subjective memory impairment: effects of severity and temporal association with cognitive impairment. *Archives of general psychiatry* **67**, 414-422, doi:10.1001/archgenpsychiatry.2010.30 (2010).

25 Reisberg, B., Shulman, M. B., Torossian, C., Leng, L. & Zhu, W. Outcome over seven years of healthy adults with and without subjective cognitive impairment. *Alzheimer's & dementia : the journal of the Alzheimer's Association* **6**, 11-24, doi:10.1016/j.jalz.2009.10.002 (2010).

26 Glodzik-Sobanska, L. *et al.* Subjective memory complaints: presence, severity and future outcome in normal older subjects. *Dementia and geriatric cognitive disorders* **24**, 177-184, doi:10.1159/000105604 (2007).

27 McKhann, G. *et al.* Clinical diagnosis of Alzheimer's disease: report of the NINCDS-ADRDA Work Group under the auspices of Department of Health and Human Services Task Force on Alzheimer's Disease. *Neurology* **34**, 939-944 (1984).

28 Crutch, S. J. *et al.* Posterior cortical atrophy. *The Lancet. Neurology* **11**, 170-178, doi:10.1016/S1474-4422(11)70289-7 (2012).

29 Gorno-Tempini, M. L. *et al.* Classification of primary progressive aphasia and its variants. *Neurology* **76**, 1006-1014, doi:10.1212/WNL.0b013e31821103e6 (2011).

30 Ossenkoppele, R. *et al.* The behavioural/dysexecutive variant of Alzheimer's disease: clinical, neuroimaging and pathological features. *Brain : a journal of neurology* **138**, 2732-2749, doi:10.1093/brain/awv191 (2015).

31 Klatka, L. A., Schiffer, R. B., Powers, J. M. & Kazee, A. M. Incorrect diagnosis of Alzheimer's disease. A clinicopathologic study. *Archives of neurology* **53**, 35-42 (1996).

32 Hyman, B. T. *et al.* National Institute on Aging-Alzheimer's Association guidelines for the neuropathologic assessment of Alzheimer's disease. *Alzheimer's & dementia : the journal of the Alzheimer's Association* **8**, 1-13, doi:10.1016/j.jalz.2011.10.007 (2012).

33 Beach, T. G., Monsell, S. E., Phillips, L. E. & Kukull, W. Accuracy of the clinical diagnosis of Alzheimer disease at National Institute on Aging Alzheimer Disease Centers, 2005-2010. *Journal of neuropathology and experimental neurology* **71**, 266-273, doi:10.1097/NEN.0b013e31824b211b (2012).

34 Corder, E. H. *et al.* Gene dose of apolipoprotein E type 4 allele and the risk of Alzheimer's disease in late onset families. *Science* **261**, 921-923 (1993).

35 Stern, Y. *et al.* Influence of education and occupation on the incidence of Alzheimer's disease. *Jama* **271**, 1004-1010 (1994).

36 Xiong, C. *et al.* Role of family history for Alzheimer biomarker abnormalities in the adult children study. *Archives of neurology* **68**, 1313-1319, doi:10.1001/archneurol.2011.208 (2011).

37 Norton, S., Matthews, F. E., Barnes, D. E., Yaffe, K. & Brayne, C. Potential for primary prevention of Alzheimer's disease: an analysis of population-based data. *The Lancet. Neurology* **13**, 788-794, doi:10.1016/S1474-4422(14)70136-X (2014).

38 Alzheimer, A., Stelzmann, R. A., Schnitzlein, H. N. & Murtagh, F. R. An English translation of Alzheimer's 1907 paper, "Uber eine eigenartige Erkankung der Hirnrinde". *Clinical anatomy* **8**, 429-431, doi:10.1002/ca.980080612 (1995).

39 Glenner, G. G. & Wong, C. W. Alzheimer's disease: initial report of the purification and characterization of a novel cerebrovascular amyloid protein. *Biochemical and biophysical research communications* **120**, 885-890 (1984).

40 Masters, C. L. *et al.* Amyloid plaque core protein in Alzheimer disease and Down syndrome. *Proceedings of the National Academy of Sciences of the United States of America* **82**, 4245-4249 (1985).

41 Yankner, B. A. & Mesulam, M. M. Seminars in medicine of the Beth Israel Hospital, Boston. beta-Amyloid and the pathogenesis of Alzheimer's disease. *The New England journal of medicine* **325**, 1849-1857, doi:10.1056/NEJM199112263252605 (1991).

42 Haass, C. & Selkoe, D. J. Cellular processing of beta-amyloid precursor protein and the genesis of amyloid beta-peptide. *Cell* **75**, 1039-1042 (1993).

43 O'Brien, R. J. & Wong, P. C. Amyloid precursor protein processing and Alzheimer's disease. *Annual review of neuroscience* **34**, 185-204, doi:10.1146/annurev-neuro-061010-113613 (2011).

44 Hyman, B. T., Marzloff, K. & Arriagada, P. V. The lack of accumulation of senile plaques or amyloid burden in Alzheimer's disease suggests a dynamic balance

between amyloid deposition and resolution. *Journal of neuropathology and experimental neurology* **52**, 594-600 (1993).

45 Glabe, C. G. Structural classification of toxic amyloid oligomers. *The Journal of biological chemistry* **283**, 29639-29643, doi:10.1074/jbc.R800016200 (2008).

46 Thal, D. R., Capetillo-Zarate, E., Del Tredici, K. & Braak, H. The development of amyloid beta protein deposits in the aged brain. *Science of aging knowledge environment : SAGE KE* **2006**, re1, doi:10.1126/sageke.2006.6.re1 (2006).

47 Alafuzoff, I. *et al.* Assessment of beta-amyloid deposits in human brain: a study of the BrainNet Europe Consortium. *Acta neuropathologica* **117**, 309-320, doi:10.1007/s00401-009-0485-4 (2009).

48 Cras, P. *et al.* Senile plaque neurites in Alzheimer disease accumulate amyloid precursor protein. *Proceedings of the National Academy of Sciences of the United States of America* **88**, 7552-7556 (1991).

49 Braak, H. & Braak, E. Neuropathological stageing of Alzheimer-related changes. *Acta neuropathologica* **82**, 239-259 (1991).

50 Thal, D. R., Rub, U., Orantes, M. & Braak, H. Phases of A beta-deposition in the human brain and its relevance for the development of AD. *Neurology* **58**, 1791-1800 (2002).

51 Braak, H., Thal, D. R., Ghebremedhin, E. & Del Tredici, K. Stages of the pathologic process in Alzheimer disease: age categories from 1 to 100 years. *Journal of neuropathology and experimental neurology* **70**, 960-969, doi:10.1097/NEN.0b013e318232a379 (2011).

52 Gao, S., Hendrie, H. C., Hall, K. S. & Hui, S. The relationships between age, sex, and the incidence of dementia and Alzheimer disease: a meta-analysis. *Archives of general psychiatry* **55**, 809-815 (1998).

53 Grundke-Iqbal, I. *et al.* Abnormal phosphorylation of the microtubule-associated protein tau (tau) in Alzheimer cytoskeletal pathology. *Proceedings of the National Academy of Sciences of the United States of America* **83**, 4913-4917 (1986).

54 Weingarten, M. D., Lockwood, A. H., Hwo, S. Y. & Kirschner, M. W. A protein factor essential for microtubule assembly. *Proceedings of the National Academy of Sciences of the United States of America* **72**, 1858-1862 (1975).

55 Morris, M., Maeda, S., Vossel, K. & Mucke, L. The many faces of tau. *Neuron* **70**, 410-426, doi:10.1016/j.neuron.2011.04.009 (2011).

56 Goedert, M., Spillantini, M. G., Jakes, R., Rutherford, D. & Crowther, R. A. Multiple isoforms of human microtubule-associated protein tau: sequences and localization in neurofibrillary tangles of Alzheimer's disease. *Neuron* **3**, 519-526 (1989).

57 Kosik, K. S., Orecchio, L. D., Bakalis, S. & Neve, R. L. Developmentally regulated expression of specific tau sequences. *Neuron* **2**, 1389-1397 (1989).

58 Ksiezak-Reding, H., Farooq, M., Yang, L. S., Dickson, D. W. & LoPresti, P. Tau protein expression in adult bovine oligodendrocytes: functional and pathological significance. *Neurochemical research* **28**, 1385-1392 (2003).

59 Muller, R., Heinrich, M., Heck, S., Blohm, D. & Richter-Landsberg, C. Expression of microtubule-associated proteins MAP2 and tau in cultured rat brain oligodendrocytes. *Cell and tissue research* **288**, 239-249 (1997).

60 Buee, L., Bussiere, T., Buee-Scherrer, V., Delacourte, A. & Hof, P. R. Tau protein isoforms, phosphorylation and role in neurodegenerative disorders. *Brain research. Brain research reviews* **33**, 95-130 (2000).

61 Gotz, J. *et al.* Somatodendritic localization and hyperphosphorylation of tau protein in transgenic mice expressing the longest human brain tau isoform. *The EMBO journal* **14**, 1304-1313 (1995).

62 Lauckner, J., Frey, P. & Geula, C. Comparative distribution of tau phosphorylated at Ser262 in pre-tangles and tangles. *Neurobiology of aging* **24**, 767-776 (2003).

63 Augustinack, J. C., Schneider, A., Mandelkow, E. M. & Hyman, B. T. Specific tau phosphorylation sites correlate with severity of neuronal cytopathology in Alzheimer's disease. *Acta neuropathologica* **103**, 26-35 (2002).

64 Uchihara, T. Pretangles and neurofibrillary changes: similarities and differences between AD and CBD based on molecular and morphological evolution. *Neuropathology : official journal of the Japanese Society of Neuropathology* **34**, 571-577, doi:10.1111/neup.12108 (2014).

65 Giannakopoulos, P. *et al.* Tangle and neuron numbers, but not amyloid load, predict cognitive status in Alzheimer's disease. *Neurology* **60**, 1495-1500 (2003).

66 Arriagada, P. V., Growdon, J. H., Hedley-Whyte, E. T. & Hyman, B. T. Neurofibrillary tangles but not senile plaques parallel duration and severity of Alzheimer's disease. *Neurology* **42**, 631-639 (1992).

67 Gomez-Isla, T. *et al.* Neuronal loss correlates with but exceeds neurofibrillary tangles in Alzheimer's disease. *Annals of neurology* **41**, 17-24, doi:10.1002/ana.410410106 (1997).

68 Nelson, P. T. *et al.* Correlation of Alzheimer disease neuropathologic changes with cognitive status: a review of the literature. *Journal of neuropathology and experimental neurology* **71**, 362-381, doi:10.1097/NEN.0b013e31825018f7 (2012).

69 Iqbal, K., Liu, F., Gong, C. X. & Grundke-Iqbal, I. Tau in Alzheimer disease and related tauopathies. *Current Alzheimer research* **7**, 656-664 (2010).

70 Spillantini, M. G. & Goedert, M. Tau pathology and neurodegeneration. *The Lancet. Neurology* **12**, 609-622, doi:10.1016/S1474-4422(13)70090-5 (2013).

71 Ballatore, C., Lee, V. M. & Trojanowski, J. Q. Tau-mediated neurodegeneration in Alzheimer's disease and related disorders. *Nature reviews. Neuroscience* **8**, 663-672, doi:10.1038/nrn2194 (2007).

72 de Calignon, A., Spires-Jones, T. L., Pitstick, R., Carlson, G. A. & Hyman, B. T. Tangle-bearing neurons survive despite disruption of membrane integrity in a mouse model of tauopathy. *Journal of neuropathology and experimental neurology* **68**, 757-761, doi:10.1097/NEN.0b013e3181a9fc66 (2009).

73 Morsch, R., Simon, W. & Coleman, P. D. Neurons may live for decades with neurofibrillary tangles. *Journal of neuropathology and experimental neurology* **58**, 188-197 (1999).

74 Buee, L. *et al.* From tau phosphorylation to tau aggregation: what about neuronal death? *Biochemical Society transactions* **38**, 967-972, doi:10.1042/BST0380967 (2010).

75 Delacourte, A. *et al.* The biochemical pathway of neurofibrillary degeneration in aging and Alzheimer's disease. *Neurology* **52**, 1158-1165 (1999).

76 Braak, H. & Del Tredici, K. Where, when, and in what form does sporadic Alzheimer's disease begin? *Current opinion in neurology* **25**, 708-714, doi:10.1097/WCO.0b013e32835a3432 (2012).

77 Royall, D. R. Location, location, location! *Neurobiology of aging* **28**, 1481-1482; discussion 1483, doi:10.1016/j.neurobiolaging.2006.09.008 (2007).

78 Braak, H. & Del Tredici, K. The preclinical phase of the pathological process underlying sporadic Alzheimer's disease. *Brain : a journal of neurology* **138**, 2814-2833, doi:10.1093/brain/awv236 (2015).

79 Jucker, M. & Walker, L. C. Self-propagation of pathogenic protein aggregates in neurodegenerative diseases. *Nature* **501**, 45-51, doi:10.1038/nature12481 (2013).

80 Clavaguera, F., Hench, J., Goedert, M. & Tolnay, M. Invited review: Prion-like transmission and spreading of tau pathology. *Neuropathology and applied neurobiology* **41**, 47-58, doi:10.1111/nan.12197 (2015).

81 Brettschneider, J., Del Tredici, K., Lee, V. M. & Trojanowski, J. Q. Spreading of pathology in neurodegenerative diseases: a focus on human studies. *Nature reviews. Neuroscience* **16**, 109-120, doi:10.1038/nrn3887 (2015).

82 Ingelsson, M. *et al.* Early Abeta accumulation and progressive synaptic loss, gliosis, and tangle formation in AD brain. *Neurology* **62**, 925-931 (2004).

83 Duyckaerts, C. & Hauw, J. J. Prevalence, incidence and duration of Braak's stages in the general population: can we know? *Neurobiology of aging* **18**, 362-369; discussion 389-392 (1997).

84 Duyckaerts, C. Tau pathology in children and young adults: can you still be unconditionally baptist? *Acta neuropathologica* **121**, 145-147, doi:10.1007/s00401-010-0794-7 (2011).

85 Duyckaerts, C. *et al.* PART is part of Alzheimer disease. *Acta neuropathologica* **129**, 749-756, doi:10.1007/s00401-015-1390-7 (2015).

86 Braak, H. & Del Tredici, K. Are cases with tau pathology occurring in the absence of Abeta deposits part of the AD-related pathological process? *Acta neuropathologica* **128**, 767-772, doi:10.1007/s00401-014-1356-1 (2014).

87 Schonheit, B., Zarski, R. & Ohm, T. G. Spatial and temporal relationships between plaques and tangles in Alzheimer-pathology. *Neurobiology of aging* **25**, 697-711, doi:10.1016/j.neurobiolaging.2003.09.009 (2004).

88 Skullerud, K. Variations in the size of the human brain. Influence of age, sex, body length, body mass index, alcoholism, Alzheimer changes, and cerebral atherosclerosis. *Acta neurologica Scandinavica. Supplementum* **102**, 1-94 (1985).

89 DeKosky, S. T. & Scheff, S. W. Synapse loss in frontal cortex biopsies in Alzheimer's disease: correlation with cognitive severity. *Annals of neurology* **27**, 457-464, doi:10.1002/ana.410270502 (1990).

90 Mouton, P. R., Martin, L. J., Calhoun, M. E., Dal Forno, G. & Price, D. L. Cognitive decline strongly correlates with cortical atrophy in Alzheimer's dementia. *Neurobiology of aging* **19**, 371-377 (1998).

91 Klucken, J., McLean, P. J., Gomez-Tortosa, E., Ingelsson, M. & Hyman, B. T. Neuritic alterations and neural system dysfunction in Alzheimer's disease and dementia with Lewy bodies. *Neurochemical research* **28**, 1683-1691 (2003).

92 Terry, R. D., Peck, A., DeTeresa, R., Schechter, R. & Horoupian, D. S. Some morphometric aspects of the brain in senile dementia of the Alzheimer type. *Annals of neurology* **10**, 184-192, doi:10.1002/ana.410100209 (1981).

93 Coleman, M. P. & Perry, V. H. Axon pathology in neurological disease: a neglected therapeutic target. *Trends in neurosciences* **25**, 532-537 (2002).

94 Crews, L. & Masliah, E. Molecular mechanisms of neurodegeneration in Alzheimer's disease. *Human molecular genetics* **19**, R12-20, doi:10.1093/hmg/ddq160 (2010).

95 Eikelenboom, P. & Stam, F. C. Immunoglobulins and complement factors in senile plaques. An immunoperoxidase study. *Acta neuropathologica* **57**, 239-242 (1982).

96 McGeer, P. L., Itagaki, S., Tago, H. & McGeer, E. G. Reactive microglia in patients with senile dementia of the Alzheimer type are positive for the histocompatibility glycoprotein HLA-DR. *Neuroscience letters* **79**, 195-200 (1987).

97 Saura, J. *et al.* Increased monoamine oxidase B activity in plaque-associated astrocytes of Alzheimer brains revealed by quantitative enzyme radioautography. *Neuroscience* **62**, 15-30 (1994).

98 Marutle, A. *et al.* (3)H-deprenyl and (3)H-PIB autoradiography show different laminar distributions of astroglia and fibrillar beta-amyloid in Alzheimer brain. *Journal of neuroinflammation* **10**, 90, doi:10.1186/1742-2094-10-90 (2013).

99 Perry, V. H. & Holmes, C. Microglial priming in neurodegenerative disease. *Nature reviews. Neurology* **10**, 217-224, doi:10.1038/nrneurol.2014.38 (2014).

100 Anderson, M. A., Ao, Y. & Sofroniew, M. V. Heterogeneity of reactive astrocytes. *Neuroscience letters* **565**, 23-29, doi:10.1016/j.neulet.2013.12.030 (2014).

101 Wyss-Coray, T. *et al.* Adult mouse astrocytes degrade amyloid-beta in vitro and in situ. *Nature medicine* **9**, 453-457, doi:10.1038/nm838 (2003).

102 Miller, G. Neuroscience. The dark side of glia. *Science* **308**, 778-781, doi:10.1126/science.308.5723.778 (2005).

103 Nagele, R. G., D'Andrea, M. R., Lee, H., Venkataraman, V. & Wang, H. Y. Astrocytes accumulate A beta 42 and give rise to astrocytic amyloid plaques in Alzheimer disease brains. *Brain research* **971**, 197-209 (2003).

104 Rossner, S., Lange-Dohna, C., Zeitschel, U. & Perez-Polo, J. R. Alzheimer's disease beta-secretase BACE1 is not a neuron-specific enzyme. *Journal of neurochemistry* **92**, 226-234, doi:10.1111/j.1471-4159.2004.02857.x (2005).

105 Montine, T. J. *et al.* National Institute on Aging-Alzheimer's Association guidelines for the neuropathologic assessment of Alzheimer's disease: a practical approach. *Acta neuropathologica* **123**, 1-11, doi:10.1007/s00401-011-0910-3 (2012).

106 Alafuzoff, I. *et al.* Staging of neurofibrillary pathology in Alzheimer's disease: a study of the BrainNet Europe Consortium. *Brain pathology* **18**, 484-496, doi:10.1111/j.1750-3639.2008.00147.x (2008).

107 Mirra, S. S. *et al.* The Consortium to Establish a Registry for Alzheimer's Disease (CERAD). Part II. Standardization of the neuropathologic assessment of Alzheimer's disease. *Neurology* **41**, 479-486 (1991).

108 Hardy, J. A. & Higgins, G. A. Alzheimer's disease: the amyloid cascade hypothesis. *Science* **256**, 184-185 (1992).

109 Goate, A. *et al.* Segregation of a missense mutation in the amyloid precursor protein gene with familial Alzheimer's disease. *Nature* **349**, 704-706, doi:10.1038/349704a0 (1991).

110 Mullan, M. *et al.* A pathogenic mutation for probable Alzheimer's disease in the APP gene at the N-terminus of beta-amyloid. *Nature genetics* **1**, 345-347, doi:10.1038/ng0892-345 (1992).

111 Glenner, G. G. & Wong, C. W. Alzheimer's disease and Down's syndrome: sharing of a unique cerebrovascular amyloid fibril protein. *Biochemical and biophysical research communications* **122**, 1131-1135 (1984).

112 Lai, F. & Williams, R. S. A prospective study of Alzheimer disease in Down syndrome. *Archives of neurology* **46**, 849-853 (1989).

113 Herrup, K. The case for rejecting the amyloid cascade hypothesis. *Nature neuroscience* **18**, 794-799, doi:10.1038/nn.4017 (2015).

114 Villemagne, V. L. *et al.* Longitudinal assessment of Abeta and cognition in aging and Alzheimer disease. *Annals of neurology* **69**, 181-192, doi:10.1002/ana.22248 (2011).

115 Wirths, O. & Bayer, T. A. Neuron loss in transgenic mouse models of Alzheimer's disease. *International journal of Alzheimer's disease* **2010**, doi:10.4061/2010/723782 (2010).

116 Webster, S. J., Bachstetter, A. D., Nelson, P. T., Schmitt, F. A. & Van Eldik, L. J. Using mice to model Alzheimer's dementia: an overview of the clinical disease and the preclinical behavioral changes in 10 mouse models. *Frontiers in genetics* **5**, 88, doi:10.3389/fgene.2014.00088 (2014).

117 Holmes, C. *et al.* Long-term effects of Abeta42 immunisation in Alzheimer's disease: follow-up of a randomised, placebo-controlled phase I trial. *Lancet* **372**, 216-223, doi:10.1016/S0140-6736(08)61075-2 (2008).

118 Doody, R. S. *et al.* Phase 3 trials of solanezumab for mild-to-moderate Alzheimer's disease. *The New England journal of medicine* **370**, 311-321, doi:10.1056/NEJMoa1312889 (2014).

119 Salloway, S. *et al.* Two phase 3 trials of bapineuzumab in mild-to-moderate Alzheimer's disease. *The New England journal of medicine* **370**, 322-333, doi:10.1056/NEJMoa1304839 (2014).

120 Musiek, E. S. & Holtzman, D. M. Three dimensions of the amyloid hypothesis: time, space and 'wingmen'. *Nature neuroscience* **18**, 800-806, doi:10.1038/nn.4018 (2015).

121 Bloom, G. S. Amyloid-beta and tau: the trigger and bullet in Alzheimer disease pathogenesis. *JAMA neurology* **71**, 505-508, doi:10.1001/jamaneurol.2013.5847 (2014).

122 Lesne, S. *et al.* A specific amyloid-beta protein assembly in the brain impairs memory. *Nature* **440**, 352-357, doi:10.1038/nature04533 (2006).

123 Haass, C. & Selkoe, D. J. Soluble protein oligomers in neurodegeneration: lessons from the Alzheimer's amyloid beta-peptide. *Nature reviews. Molecular cell biology* **8**, 101-112, doi:10.1038/nrm2101 (2007).

124 Benilova, I., Karran, E. & De Strooper, B. The toxic Abeta oligomer and Alzheimer's disease: an emperor in need of clothes. *Nature neuroscience* **15**, 349-357, doi:10.1038/nn.3028 (2012).

125 Lambert, M. P. *et al.* Diffusible, nonfibrillar ligands derived from Abeta1-42 are potent central nervous system neurotoxins. *Proceedings of the National Academy of Sciences of the United States of America* **95**, 6448-6453 (1998).

126 Small, S. A. & Duff, K. Linking Abeta and tau in late-onset Alzheimer's disease: a dual pathway hypothesis. *Neuron* **60**, 534-542, doi:10.1016/j.neuron.2008.11.007 (2008).

127 Herrup, K. Reimagining Alzheimer's disease--an age-based hypothesis. *The Journal of neuroscience : the official journal of the Society for Neuroscience* **30**, 16755-16762, doi:10.1523/JNEUROSCI.4521-10.2010 (2010).

128 Roberson, E. D. *et al.* Reducing endogenous tau ameliorates amyloid beta-induced deficits in an Alzheimer's disease mouse model. *Science* **316**, 750-754, doi:10.1126/science.1141736 (2007).

129 Heneka, M. T. & O'Banion, M. K. Inflammatory processes in Alzheimer's disease. *Journal of neuroimmunology* **184**, 69-91, doi:10.1016/j.jneuroim.2006.11.017 (2007).

130 de Toledo-Morrell, L., Goncharova, I., Dickerson, B., Wilson, R. S. & Bennett, D. A. From healthy aging to early Alzheimer's disease: in vivo detection of entorhinal cortex atrophy. *Annals of the New York Academy of Sciences* **911**, 240-253 (2000).

131 Nelson, P. T., Braak, H. & Markesbery, W. R. Neuropathology and cognitive impairment in Alzheimer disease: a complex but coherent relationship. *Journal of neuropathology and experimental neurology* **68**, 1-14, doi:10.1097/NEN.0b013e3181919a48 (2009).

132 Cerami, C. *et al.* Clinical validity of delayed recall tests as a gateway biomarker for Alzheimer's disease in the context of a structured 5-phase development framework. *Neurobiology of aging* **52**, 153-166, doi:10.1016/j.neurobiolaging.2016.03.034 (2017).

133 Reul, S., Lohmann, H., Wiendl, H., Duning, T. & Johnen, A. Can cognitive assessment really discriminate early stages of Alzheimer's and behavioural variant frontotemporal dementia at initial clinical presentation? *Alzheimer's research & therapy* **9**, 61, doi:10.1186/s13195-017-0287-1 (2017).

134 Lebouvier, T., Pasquier, F. & Buee, L. Update on tauopathies. *Current opinion in neurology*, doi:10.1097/WCO.0000000000000502 (2017).

135 Forman, M. S. *et al.* Signature tau neuropathology in gray and white matter of corticobasal degeneration. *The American journal of pathology* **160**, 2045-2053, doi:10.1016/S0002-9440(10)61154-6 (2002).

136 Steele, J. C., Richardson, J. C. & Olszewski, J. Progressive Supranuclear Palsy. A Heterogeneous Degeneration Involving the Brain Stem, Basal Ganglia and Cerebellum with Vertical Gaze and Pseudobulbar Palsy, Nuchal Dystonia and Dementia. *Archives of neurology* **10**, 333-359 (1964).

137 Litvan, I. Diagnosis and management of progressive supranuclear palsy. *Seminars in neurology* **21**, 41-48 (2001).

138 Armstrong, M. J. *et al.* Criteria for the diagnosis of corticobasal degeneration. *Neurology* **80**, 496-503, doi:10.1212/WNL.0b013e31827f0fd1 (2013).

139 Dickson, D. W., Kouri, N., Murray, M. E. & Josephs, K. A. Neuropathology of frontotemporal lobar degeneration-tau (FTLD-tau). *Journal of molecular neuroscience : MN* **45**, 384-389, doi:10.1007/s12031-011-9589-0 (2011).

140 Feany, M. B., Mattiace, L. A. & Dickson, D. W. Neuropathologic overlap of progressive supranuclear palsy, Pick's disease and corticobasal degeneration. *Journal of neuropathology and experimental neurology* **55**, 53-67 (1996).

141 Litvan, I. *et al.* Validity and reliability of the preliminary NINDS neuropathologic criteria for progressive supranuclear palsy and related disorders. *Journal of neuropathology and experimental neurology* **55**, 97-105 (1996).

142 Boeve, B. F. *et al.* Pathologic heterogeneity in clinically diagnosed corticobasal degeneration. *Neurology* **53**, 795-800 (1999).

143 Josephs, K. A. & Dickson, D. W. Diagnostic accuracy of progressive supranuclear palsy in the Society for Progressive Supranuclear Palsy brain bank. *Movement disorders : official journal of the Movement Disorder Society* **18**, 1018-1026, doi:10.1002/mds.10488 (2003).

144 Respondek, G. *et al.* The phenotypic spectrum of progressive supranuclear palsy: a retrospective multicenter study of 100 definite cases. *Movement disorders : official journal of the Movement Disorder Society* **29**, 1758-1766, doi:10.1002/mds.26054 (2014).

145 Williams, D. R. & Lees, A. J. Progressive supranuclear palsy: clinicopathological concepts and diagnostic challenges. *The Lancet. Neurology* **8**, 270-279, doi:10.1016/S1474-4422(09)70042-0 (2009).

146 Lee, S. E. *et al.* Clinicopathological correlations in corticobasal degeneration. *Annals of neurology* **70**, 327-340, doi:10.1002/ana.22424 (2011).

147 Biomarkers Definitions Working Group. Biomarkers and surrogate endpoints: preferred definitions and conceptual framework. *Clinical pharmacology and therapeutics* **69**, 89-95, doi:10.1067/mcp.2001.113989 (2001).

148 Frisoni, G. B. *et al.* Strategic roadmap for an early diagnosis of Alzheimer's disease based on biomarkers. *The Lancet. Neurology* **16**, 661-676, doi:10.1016/S1474-4422(17)30159-X (2017).

149 Phelps, M. E. Positron emission tomography provides molecular imaging of biological processes. *Proceedings of the National Academy of Sciences of the United States of America* **97**, 9226-9233 (2000).

150 Frisoni, G. B. *et al.* Imaging markers for Alzheimer disease: which vs how. *Neurology* **81**, 487-500, doi:10.1212/WNL.0b013e31829d86e8 (2013).

151 Rohrer, J. D. *et al.* Clinical and neuroanatomical signatures of tissue pathology in frontotemporal lobar degeneration. *Brain : a journal of neurology* **134**, 2565-2581, doi:10.1093/brain/awr198 (2011).

152 Dickerson, B. C. *et al.* The cortical signature of Alzheimer's disease: regionally specific cortical thinning relates to symptom severity in very mild to mild AD

dementia and is detectable in asymptomatic amyloid-positive individuals. *Cerebral cortex* **19**, 497-510, doi:10.1093/cercor/bhn113 (2009).

153 Ferreira, D. *et al.* Distinct subtypes of Alzheimer's disease based on patterns of brain atrophy: longitudinal trajectories and clinical applications. *Scientific reports* **7**, 46263, doi:10.1038/srep46263 (2017).

154 Bobinski, M. *et al.* The histological validation of post mortem magnetic resonance imaging-determined hippocampal volume in Alzheimer's disease. *Neuroscience* **95**, 721-725 (2000).

155 Fox, N. C., Scahill, R. I., Crum, W. R. & Rossor, M. N. Correlation between rates of brain atrophy and cognitive decline in AD. *Neurology* **52**, 1687-1689 (1999).

156 Whitwell, J. L. *et al.* MRI correlates of neurofibrillary tangle pathology at autopsy: a voxel-based morphometry study. *Neurology* **71**, 743-749, doi:10.1212/01.wnl.0000324924.91351.7d (2008).

157 Jack, C. R., Jr. *et al.* Antemortem MRI findings correlate with hippocampal neuropathology in typical aging and dementia. *Neurology* **58**, 750-757 (2002).

158 Scheltens, P. *et al.* Atrophy of medial temporal lobes on MRI in "probable" Alzheimer's disease and normal ageing: diagnostic value and neuropsychological correlates. *Journal of neurology, neurosurgery, and psychiatry* **55**, 967-972 (1992).

159 Ten Kate, M. *et al.* Clinical validity of medial temporal atrophy as a biomarker for Alzheimer's disease in the context of a structured 5-phase development framework. *Neurobiology of aging* **52**, 167-182 e161, doi:10.1016/j.neurobiolaging.2016.05.024 (2017).

160 Voevodskaya, O. *et al.* Myo-inositol changes precede amyloid pathology and relate to APOE genotype in Alzheimer disease. *Neurology* **86**, 1754-1761, doi:10.1212/WNL.0000000000002672 (2016).

161 Li, X. *et al.* Ratio of Abeta42/P-tau181p in CSF is associated with aberrant default mode network in AD. *Scientific reports* **3**, 1339, doi:10.1038/srep01339 (2013).

162 Haller, S. *et al.* Arterial Spin Labeling Perfusion of the Brain: Emerging Clinical Applications. *Radiology* **281**, 337-356, doi:10.1148/radiol.2016150789 (2016).

163 Li, X. *et al.* White matter changes in familial Alzheimer's disease. *Journal of internal medicine* **278**, 211-218, doi:10.1111/joim.12352 (2015).

164 Phelps, M. E., Hoffman, E. J., Mullani, N. A. & Ter-Pogossian, M. M. Application of annihilation coincidence detection to transaxial reconstruction tomography. *Journal of nuclear medicine : official publication, Society of Nuclear Medicine* **16**, 210-224 (1975).

165 Moses, W. W. Fundamental Limits of Spatial Resolution in PET. *Nuclear instruments & methods in physics research. Section A, Accelerators, spectrometers, detectors and associated equipment* **648 Supplement 1**, S236-S240, doi:10.1016/j.nima.2010.11.092 (2011).

166 Pike, V. W. PET radiotracers: crossing the blood-brain barrier and surviving metabolism. *Trends in pharmacological sciences* **30**, 431-440, doi:10.1016/j.tips.2009.05.005 (2009).

167 Jones, T., Rabiner, E. A. & Company, P. E. T. R. A. The development, past achievements, and future directions of brain PET. *Journal of cerebral blood flow and*

metabolism : official journal of the International Society of Cerebral Blood Flow and Metabolism **32**, 1426-1454, doi:10.1038/jcbfm.2012.20 (2012).

168 de Leon, M. J. *et al.* Regional correlation of PET and CT in senile dementia of the Alzheimer type. *AJNR. American journal of neuroradiology* **4**, 553-556 (1983).

169 Foster, N. L. *et al.* Alzheimer's disease: focal cortical changes shown by positron emission tomography. *Neurology* **33**, 961-965 (1983).

170 Sokoloff, L. Relation between physiological function and energy metabolism in the central nervous system. *Journal of neurochemistry* **29**, 13-26 (1977).

171 Kushner, M. J. *et al.* Cerebral metabolism and patterned visual stimulation: a positron emission tomographic study of the human visual cortex. *Neurology* **38**, 89-95 (1988).

172 Mazziotta, J. C., Phelps, M. E., Carson, R. E. & Kuhl, D. E. Tomographic mapping of human cerebral metabolism: auditory stimulation. *Neurology* **32**, 921-937 (1982).

173 Mielke, R. *et al.* Regional cerebral glucose metabolism and postmortem pathology in Alzheimer's disease. *Acta neuropathologica* **91**, 174-179 (1996).

174 Friedland, R. P., Brun, A. & Budinger, T. F. Pathological and positron emission tomographic correlations in Alzheimer's disease. *Lancet* **1**, 228 (1985).

175 McGeer, P. L. *et al.* Comparison of PET, MRI, and CT with pathology in a proven case of Alzheimer's disease. *Neurology* **36**, 1569-1574 (1986).

176 Zimmer, E. R. *et al.* [18F]FDG PET signal is driven by astroglial glutamate transport. *Nature neuroscience* **20**, 393-395, doi:10.1038/nn.4492 (2017).

177 Heiss, W. D., Szelies, B., Kessler, J. & Herholz, K. Abnormalities of energy metabolism in Alzheimer's disease studied with PET. *Annals of the New York Academy of Sciences* **640**, 65-71 (1991).

178 Minoshima, S. *et al.* Metabolic reduction in the posterior cingulate cortex in very early Alzheimer's disease. *Annals of neurology* **42**, 85-94, doi:10.1002/ana.410420114 (1997).

179 Kadir, A. *et al.* Positron emission tomography imaging and clinical progression in relation to molecular pathology in the first Pittsburgh Compound B positron emission tomography patient with Alzheimer's disease. *Brain : a journal of neurology* **134**, 301-317, doi:10.1093/brain/awq349 (2011).

180 Jagust, W. J. *et al.* Relationships between biomarkers in aging and dementia. *Neurology* **73**, 1193-1199, doi:10.1212/WNL.0b013e3181bc010c (2009).

181 Madhavan, A. *et al.* FDG PET and MRI in logopenic primary progressive aphasia versus dementia of the Alzheimer's type. *PloS one* **8**, e62471, doi:10.1371/journal.pone.0062471 (2013).

182 Woodward, M. C., Rowe, C. C., Jones, G., Villemagne, V. L. & Varos, T. A. Differentiating the frontal presentation of Alzheimer's disease with FDG-PET. *Journal of Alzheimer's disease : JAD* **44**, 233-242, doi:10.3233/JAD-141110 (2015).

183 Singh, T. D. *et al.* Clinical, FDG and amyloid PET imaging in posterior cortical atrophy. *Journal of neurology* **262**, 1483-1492, doi:10.1007/s00415-015-7732-5 (2015).

184 Teune, L. K. *et al.* Typical cerebral metabolic patterns in neurodegenerative brain diseases. *Movement disorders : official journal of the Movement Disorder Society* **25**, 2395-2404, doi:10.1002/mds.23291 (2010).

185 Drzezga, A. *et al.* Cerebral metabolic changes accompanying conversion of mild cognitive impairment into Alzheimer's disease: a PET follow-up study. *European journal of nuclear medicine and molecular imaging* **30**, 1104-1113, doi:10.1007/s00259-003-1194-1 (2003).

186 Garibotto, V. *et al.* Clinical validity of brain fluorodeoxyglucose positron emission tomography as a biomarker for Alzheimer's disease in the context of a structured 5-phase development framework. *Neurobiology of aging* **52**, 183-195, doi:10.1016/j.neurobiolaging.2016.03.033 (2017).

187 Jagust, W., Reed, B., Mungas, D., Ellis, W. & Decarli, C. What does fluorodeoxyglucose PET imaging add to a clinical diagnosis of dementia? *Neurology* **69**, 871-877, doi:10.1212/01.wnl.0000269790.05105.16 (2007).

188 Klunk, W. E. *et al.* Imaging brain amyloid in Alzheimer's disease with Pittsburgh Compound-B. *Annals of neurology* **55**, 306-319, doi:10.1002/ana.20009 (2004).

189 Bacskai, B. J. *et al.* Four-dimensional multiphoton imaging of brain entry, amyloid binding, and clearance of an amyloid-beta ligand in transgenic mice. *Proceedings of the National Academy of Sciences of the United States of America* **100**, 12462-12467, doi:10.1073/pnas.2034101100 (2003).

190 Johnson, K. A. *et al.* Imaging of amyloid burden and distribution in cerebral amyloid angiopathy. *Annals of neurology* **62**, 229-234, doi:10.1002/ana.21164 (2007).

191 Ikonomovic, M. D. *et al.* Post-mortem correlates of in vivo PiB-PET amyloid imaging in a typical case of Alzheimer's disease. *Brain : a journal of neurology* **131**, 1630-1645, doi:10.1093/brain/awn016 (2008).

192 Murray, M. E. *et al.* Clinicopathologic and 11C-Pittsburgh compound B implications of Thal amyloid phase across the Alzheimer's disease spectrum. *Brain : a journal of neurology* **138**, 1370-1381, doi:10.1093/brain/awv050 (2015).

193 Landau, S. M. *et al.* Amyloid PET imaging in Alzheimer's disease: a comparison of three radiotracers. *European journal of nuclear medicine and molecular imaging* **41**, 1398-1407, doi:10.1007/s00259-014-2753-3 (2014).

194 Landau, S. M. *et al.* Amyloid-beta imaging with Pittsburgh compound B and florbetapir: comparing radiotracers and quantification methods. *Journal of nuclear medicine : official publication, Society of Nuclear Medicine* **54**, 70-77, doi:10.2967/jnumed.112.109009 (2013).

195 Wolk, D. A. *et al.* Amyloid imaging in Alzheimer's disease: comparison of florbetapir and Pittsburgh compound-B positron emission tomography. *Journal of neurology, neurosurgery, and psychiatry* **83**, 923-926, doi:10.1136/jnnp-2012-302548 (2012).

196 Jansen, W. J. *et al.* Prevalence of cerebral amyloid pathology in persons without dementia: a meta-analysis. *Jama* **313**, 1924-1938, doi:10.1001/jama.2015.4668 (2015).

197 Villemagne, V. L. *et al.* Amyloid beta deposition, neurodegeneration, and cognitive decline in sporadic Alzheimer's disease: a prospective cohort study. *The Lancet. Neurology* **12**, 357-367, doi:10.1016/S1474-4422(13)70044-9 (2013).

198 Jack, C. R., Jr. *et al.* Brain beta-amyloid load approaches a plateau. *Neurology* **80**, 890-896, doi:10.1212/WNL.0b013e3182840bbe (2013).

199 Ma, Y. *et al.* Predictive accuracy of amyloid imaging for progression from mild cognitive impairment to Alzheimer disease with different lengths of follow-up: a meta-analysis. [Corrected]. *Medicine* **93**, e150, doi:10.1097/MD.0000000000000150 (2014).

200 Forsberg, A. *et al.* PET imaging of amyloid deposition in patients with mild cognitive impairment. *Neurobiology of aging* **29**, 1456-1465, doi:10.1016/j.neurobiolaging.2007.03.029 (2008).

201 Nordberg, A. *et al.* A European multicentre PET study of fibrillar amyloid in Alzheimer's disease. *European journal of nuclear medicine and molecular imaging* **40**, 104-114, doi:10.1007/s00259-012-2237-2 (2013).

202 Clark, C. M. *et al.* Cerebral PET with florbetapir compared with neuropathology at autopsy for detection of neuritic amyloid-beta plaques: a prospective cohort study. *The Lancet. Neurology* **11**, 669-678, doi:10.1016/S1474-4422(12)70142-4 (2012).

203 Rinne, J. O. *et al.* [(18)F]Flutemetamol PET imaging and cortical biopsy histopathology for fibrillar amyloid beta detection in living subjects with normal pressure hydrocephalus: pooled analysis of four studies. *Acta neuropathologica* **124**, 833-845, doi:10.1007/s00401-012-1051-z (2012).

204 Thurfjell, L. *et al.* Automated quantification of 18F-flutemetamol PET activity for categorizing scans as negative or positive for brain amyloid: concordance with visual image reads. *Journal of nuclear medicine : official publication, Society of Nuclear Medicine* **55**, 1623-1628, doi:10.2967/jnumed.114.142109 (2014).

205 Sabri, O. *et al.* Florbetaben PET imaging to detect amyloid beta plaques in Alzheimer's disease: phase 3 study. *Alzheimer's & dementia : the journal of the Alzheimer's Association* **11**, 964-974, doi:10.1016/j.jalz.2015.02.004 (2015).

206 Laforce, R., Jr. & Rabinovici, G. D. Amyloid imaging in the differential diagnosis of dementia: review and potential clinical applications. *Alzheimer's research & therapy* **3**, 31, doi:10.1186/alzrt93 (2011).

207 Johnson, K. A. *et al.* Appropriate use criteria for amyloid PET: a report of the Amyloid Imaging Task Force, the Society of Nuclear Medicine and Molecular Imaging, and the Alzheimer's Association. *Alzheimer's & dementia : the journal of the Alzheimer's Association* **9**, e-1-16, doi:10.1016/j.jalz.2013.01.002 (2013).

208 Villemagne, V. L., Fodero-Tavoletti, M. T., Masters, C. L. & Rowe, C. C. Tau imaging: early progress and future directions. *The Lancet. Neurology* **14**, 114-124, doi:10.1016/S1474-4422(14)70252-2 (2015).

209 Thompson, P. W. *et al.* Interaction of the amyloid imaging tracer FDDNP with hallmark Alzheimer's disease pathologies. *Journal of neurochemistry* **109**, 623-630, doi:10.1111/j.1471-4159.2009.05996.x (2009).

210 Shin, J., Kepe, V., Barrio, J. R. & Small, G. W. The merits of FDDNP-PET imaging in Alzheimer's disease. *Journal of Alzheimer's disease : JAD* **26 Suppl 3**, 135-145, doi:10.3233/JAD-2011-0008 (2011).

211 Klunk, W. E. & Mathis, C. A. The future of amyloid-beta imaging: a tale of radionuclides and tracer proliferation. *Current opinion in neurology* **21**, 683-687, doi:10.1097/WCO.0b013e3283168e1a (2008).

212 Shah, M. & Catafau, A. M. Molecular Imaging Insights into Neurodegeneration: Focus on Tau PET Radiotracers. *Journal of nuclear medicine : official publication, Society of Nuclear Medicine* **55**, 871-874, doi:10.2967/jnumed.113.136069 (2014).

213 Martin, L., Latypova, X. & Terro, F. Post-translational modifications of tau protein: implications for Alzheimer's disease. *Neurochemistry international* **58**, 458-471, doi:10.1016/j.neuint.2010.12.023 (2011).

214 Dani, M., Brooks, D. J. & Edison, P. Tau imaging in neurodegenerative diseases. *European journal of nuclear medicine and molecular imaging*, doi:10.1007/s00259-015-3231-2 (2015).

215 Murray, M. E. *et al.* Clinicopathologic assessment and imaging of tauopathies in neurodegenerative dementias. *Alzheimer's research & therapy* **6**, 1, doi:10.1186/alzrt231 (2014).

216 Kowall, N. W. & Kosik, K. S. Axonal disruption and aberrant localization of tau protein characterize the neuropil pathology of Alzheimer's disease. *Annals of neurology* **22**, 639-643, doi:10.1002/ana.410220514 (1987).

217 Marquie, M. *et al.* Validating novel tau positron emission tomography tracer [F-18]-AV-1451 (T807) on postmortem brain tissue. *Annals of neurology* **78**, 787-800, doi:10.1002/ana.24517 (2015).

218 Lemoine, L. *et al.* Visualization of regional tau deposits using (3)H-THK5117 in Alzheimer brain tissue. *Acta neuropathologica communications* **3**, 40, doi:10.1186/s40478-015-0220-4 (2015).

219 Chien, D. T. *et al.* Early clinical PET imaging results with the novel PHF-tau radioligand [F-18]-T807. *Journal of Alzheimer's disease : JAD* **34**, 457-468, doi:10.3233/JAD-122059 (2013).

220 Maruyama, M. *et al.* Imaging of tau pathology in a tauopathy mouse model and in Alzheimer patients compared to normal controls. *Neuron* **79**, 1094-1108, doi:10.1016/j.neuron.2013.07.037 (2013).

221 Xia, C. F. *et al.* [(18)F]T807, a novel tau positron emission tomography imaging agent for Alzheimer's disease. *Alzheimer's & dementia : the journal of the Alzheimer's Association* **9**, 666-676, doi:10.1016/j.jalz.2012.11.008 (2013).

222 Harada, R. *et al.* 18F-THK5351: A Novel PET Radiotracer for Imaging Neurofibrillary Pathology in Alzheimer Disease. *Journal of nuclear medicine : official publication, Society of Nuclear Medicine* **57**, 208-214, doi:10.2967/jnumed.115.164848 (2016).

223 Saint-Aubert, L. *et al.* Tau PET imaging: present and future directions. *Molecular neurodegeneration* **12**, 19, doi:10.1186/s13024-017-0162-3 (2017).

224 Ono, M. *et al.* Distinct binding of PET ligands PBB3 and AV-1451 to tau fibril strains in neurodegenerative tauopathies. *Brain : a journal of neurology* **140**, 764-780, doi:10.1093/brain/aww339 (2017).

225 Lemoine, L. *et al.* Comparative binding properties of the tau PET tracers THK5117, THK5351, PBB3 and T807 in post-mortem Alzheimer brains. (under review).

226 Kimura, Y. *et al.* PET Quantification of Tau Pathology in Human Brain with 11C-PBB3. *Journal of nuclear medicine : official publication, Society of Nuclear Medicine* **56**, 1359-1365, doi:10.2967/jnumed.115.160127 (2015).

227 Jonasson, M. *et al.* Tracer kinetic analysis of (S)-18F-THK5117 as a PET tracer for assessing tau pathology. *Journal of nuclear medicine : official publication, Society of Nuclear Medicine*, doi:10.2967/jnumed.115.158519 (2016).

228 Barret, O. *et al.* Kinetic Modeling of the Tau PET Tracer 18F-AV-1451 in Human Healthy Volunteers and Alzheimer Disease Subjects. *Journal of nuclear medicine : official publication, Society of Nuclear Medicine* **58**, 1124-1131, doi:10.2967/jnumed.116.182881 (2017).

229 Baker, S. L. *et al.* Reference Tissue-Based Kinetic Evaluation of 18F-AV-1451 for Tau Imaging. *Journal of nuclear medicine : official publication, Society of Nuclear Medicine* **58**, 332-338, doi:10.2967/jnumed.116.175273 (2017).

230 Harada, R. *et al.* [(18)F]THK-5117 PET for assessing neurofibrillary pathology in Alzheimer's disease. *European journal of nuclear medicine and molecular imaging* **42**, 1052-1061, doi:10.1007/s00259-015-3035-4 (2015).

231 Johnson, K. A. *et al.* Tau PET imaging in aging and early Alzheimer's disease. *Annals of neurology*, doi:10.1002/ana.24546 (2015).

232 Harada, R. *et al.* 18F-THK5351: A Novel PET Radiotracer for Imaging Neurofibrillary Pathology in Alzheimer's Disease. *Journal of nuclear medicine : official publication, Society of Nuclear Medicine*, doi:10.2967/jnumed.115.164848 (2015).

233 Cho, H. *et al.* In vivo cortical spreading pattern of tau and amyloid in the Alzheimer disease spectrum. *Annals of neurology* **80**, 247-258, doi:10.1002/ana.24711 (2016).

234 Scholl, M. *et al.* PET Imaging of Tau Deposition in the Aging Human Brain. *Neuron* **89**, 971-982, doi:10.1016/j.neuron.2016.01.028 (2016).

235 Schwarz, A. J. *et al.* Regional profiles of the candidate tau PET ligand 18F-AV-1451 recapitulate key features of Braak histopathological stages. *Brain : a journal of neurology* **139**, 1539-1550, doi:10.1093/brain/aww023 (2016).

236 Harada, R. *et al.* Correlations of 18F-THK5351 PET with post-mortem burden of tau and astrogliosis in Alzheimer's disease. *Journal of nuclear medicine : official publication, Society of Nuclear Medicine*, doi:10.2967/jnumed.117.197426 (2017).

237 Kang, J. M. *et al.* Tau positron emission tomography using [18F]THK5351 and cerebral glucose hypometabolism in Alzheimer's disease. *Neurobiology of aging* **59**, 210-219, doi:10.1016/j.neurobiolaging.2017.08.008 (2017).

238 Sone, D. *et al.* Regional tau deposition and subregion atrophy of medial temporal structures in early Alzheimer's disease: A combined positron emission tomography/magnetic resonance imaging study. *Alzheimer's & dementia* **9**, 35-40, doi:10.1016/j.dadm.2017.07.001 (2017).

239 Sepulcre, J. *et al.* In Vivo Tau, Amyloid, and Gray Matter Profiles in the Aging Brain. *The Journal of neuroscience : the official journal of the Society for Neuroscience* **36**, 7364-7374, doi:10.1523/JNEUROSCI.0639-16.2016 (2016).

240 Dronse, J. *et al.* In vivo Patterns of Tau Pathology, Amyloid-beta Burden, and Neuronal Dysfunction in Clinical Variants of Alzheimer's Disease. *Journal of Alzheimer's disease : JAD* **55**, 465-471, doi:10.3233/JAD-160316 (2017).

241 Pontecorvo, M. J. *et al.* Relationships between flortaucipir PET tau binding and amyloid burden, clinical diagnosis, age and cognition. *Brain : a journal of neurology* **140**, 748-763, doi:10.1093/brain/aww334 (2017).

242 Bischof, G. N. *et al.* Impact of tau and amyloid burden on glucose metabolism in Alzheimer's disease. *Annals of clinical and translational neurology* **3**, 934-939, doi:10.1002/acn3.339 (2016).

243 Lockhart, S. N. *et al.* Amyloid and tau PET demonstrate region-specific associations in normal older people. *NeuroImage* **150**, 191-199, doi:10.1016/j.neuroimage.2017.02.051 (2017).

244 Tosun, D. *et al.* Association between tau deposition and antecedent amyloid-beta accumulation rates in normal and early symptomatic individuals. *Brain : a journal of neurology*, doi:10.1093/brain/awx046 (2017).

245 LaPoint, M. R. *et al.* The association between tau PET and retrospective cortical thinning in clinically normal elderly. *NeuroImage* **157**, 612-622, doi:10.1016/j.neuroimage.2017.05.049 (2017).

246 Ossenkoppele, R. *et al.* Tau PET patterns mirror clinical and neuroanatomical variability in Alzheimer's disease. *Brain : a journal of neurology* **139**, 1551-1567, doi:10.1093/brain/aww027 (2016).

247 Kikuchi, A. *et al.* In vivo visualization of tau deposits in corticobasal syndrome by 18F-THK5351 PET. *Neurology* **87**, 2309-2316, doi:10.1212/WNL.0000000000003375 (2016).

248 Cho, H. *et al.* 18F-AV-1451 binds to motor-related subcortical gray and white matter in corticobasal syndrome. *Neurology* **89**, 1170-1178, doi:10.1212/WNL.0000000000004364 (2017).

249 Smith, R. *et al.* In vivo retention of 18F-AV-1451 in corticobasal syndrome. *Neurology* **89**, 845-853, doi:10.1212/WNL.0000000000004264 (2017).

250 Passamonti, L. *et al.* 18F-AV-1451 positron emission tomography in Alzheimer's disease and progressive supranuclear palsy. *Brain : a journal of neurology* **140**, 781-791, doi:10.1093/brain/aww340 (2017).

251 Whitwell, J. L. *et al.* [18 F]AV-1451 tau positron emission tomography in progressive supranuclear palsy. *Movement disorders : official journal of the Movement Disorder Society* **32**, 124-133, doi:10.1002/mds.26834 (2017).

252 Schonhaut, D. R. *et al.* 18 F-flortaucipir tau PET distinguishes established progressive supranuclear palsy from controls and Parkinson's disease: A multicenter study. *Annals of neurology*, doi:10.1002/ana.25060 (2017).

253 Josephs, K. A. *et al.* [18F]AV-1451 tau-PET uptake does correlate with quantitatively measured 4R-tau burden in autopsy-confirmed corticobasal degeneration. *Acta neuropathologica* **132**, 931-933, doi:10.1007/s00401-016-1618-1 (2016).

254 Smith, R. *et al.* Tau neuropathology correlates with FDG-PET, but not AV-1451-PET, in progressive supranuclear palsy. *Acta neuropathologica* **133**, 149-151, doi:10.1007/s00401-016-1650-1 (2017).

255 McMillan, C. T. *et al.* Multimodal evaluation demonstrates in vivo 18F-AV-1451 uptake in autopsy-confirmed corticobasal degeneration. *Acta neuropathologica* **132**, 935-937, doi:10.1007/s00401-016-1640-3 (2016).

256 Coakeley, S. *et al.* Positron emission tomography imaging of tau pathology in progressive supranuclear palsy. *Journal of cerebral blood flow and metabolism : official journal of the International Society of Cerebral Blood Flow and Metabolism* **37**, 3150-3160, doi:10.1177/0271678X16683695 (2017).

257 Perez-Soriano, A. *et al.* PBB3 imaging in Parkinsonian disorders: Evidence for binding to tau and other proteins. *Movement disorders : official journal of the Movement Disorder Society* **32**, 1016-1024, doi:10.1002/mds.27029 (2017).

258 Bevan-Jones, W. R. *et al.* [18F]AV-1451 binding in vivo mirrors the expected distribution of TDP-43 pathology in the semantic variant of primary progressive aphasia. *Journal of neurology, neurosurgery, and psychiatry*, doi:10.1136/jnnp-2017-316402 (2017).

259 Lowe, V. J. *et al.* An autoradiographic evaluation of AV-1451 Tau PET in dementia. *Acta neuropathologica communications* **4**, 58, doi:10.1186/s40478-016-0315-6 (2016).

260 Hostetler, E. D. *et al.* Preclinical Characterization of 18F-MK-6240, a Promising PET Tracer for In Vivo Quantification of Human Neurofibrillary Tangles. *Journal of nuclear medicine : official publication, Society of Nuclear Medicine* **57**, 1599-1606, doi:10.2967/jnumed.115.171678 (2016).

261 Marquie, M. *et al.* Lessons learned about [F-18]-AV-1451 off-target binding from an autopsy-confirmed Parkinson's case. *Acta neuropathologica communications* **5**, 75, doi:10.1186/s40478-017-0482-0 (2017).

262 Seubert, P. *et al.* Isolation and quantification of soluble Alzheimer's beta-peptide from biological fluids. *Nature* **359**, 325-327, doi:10.1038/359325a0 (1992).

263 Kawarabayashi, T. *et al.* Age-dependent changes in brain, CSF, and plasma amyloid (beta) protein in the Tg2576 transgenic mouse model of Alzheimer's disease. *The Journal of neuroscience : the official journal of the Society for Neuroscience* **21**, 372-381 (2001).

264 DeMattos, R. B. *et al.* Plaque-associated disruption of CSF and plasma amyloid-beta (Abeta) equilibrium in a mouse model of Alzheimer's disease. *Journal of neurochemistry* **81**, 229-236 (2002).

265 Tapiola, T. *et al.* Cerebrospinal fluid {beta}-amyloid 42 and tau proteins as biomarkers of Alzheimer-type pathologic changes in the brain. *Archives of neurology* **66**, 382-389, doi:10.1001/archneurol.2008.596 (2009).

266 Seppala, T. T. *et al.* CSF biomarkers for Alzheimer disease correlate with cortical brain biopsy findings. *Neurology* **78**, 1568-1575, doi:10.1212/WNL.0b013e3182563bd0 (2012).

267 Leuzy, A. *et al.* Concordance and Diagnostic Accuracy of [11C]PIB PET and Cerebrospinal Fluid Biomarkers in a Sample of Patients with Mild Cognitive Impairment and Alzheimer's Disease. *Journal of Alzheimer's disease : JAD* **45**, 1077-1088, doi:10.3233/JAD-142952 (2015).

268 Leuzy, A. *et al.* Pittsburgh compound B imaging and cerebrospinal fluid amyloid-beta in a multicentre European memory clinic study. *Brain : a journal of neurology* **139**, 2540-2553, doi:10.1093/brain/aww160 (2016).

269 Palmqvist, S. *et al.* Detailed comparison of amyloid PET and CSF biomarkers for identifying early Alzheimer disease. *Neurology* **85**, 1240-1249, doi:10.1212/WNL.0000000000001991 (2015).

270 Palmqvist, S., Mattsson, N., Hansson, O. & Alzheimer's Disease Neuroimaging, I. Cerebrospinal fluid analysis detects cerebral amyloid-beta accumulation earlier than positron emission tomography. *Brain : a journal of neurology* **139**, 1226-1236, doi:10.1093/brain/aww015 (2016).

271 Blennow, K. Cerebrospinal fluid protein biomarkers for Alzheimer's disease. *NeuroRx : the journal of the American Society for Experimental NeuroTherapeutics* **1**, 213-225, doi:10.1602/neurorx.1.2.213 (2004).

272 Blennow, K. *et al.* Tau protein in cerebrospinal fluid: a biochemical marker for axonal degeneration in Alzheimer disease? *Molecular and chemical neuropathology / sponsored by the International Society for Neurochemistry and the World Federation of Neurology and research groups on neurochemistry and cerebrospinal fluid* **26**, 231-245, doi:10.1007/BF02815140 (1995).

273 Iqbal, K. & Grundke-Iqbal, I. Elevated levels of tau and ubiquitin in brain and cerebrospinal fluid in Alzheimer's disease. *International psychogeriatrics / IPA* **9 Suppl 1**, 289-296; discussion 317-221 (1997).

274 Tapiola, T. *et al.* The level of cerebrospinal fluid tau correlates with neurofibrillary tangles in Alzheimer's disease. *Neuroreport* **8**, 3961-3963 (1997).

275 Buerger, K. *et al.* CSF phosphorylated tau protein correlates with neocortical neurofibrillary pathology in Alzheimer's disease. *Brain : a journal of neurology* **129**, 3035-3041, doi:10.1093/brain/awl269 (2006).

276 Buerger, K. *et al.* No correlation between CSF tau protein phosphorylated at threonine 181 with neocortical neurofibrillary pathology in Alzheimer's disease. *Brain : a journal of neurology* **130**, e82, doi:10.1093/brain/awm140 (2007).

277 Mattsson, N. *et al.* 18F-AV-1451 and CSF T-tau and P-tau as biomarkers in Alzheimer's disease. *EMBO molecular medicine* **9**, 1212-1223, doi:10.15252/emmm.201707809 (2017).

278 Gordon, B. A. *et al.* The relationship between cerebrospinal fluid markers of Alzheimer pathology and positron emission tomography tau imaging. *Brain : a journal of neurology* **139**, 2249-2260, doi:10.1093/brain/aww139 (2016).

279 Brier, M. R. *et al.* Tau and Abeta imaging, CSF measures, and cognition in Alzheimer's disease. *Science translational medicine* **8**, 338ra366, doi:10.1126/scitranslmed.aaf2362 (2016).

280 Chhatwal, J. P. *et al.* Temporal T807 binding correlates with CSF tau and phospho-tau in normal elderly. *Neurology* **87**, 920-926, doi:10.1212/WNL.0000000000003050 (2016).

281 Nationella riktlinjer för vård och omsorg vid demenssjukdom. *Swedish National Board of Health and Welfare - Socialstyrelsen* (2016).

282 Dubois, B. *et al.* Advancing research diagnostic criteria for Alzheimer's disease: the IWG-2 criteria. *The Lancet. Neurology* **13**, 614-629, doi:10.1016/S1474-4422(14)70090-0 (2014).

283 Albert, M. S. *et al.* The diagnosis of mild cognitive impairment due to Alzheimer's disease: recommendations from the National Institute on Aging-Alzheimer's Association workgroups on diagnostic guidelines for Alzheimer's disease. *Alzheimer's & dementia : the journal of the Alzheimer's Association* **7**, 270-279, doi:10.1016/j.jalz.2011.03.008 (2011).

284 Sperling, R. A. *et al.* Toward defining the preclinical stages of Alzheimer's disease: recommendations from the National Institute on Aging-Alzheimer's Association workgroups on diagnostic guidelines for Alzheimer's disease. *Alzheimer's & dementia : the journal of the Alzheimer's Association* **7**, 280-292, doi:10.1016/j.jalz.2011.03.003 (2011).

285 McKhann, G. M. *et al.* The diagnosis of dementia due to Alzheimer's disease: recommendations from the National Institute on Aging-Alzheimer's Association workgroups on diagnostic guidelines for Alzheimer's disease. *Alzheimer's & dementia : the journal of the Alzheimer's Association* **7**, 263-269, doi:10.1016/j.jalz.2011.03.005 (2011).

286 Jack, C. R., Jr. *et al.* Tracking pathophysiological processes in Alzheimer's disease: an updated hypothetical model of dynamic biomarkers. *The Lancet. Neurology* **12**, 207-216, doi:10.1016/S1474-4422(12)70291-0 (2013).

287 Nordberg, A. Molecular imaging in Alzheimer's disease: new perspectives on biomarkers for early diagnosis and drug development. *Alzheimer's research & therapy* **3**, 34, doi:10.1186/alzrt96 (2011).

288 Petersen, R. C. Alzheimer's disease: progress in prediction. *The Lancet. Neurology* **9**, 4-5, doi:10.1016/S1474-4422(09)70330-8 (2010).

289 Petersen, R. C. *et al.* Alzheimer's Disease Neuroimaging Initiative (ADNI): clinical characterization. *Neurology* **74**, 201-209, doi:10.1212/WNL.0b013e3181cb3e25 (2010).

290 Wechsler, D. *Manual for the Wechsler Adult Intelligence Scale.*, (Psychological Corp., 1955).

291 Tallberg, I. M., Wenneborg, K. & Almkvist, O. Reading words with irregular decoding rules: a test of premorbid cognitive function? *Scandinavian journal of psychology* **47**, 531-539, doi:10.1111/j.1467-9450.2006.00547.x (2006).

292 Bergman, I., Blomberg, M. & Almkvist, O. The importance of impaired physical health and age in normal cognitive aging. *Scandinavian journal of psychology* **48**, 115-125, doi:10.1111/j.1467-9450.2007.00594.x (2007).

293 Edison, P. *et al.* Comparison of MRI based and PET template based approaches in the quantitative analysis of amyloid imaging with PIB-PET. *NeuroImage* **70**, 423-433, doi:10.1016/j.neuroimage.2012.12.014 (2013).

294 Tzourio-Mazoyer, N. *et al.* Automated anatomical labeling of activations in SPM using a macroscopic anatomical parcellation of the MNI MRI single-subject brain. *NeuroImage* **15**, 273-289, doi:10.1006/nimg.2001.0978 (2002).

295 Desikan, R. S. *et al.* An automated labeling system for subdividing the human cerebral cortex on MRI scans into gyral based regions of interest. *NeuroImage* **31**, 968-980, doi:10.1016/j.neuroimage.2006.01.021 (2006).

296 Frazier, J. A. *et al.* Structural brain magnetic resonance imaging of limbic and thalamic volumes in pediatric bipolar disorder. *The American journal of psychiatry* **162**, 1256-1265, doi:10.1176/appi.ajp.162.7.1256 (2005).

297 Goldstein, J. M. *et al.* Hypothalamic abnormalities in schizophrenia: sex effects and genetic vulnerability. *Biological psychiatry* **61**, 935-945, doi:10.1016/j.biopsych.2006.06.027 (2007).

298 Makris, N. *et al.* Decreased volume of left and total anterior insular lobule in schizophrenia. *Schizophrenia research* **83**, 155-171, doi:10.1016/j.schres.2005.11.020 (2006).

299 Hammers, A. *et al.* Three-dimensional maximum probability atlas of the human brain, with particular reference to the temporal lobe. *Human brain mapping* **19**, 224-247, doi:10.1002/hbm.10123 (2003).

300 Logan, J. *et al.* Distribution volume ratios without blood sampling from graphical analysis of PET data. *Journal of cerebral blood flow and metabolism : official journal of the International Society of Cerebral Blood Flow and Metabolism* **16**, 834-840, doi:10.1097/00004647-199609000-00008 (1996).

301 Cselenyi, Z., Olsson, H., Farde, L. & Gulyas, B. Wavelet-aided parametric mapping of cerebral dopamine D2 receptors using the high affinity PET radioligand [11C]FLB 457. *NeuroImage* **17**, 47-60 (2002).

302 Ichise, M. *et al.* Linearized reference tissue parametric imaging methods: application to [11C]DASB positron emission tomography studies of the serotonin transporter in human brain. *Journal of cerebral blood flow and metabolism : official journal of the International Society of Cerebral Blood Flow and Metabolism* **23**, 1096-1112, doi:10.1097/01.WCB.0000085441.37552.CA (2003).

303 Muller-Gartner, H. W. *et al.* Measurement of radiotracer concentration in brain gray matter using positron emission tomography: MRI-based correction for partial volume effects. *Journal of cerebral blood flow and metabolism : official journal of the International Society of Cerebral Blood Flow and Metabolism* **12**, 571-583, doi:10.1038/jcbfm.1992.81 (1992).

304 Rousset, O. G., Ma, Y. & Evans, A. C. Correction for partial volume effects in PET: principle and validation. *Journal of nuclear medicine : official publication, Society of Nuclear Medicine* **39**, 904-911 (1998).

305 Maass, A. *et al.* Comparison of multiple tau-PET measures as biomarkers in aging and Alzheimer's disease. *NeuroImage* **157**, 448-463, doi:10.1016/j.neuroimage.2017.05.058 (2017).

306 Landau, S. M. *et al.* Association of lifetime cognitive engagement and low beta-amyloid deposition. *Archives of neurology* **69**, 623-629, doi:10.1001/archneurol.2011.2748 (2012).

307 Wirth, M., Villeneuve, S., La Joie, R., Marks, S. M. & Jagust, W. J. Gene-environment interactions: lifetime cognitive activity, APOE genotype, and beta-amyloid burden. *The Journal of neuroscience : the official journal of the Society for Neuroscience* **34**, 8612-8617, doi:10.1523/JNEUROSCI.4612-13.2014 (2014).

308 Yasuno, F. *et al.* Low amyloid-beta deposition correlates with high education in cognitively normal older adults: a pilot study. *International journal of geriatric psychiatry* **30**, 919-926, doi:10.1002/gps.4235 (2015).

309 Kemppainen, N. M. *et al.* Cognitive reserve hypothesis: Pittsburgh Compound B and fluorodeoxyglucose positron emission tomography in relation to education in mild Alzheimer's disease. *Annals of neurology* **63**, 112-118, doi:10.1002/ana.21212 (2008).

310 Rowe, C. C. *et al.* Amyloid imaging results from the Australian Imaging, Biomarkers and Lifestyle (AIBL) study of aging. *Neurobiology of aging* **31**, 1275-1283, doi:10.1016/j.neurobiolaging.2010.04.007 (2010).

311 Ossenkoppele, R. *et al.* Prevalence of amyloid PET positivity in dementia syndromes: a meta-analysis. *Jama* **313**, 1939-1949, doi:10.1001/jama.2015.4669 (2015).

312 Johnson, K. A. *et al.* Tau positron emission tomographic imaging in aging and early Alzheimer disease. *Annals of neurology* **79**, 110-119, doi:10.1002/ana.24546 (2016).

313 Shimada, H. *et al.* Association between Abeta and tau accumulations and their influence on clinical features in aging and Alzheimer's disease spectrum brains: A [11C]PBB3-PET study. *Alzheimer's & dementia* **6**, 11-20, doi:10.1016/j.dadm.2016.12.009 (2017).

314 Dowling, N. M., Johnson, S. C., Gleason, C. E., Jagust, W. J. & Alzheimer's Disease Neuroimaging, I. The mediational effects of FDG hypometabolism on the association between cerebrospinal fluid biomarkers and neurocognitive function. *NeuroImage* **105**, 357-368, doi:10.1016/j.neuroimage.2014.10.050 (2015).

315 Bejanin, A. *et al.* Tau pathology and neurodegeneration contribute to cognitive impairment in Alzheimer's disease. *Brain : a journal of neurology*, doi:10.1093/brain/awx243 (2017).

316 Hanseeuw, B. J. *et al.* Fluorodeoxyglucose metabolism associated with tau-amyloid interaction predicts memory decline. *Annals of neurology* **81**, 583-596, doi:10.1002/ana.24910 (2017).

317 Dickson, D. W. *et al.* Office of Rare Diseases neuropathologic criteria for corticobasal degeneration. *Journal of neuropathology and experimental neurology* **61**, 935-946 (2002).

318 Hauw, J. J. *et al.* Preliminary NINDS neuropathologic criteria for Steele-Richardson-Olszewski syndrome (progressive supranuclear palsy). *Neurology* **44**, 2015-2019 (1994).

319 Arnold, S. E., Hyman, B. T., Flory, J., Damasio, A. R. & Van Hoesen, G. W. The topographical and neuroanatomical distribution of neurofibrillary tangles and neuritic plaques in the cerebral cortex of patients with Alzheimer's disease. *Cerebral cortex* **1**, 103-116 (1991).

320 Serrano-Pozo, A., Frosch, M. P., Masliah, E. & Hyman, B. T. Neuropathological alterations in Alzheimer disease. *Cold Spring Harbor perspectives in medicine* **1**, a006189, doi:10.1101/cshperspect.a006189 (2011).

321 Harada, R. *et al.* Characteristics of Tau and Its Ligands in PET Imaging. *Biomolecules* **6**, 7, doi:10.3390/biom6010007 (2016).

322 Jang, Y. *et al.* Head to Head Comparison of [18f] AV-1451 and [18f] THK5351 for Tau Imaging in Alzheimer’s Disease and Frontotemporal Dementia. *Alzheimer's Association International Conference, London, U.K.* **P4-212** (2017).

323 Fitzpatrick, A. W. P. *et al.* Cryo-EM structures of tau filaments from Alzheimer's disease. *Nature* **547**, 185-190, doi:10.1038/nature23002 (2017).

324 Okamura, N. *et al.* Non-invasive assessment of Alzheimer's disease neurofibrillary pathology using 18F-THK5105 PET. *Brain : a journal of neurology* **137**, 1762-1771, doi:10.1093/brain/awu064 (2014).

325 Lee, H. *et al.* [18F]-THK5351 PET Imaging in Patients With Semantic Variant Primary Progressive Aphasia. *Alzheimer disease and associated disorders*, doi:10.1097/WAD.0000000000000216 (2017).

326 Makaretz, S. J. *et al.* Flortaucipir tau PET imaging in semantic variant primary progressive aphasia. *Journal of neurology, neurosurgery, and psychiatry*, doi:10.1136/jnnp-2017-316409 (2017).

327 Wintmolders, C., Bottelbergs, A., Mariën, J., Moechars, D. & Langlois, X. Characterization of the tau radioligand [3H]THK-5351 binding in Alzheimer brain tissue. *Alzheimer's & Parkinson's Diseases Congress, Vienna, Austria* **B04.c-236** (2017).

328 Koga, S., Ono, M., Sahara, N., Higuchi, M. & Dickson, D. W. Fluorescence and autoradiographic evaluation of tau PET ligand PBB3 to alpha-synuclein pathology. *Movement disorders : official journal of the Movement Disorder Society* **32**, 884-892, doi:10.1002/mds.27013 (2017).

329 Chiotis, K. *et al.* Imaging in-vivo tau pathology in Alzheimer's disease with THK5317 PET in a multimodal paradigm. *European journal of nuclear medicine and molecular imaging* **43**, 1686-1699, doi:10.1007/s00259-016-3363-z (2016).

330 Tong, J. *et al.* Distribution of monoamine oxidase proteins in human brain: implications for brain imaging studies. *Journal of cerebral blood flow and metabolism : official journal of the International Society of Cerebral Blood Flow and Metabolism* **33**, 863-871, doi:10.1038/jcbfm.2013.19 (2013).

331 Thomas, T. Monoamine oxidase-B inhibitors in the treatment of Alzheimer's disease. *Neurobiology of aging* **21**, 343-348 (2000).

332 Ikonomovic, M. D., Abrahamson, E. E., Price, J. C., Mathis, C. A. & Klunk, W. E. [F-18]AV-1451 positron emission tomography retention in choroid plexus: More than "off-target" binding. *Annals of neurology* **80**, 307-308, doi:10.1002/ana.24706 (2016).

333 Saint-Aubert, L. *et al.* Regional tau deposition measured by [18F]THK5317 positron emission tomography is associated to cognition via glucose metabolism in Alzheimer's disease. *Alzheimer's research & therapy* **8**, 38, doi:10.1186/s13195-016-0204-z (2016).

334 Chiotis, K. *et al.* Longitudinal changes of tau PET imaging in relation to hypometabolism in prodromal and Alzheimer's disease dementia. *Molecular psychiatry*, doi:10.1038/mp.2017.108 (2017).